UNIVERSITEIT VAN PRETORIA
UNIVERSITY OF PRETORIA
YUNIBESITHI YA PRETORIA

Mixture interactions of two metal oxides engineered nanoparticles and an organic pollutant in river water systems

By

Aston Frankline Nanja

Thesis submitted in fulfilment of the requirement for the degree of

Doctor of Philosophy

in

Chemical Technology

In the

Department of Chemical Engineering

Faculty of Engineering, Built Environment and Information Technology

University of Pretoria

Pretoria

Supervisors: Prof Ndeke Musee and Prof Walter W. Focke

November 2020

DECLARATION BY CANDIDATE

I hereby declare that the thesis submitted for the degree PhD: Chemical Technology, at the university of Pretoria, is my original work and has not been previously submitted to any other institution of higher education. In addition, I declare that all sources cited or quoted in this thesis are indicated and acknowledged by means of a comprehensive list of references.

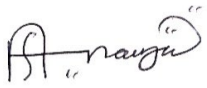

Aston Frankline Nanja

18/11/2020

Date

© University of Pretoria

DEDICATION

Dedicated to

My father (Delano. F. Nanja), Batra. H. Mainza, Winston Nanja and Moses. A. Nanja

© University of Pretoria

ACKNOWLEDGEMENTS

I am grateful to my supervisors, Prof Ndeke Musee and Prof Walter W Focke for their assistance, guidance and support during the course of this work. In addition, I would also like to thank my supervisors for the mentorship that they have given me during the time we have worked together.

I would like to acknowledge the Copperbelt University (CBU), Water Research Commission (WRC) and the University of Pretoria for their financial support which was so critical in accomplishing this work.

I acknowledge and thank the team at the Laboratory for Microscopy and Microanalysis at University of Pretoria for assistance with microscopy sample analysis. I extend my gratitude to the Botswana International University of Science and Technology (BIUST) for PXRD analysis. I am grateful to Prof Philiswa Nomgongo at the University of Johannesburg for her assistance with ICP-MS analysis.

I am grateful to my lab Colleagues Samuel Keeng Leareng, Dr Ntombi Mahaye, Mpho Makofane, Ernst Bekker and Ntsikelelo Yalezo, for their support. I would also like to express my gratitude to Batra. H. Mainza, Winston Nanja, Moses. A. Nanja and my father, Delano. F. Nanja for their encouragement, support, motivation and endurance with my absence for such a long period during the years of this study.

Finally, I give all the glory to God the Almighty for the blessings and grace that He has abundantly bestowed on me during the course of this study.

© University of Pretoria

LIST OF PAPERS AND CONFERENCES

The publications in peer-reviewed journals and conference presentations from this work are as follows:

Journal articles

Nanja, A. F., Focke, W.W., Musee, N., 2020. Aggregation and dissolution of aluminium oxide and copper nanoparticles in natural aqueous matrixes. SN Applied Sciences, **2**:1164.

Nanja, A. F., Focke, W.W., Musee, N., 2020. Binary interactions of aluminium oxide and copper oxide nanoparticles in freshwater systems (In progress)

Technical Report Chapters

Nanja, A.F., Focke, W.W., Musee, N., 2019. Aggregation and dissolution of singles and binary mixtures of metal oxide nanoparticles and triclosan in freshwater systems (WRC, K5 2509 Report; Vol. I. Chapter 6).

List of Conferences presentations

Musee, N., Leareng, S. K., Mahaye, N., **Nanja, A. F.,** Bekker, E. H., Yalezo, N., 2018. Trends on environmental transformations and effects of nanomaterials mixtures in aquatic systems: an overview. In: 6th Nanosafe International Conference: Health and safety issues related to nanomaterials for a socially responsible approach, Minatec, Grenoble, France, 5th – 9th November 2018.

Nanja, A. F., Focke, W.W., Musee, N., 2018. Aggregation of binary mixtures of aluminium oxide and copper oxide engineered nanoparticles in aqueous systems was accepted for international conference. NanoSafe 2018 - 5-9 November 2018 – MINATEC, Grenoble, France (Oral presentation).

Nanja A. F., Focke, W.W., Musee, N., 2020. Aggregation and dissolution of binary mixtures of aluminium oxide and copper oxide engineered nanoparticles in aqueous systems: 8th International conference on Nanoscience and Nanotechnology, NanoAfrica 2020, Enabling the Commercialization of Nanotechnological Innovation, Birchwood Hotel and OR Tambo Conference Centre, Johannesburg, South Africa, 18th–20th April 2020. (Accepted: Oral presentation).

© University of Pretoria

SYNOPSIS

Widespread use of engineered nanoparticles (ENPs) in consumer products and industrial applications has increased rapidly in recent years. Among the commonly used metal oxide ENPs are aluminium oxide (nAl_2O_3) and copper oxide nanoparticles (nCuO). These ENPs are commonly applied in consumer products such as personal care products (PCPs), and therefore are likely to co-exist in the aquatic systems. Hence, it is critical to consider the fate and transformation of ENPs and other pollutants as mixtures in the aquatic systems. The influence of water chemistry parameters such as ionic strength (IS), pH and natural organic matter (NOM) in synthetic and natural water on the fate of ENPs were investigated. The transformation processes considered, were aggregation and dissolution. The interplay of these processes may have diverse pollutant implications for the aquatic organisms.

To date, numerous studies have reported on the fate and transformation of individual ENPs in aqueous media. However, typically high exposure dosages were used that are unlikely to be found in the natural aquatic environments. In addition, only a few studies have considered mixtures of ENPs with organic pollutants such as triclosan (TCS). To address this knowledge gap, the fate and transformation of individual, binary and ternary mixtures of nAl_2O_3, nCuO, and TCS were investigated in deionised water (DIW) and natural river water. The latter was sourced from the Elands river (ER) and Bloubank river (BR) both in South Africa.

All aggregation and dissolution kinetics were performed at low concentrations of ENPs. This was to reflect the likely situation to be found in the environment. In DIW, humic acid (HA) (a NOM surrogate) showed a concentration-dependent stabilization effect on aggregation for both individual and mixtures of ENPs. High IS induced higher aggregation of ENPs in DIW. Hence, NOM inhibits aggregation of ENPs whereas IS enhances aggregation. The pH inhibits aggregation of ENPs to a lesser extent compared to NOM, but it enhances aggregation around the point of zero charge. Both ENPs were found to be more highly stabilized in river water compared to DIW.

Broadly speaking, ENPs exhibited concentration-dependent aggregation, it being lower in ER compared to BR. The differences are attributed to variations in water chemistry, e.g. NOM and the presence of electrolytes. Dissolution of ENPs was higher in ER than in BR water, and higher at lower concentrations of ENPs. Dissolution of nCuO was enhanced in the presence of nAl_2O_3. Binary mixtures of ENPs had higher tendency to aggregate compared to the individual

© University of Pretoria

components. Combinations of nCuO or nAl_2O_3 with TCS were less likely to aggregate in river water. This implies that the TCS acted as a stabiliser for the nanoparticles. However, this stabilisation effect was compromised when both ENPs were present.

Since the ENPs do form agglomerates, they may undergo sedimentation. Consequently, this could lead to interaction with benthic organisms. However, if they are stabilized in natural waters, they might interact with pelagic organisms. Both cases imply the possibility of inducing deleterious consequences.

The most important finding of the present study is that the behaviour of ENPs in water is very complicated. In DIW, HA strongly inhibits aggregation of ENPs whereas IS promotes their aggregation. However, in freshwater systems the aggregation of ENPs is uniquely influenced by source-specific water chemistry factors that counteract with each other. This makes it difficult to predict the fate and transformation of ENPs in natural aquatic systems. Hence, it may not be possible to generalize on ENPs transformation outcomes, even of the same ENPs type, in different water matrixes.

Keywords: aggregation kinetics, Al_2O_3 nanoparticles, binary mixture, CuO nanoparticles, dissolution, monovalent electrolyte, river water, ternary mixture.

© University of Pretoria

TABLE OF CONTENTS

© University of Pretoria

© University of Pretoria

© University of Pretoria

© University of Pretoria

LIST OF FIGURES

© University of Pretoria

© University of Pretoria

© University of Pretoria

LIST OF TABLES

© University of Pretoria

LIST OF ABBREVIATIONS AND ACRONYMS

BET	Braunner Emmett and Teller
BR	Bloubank River
DIW	Deionised water
DLS	Dynamic light scattering
DOC	Dissolved organic carbon
ECs	Emerging contaminants
EDL	Electric double layer
EDS	Energy dispersive spectroscopy
ENMs	Engineered nanomaterials
ENPs	Engineered nanoparticles
ER	Elands River
EU	European Union
FA	Fulvic acid
FTIR	Fourier–transform infrared
HA	Humic acid
HCl	Hydrochloric acid
HDD	Hydrodynamic diameter
ICP-MS	Inductively Coupled Plasma Mass spectrometry
ICP–OES	Inductively Coupled Plasma optical emission spectrometry
IEP	Isoelectric point
IS	Ionic strength
NOM	Natural organic matter
PCPs	personal care products
PECs	Predicted environmental concentrations
PEG	Polyethylene glycol
pH	Potential of hydrogen
PVP	Polyvinylpyrrolidone
PXRD	Powder X-ray diffraction

© University of Pretoria

PZC	Point of zero charge
SD	Standard deviation
SEM	Scanning electron microscope
SP–ICP–MS	Single particle inductively coupled plasma mass spectrometry
SWTPs	Sewage water treatment plants
TCS	Triclosan
TEM	Transmission electron microscope
WWTPs	Wastewater treatment plants
XRD	X-ray diffraction
ZPC	Zero-point charge
ZP (ζ)	Zeta potential

© University of Pretoria

LIST OF SYMBOLS

mg/L	Milligrams per litre
mM	Millimolar
mV	millivolts
nAl_2O_3	Aluminium oxide nanoparticles
NaOH	Sodium hydroxide
nCuO	Copper oxide nanoparticles
ng/L	Nanograms per litre
nm	Nanometer

© University of Pretoria

Chapter 1: Introduction

1.1. Background

Engineered nanoparticles (ENPs) find widespread use in various fields. They are applied in fields such as cosmetics, electronics, agriculture pharmaceuticals and personal care products (PCPs) due to their novel properties such as magnetic, electrical, antibacterial etc, which are not observed in their bulk counterparts (Chen et al., 2003b; Li et al., 2012; Matsoukas et al., 2015; Piccinno et al., 2012). The widespread use of ENPs has led to their release into various natural environmental compartments via intentional via unintentional routes as detailed in Figure 1.1. Their release in the aquatic environment has become an environmental concern, where their increasing presence has been indicated by both field measurements (Donovan et al., 2016; Johnson et al., 2011) and modelling based on predicted environment concentrations (PECs) (Boxall et al., 2007b; Keller and Lazareva, 2013; Mueller and Nowack, 2008). In aquatic systems, ENPs can interact with biological lifeforms, and in turn, induce various toxic effects to individual cells (Ivask et al., 2014; Wilke et al., 2016), whole organisms (Manusadžianas et al., 2012; Pakrashi et al., 2013; Pakrashi et al., 2012; Sadiq et al., 2011; Wang et al., 2011; Ye et al., 2017; Ye et al., 2018b), organs (Heinlaan et al., 2011; Thit et al., 2017; Zhu et al., 2009), and fish (Abdel-Khalek et al., 2015; Benavides et al., 2016; Vidya and Chitra, 2017).

The observed toxic effects depend on exposure linked to the nature of the transformed ENPs released into the aquatic systems (Lowry et al., 2012; Lv et al., 2014; Omar et al., 2014). In these, ENPs undergo numerous transformation processes including the physical and chemical processes summarised in Figure 1.1. These processes are driven by the influence of the inherent physicochemical properties of ENPs (e.g. size, shape, surface chemistry, etc.) (Fabrega et al., 2011; Lowry et al., 2012; Wang et al., 2016). The chemical transformation processes include effects arising from as pH, ionic strength (IS), the nature of natural organic matter (NOM) present, etc. (Conway et al., 2015; Odzak et al., 2014; Peng et al., 2017a; Sousa and Teixeira, 2013; Yang et al., 2009; Ye et al., 2018a; Zheng et al., 2011). The transformation of ENPs may lead to alteration of their behaviour, and ultimately the observed effects on biological lifeforms (Musee, 2011a). The key transformation processes of ENPs include; dissolution, adsorption, complexation, aggregation, and dispersion (Baalousha, 2009; Hotze et al., 2010; Lowry et al., 2012; Misra et al., 2012; Wang et al., 2016). These processes control the fate, behaviour,

© University of Pretoria

bioavailability and toxic effects of ENPs (Amde et al., 2017; Thwala et al., 2016; Thwala et al., 2013).

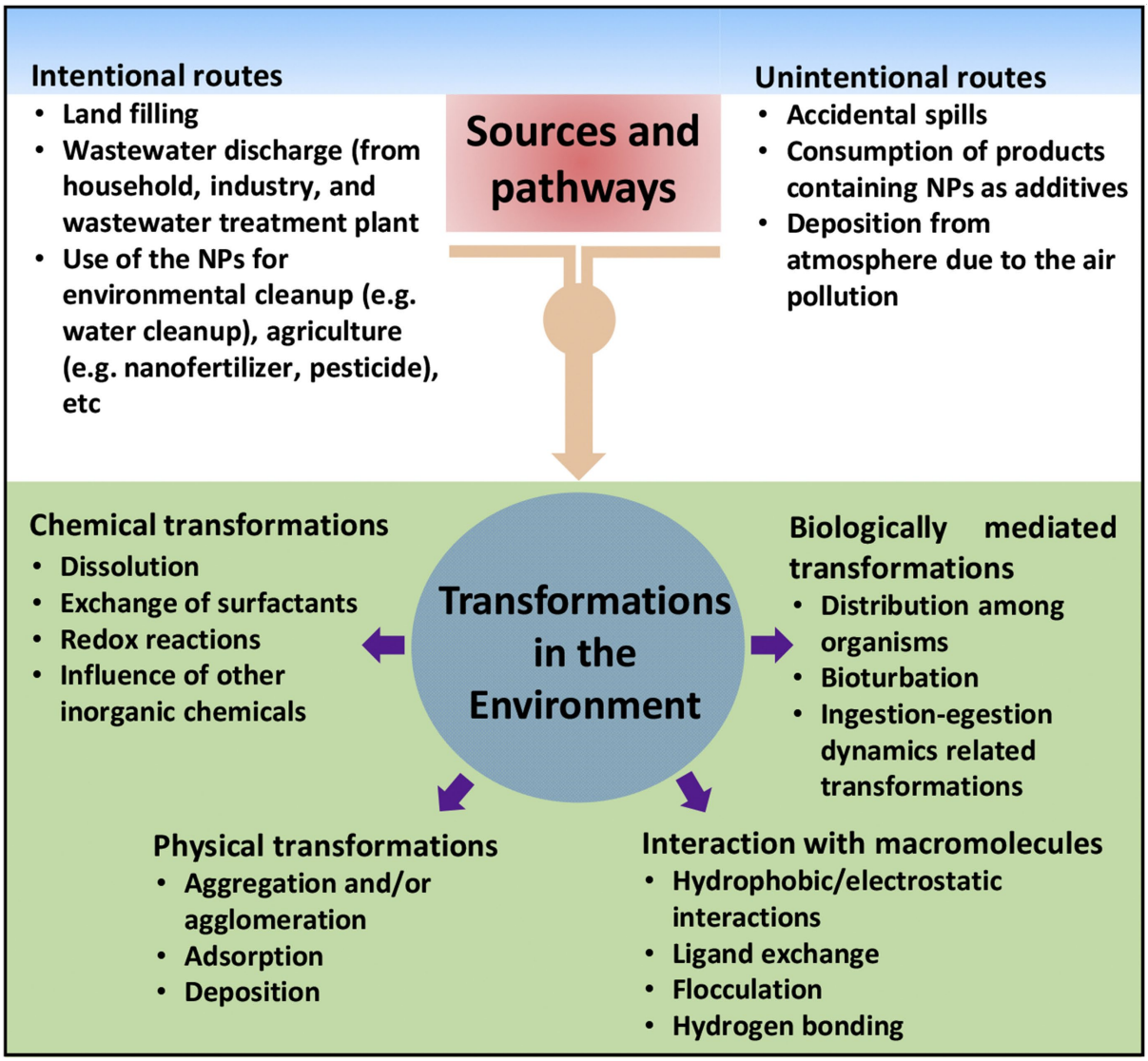

Figure 1.1: Sources, introduction routes, and summary of the transformations that ENPs experience in the environment. (source: Amde et al. 2017; Reproduced with permission from Elsevier)

The adsorption of NOM onto surfaces of ENPs may modify their surface properties. For example, adsorption of NOM may impart a net negative surface charge. This increases the interparticle repulsions of ENPs, thus rendering them highly stabilized via electrostatic repulsion mechanisms (Chen et al., 2012; Ghosh et al., 2008; Lv et al., 2014; Mui et al., 2016; Omar et al., 2014; Wang et al., 2014). The exposure media pH can influence the aggregation and disaggregation by either increasing or decreasing the ζ-potential of ENPs (Baalousha,

© University of Pretoria

2009; Odzak et al., 2014). The IS, type and valence of the electrolytes (monovalent or divalent) influence the behaviour of ENPs by compressing the electric double layer (EDL). This leads to a reduction in ζ-potential promoting aggregation because of reduced inter-particle repulsion (Peng et al., 2017a; Son et al., 2015).

Numerous studies have investigated the fate and behaviour of ENPs under various environmental media including synthetic aqueous media (Godymchuk et al., 2015; Odzak et al., 2014; Peng et al., 2017a; Romanello and De Cortalezzi, 2013), freshwater (Adam et al., 2016; Conway et al., 2015; Van Koetsem et al., 2015) and wastewater systems (Brunetti et al., 2015; Chaúque et al., 2014; Musee et al., 2014). However, the studies largely focused on single ENPs. Yet, in actual environmental systems, ENPs co-exist as mixtures, either with other ENPs or other pollutants ubiquitous in the environment. As a result, data for individual ENPs are inadequate to predict ENPs fate and behaviour where they exist as mixtures. The products of ENPs interactions may be unique and different from the constitute individual ENPs, therefore, they would have different fate and behaviour and may exhibit different toxicity on aquatic organisms.

1.2. Rationale for Study

The 21st century has been characterised by production and application of chemicals of environmental concern. These chemicals are generally referred to as emerging contaminants (ECs). ECs include a diverse collection of thousands of chemical substances that are largely outside the scope of monitoring and regulation. These ECs may be broadly categorised as micro-pollutants (MPOs) and engineered nanomaterials (ENMs) (nano-sized). MPOs encompass a wide range of chemical substances most of which are largely outside the scope of monitoring and regulation (Amoatey and Baawain, 2019; Naidu et al., 2016). Dominant classes of ECs encompass numerous classes of compounds including pesticides, microplastics, pharmaceuticals, personal care products (PCPs), hormones, endocrine disrupters, antibiotics surfactants and their degradation products etc. (Naidu et al., 2016; Yan et al., 2009). The pharmaceuticals and PCPs include thousands of chemical substances used by humans for personal health or cosmetic reasons and in animal husbandry (Liu et al., 2013; Naidu et al., 2016; Yang et al., 2017). Different types of ENMs include: metal, metal oxide, carbonaceous, fullerenes and quantum dots with metal and metal oxides being the most commonly used (Fabrega et al., 2011). These ECs and their metabolites enter into the aquatic system via various

© University of Pretoria

routes including land filling, accidental spills, discharge from sewage water treatment plants (SWTPs), runoff water from the surface, leaching from soil, surface water drainage after application of manure on the land as summarised in Figure 1.1 (Amde et al., 2017; Derksen et al., 2004).

Among various types of ENPs, aluminium oxide nanoparticles (nAl_2O_3) and copper oxide nanoparticles (nCuO) have received a great deal of attention. This is because of their large production volumes, widespread applications including in PCPs due to novel properties which include: quantum effects, unique antimicrobial, electronic, optical, and structural strength enhancement which not observed in their macroscopic counterparts (Lee et al., 2010; Singh et al., 2011). The nAl_2O_3 are widely used, for example in commercial products such as high-performance ceramics, cosmetic fillers, packing materials, polishing materials, semiconductor materials, deodorants, paints, composite materials, heat transfer fluids and resins, wear-resistant reinforcement and advanced waterproof materials, catalyst, and catalyst carriers (Defriend et al., 2003; Khanna, 2008; Landry et al., 2008; Lewis et al., 2010; Wong and Kurma, 2008). Whereas nCuO find application in semiconductors, cosmetics, textiles, heat transfer fluids and catalysts, e.g. in rocket propellant (Applerot et al., 2012; Das et al., 2013; Le Van et al., 2016; Zhao et al., 2013). The increased use and production led to their release into various environmental compartments including aquatic systems. However, not all these applications lead to release into the natural environment as the ENPs are firmly embedded into the product matrix e.g. in semiconductors where ENPs are supported in a solid matrix. However, cosmetics, paints, catalysts, catalyst carriers, and textiles, among others, readily release ENPs into various natural environmental compartments. Estimates suggest that 35% of globally-produced ENPs are released into various aquatic systems (Sun et al., 2016).

Among chemical compounds used in PCPs, triclosan (TCS) was selected in this study. It was selected because it is widely used and released in large quantities into the environment and has a distinctive risk profile (Brausch and Rand, 2011). Because of numerous ECs in the environment, organisms are concurrently exposed to a cocktail mixture of pollutants as opposed to individual pollutants. In the aquatic environment, ENPs will co-exist with other contaminants, e.g. TCS. This in turn, can result in transformations that lead to unique effects on aquatic organisms. Both ENPs and TCS are toxic to aquatic organisms. For example, nCuO has negative effects on the survival and growth of organisms (Galhardi et al., 2004; Nations et al., 2011; Zietz et al., 2003). The nAl_2O_3 is toxic towards bacteria, algae, nematodes and other

© University of Pretoria

species in the environment (Fajardo et al., 2014; Ji et al., 2011; Wang et al., 2009). TCS is toxic to a range of organisms in aquatic systems, including fish (Brausch and Rand, 2011; Gardner et al., 2012).

The risk assessment of chemicals, for regulatory purposes, relies on the assessment of individual chemicals and seldom considers exposure to multiple chemicals (Bopp et al., 2018; Kienzler et al., 2016). ECs have raised toxicological concerns especially with regard to the risk profile for individual chemicals. However, their potential interactions as mixtures of ECs or other pollutants have not been critically considered (Batley et al., 2012). Toxicological studies of organic-organic (Laetz et al., 2008; Pape-Lindstrom and Lydy, 1997), metal-metal (Chu and Chow, 2002; Preston et al., 2000), organic-inorganic contaminant mixtures (Gauthier et al., 2014; Wang et al., 2009) and EMNs-EMNs (Tong et al., 2015), were found to exert toxic effects that markedly differ from those of the constituent individual contaminants. As such, even though the toxic effects of individual contaminants may be well established, the environmental risks posed by contaminant mixtures may not be predicted based on such data. Ecosystems are exposed to complex mixtures of chemicals ubiquitous in the environment whose effects may be different from the effects of individual components. For example, an environmentally realistic mixture of 25 pesticides was observed to reduce the reproduction of freshwater alga *Scenedesmus vacuolatus* by 46% whereas the individual components on their own had close to zero effect (Junghans et al., 2006). Mixtures have been reported to exhibit additive toxicity at low, environmentally relevant concentrations. However, synergistic effects at higher concentration were observed (Bosgra et al., 2009). ENMs have been observed to be carriers of other environmental pollutants through various mechanisms such as adsorption (Trojan horse effects) (Baun et al., 2008). Lack of comprehensive data on the fate and transformation of pollutants mixtures impedes the ability to draw systematic conclusions on how to manage them to protect the environment. Therefore, for the regulatory purposes on environmental monitoring, understanding the behaviour of mixtures of chemical pollutants is critical.

The effects of ECs to aquatic organisms are controlled by their fate and behaviour (Tong et al., 2015). The transformation processes detailed in subsection 1.1 influence the fate, behaviour and bioavailability of ECs in the aquatic environment. The transformation of nAl_2O_3 (Godymchuk et al., 2015; Mui et al., 2016; Pakrashi et al., 2012) and nCuO (Conway et al., 2015; Heinlaan et al., 2016) has been studied in deionised water (DIW) and freshwater systems.

© University of Pretoria

However, studies based on the transformation of individual ENPs may not be adequate to predict the fate, behaviour and potential impact of mixtures of ENPs and other co-existing contaminants in the aquatic systems. Hence, recently an increasing focus on the implications for cocktail mixtures of ENPs and other contaminants concurrently from diverse sources has gained traction. Several studies have reported on the transformation joint effects of ENPs mixtures (Huynh et al., 2014; Jun et al., 2013; Miranda et al., 2016; Tong et al., 2015; Wilke et al., 2016) and ENPs-organic mixtures (Chen et al., 2018; Lopez-Doval et al., 2019) in aqueous media. The current study is based on the fate and behaviour of binary and ternary mixtures of nAl_2O_3, nCuO and TCS in freshwater systems. To the best of our knowledge, no study has been reported on these aspects. Therefore, the current study is significant in reducing this knowledge gap.

1.3. Study approach and aims

1.3.1. Hypothesis

It is hypothesized that the transformation of ENPs in aqueous media is not only dependent on exposure media chemistry parameters (e.g., pH, IS, NOM, etc.,), but also on other contaminants in macroscale and nanoscale dimensions. To test this hypothesis, aggregation and dissolution of two metal oxides ENPs ($nAl_2O_3$and nCuO) and organic contaminant TCS in synthetic and natural exposure media systems were investigated.

1.3.2. Aims

The aim of the current study was to investigate the aggregation and dissolution of individual, binary and ternary mixtures of ENPs (nAl_2O_3 and nCuO) and organic pollutant TCS in freshwater systems. The influence of water chemistry on dissolution and aggregation of individual and mixtures of ENPs and TCS in river water systems were studied.

1.3.3. Objectives

The specific objectives of the project were to;

i. Study the transformation of nCuO and nAl_2O_3 in synthetic and river water systems.
ii. Assess the interactions of binary mixtures of nCuO and nAl_2O_3 in synthetic and river water systems

© University of Pretoria

iii. Investigate the influence of TCS on transformation of ENPs as binary and ternary mixtures in river water systems

1.4. Outline of Thesis

The thesis is outlined in five chapters. Each of the chapters is detailed below.

Chapter 1 provides the background of the research, rationale of the project, aims specific objectives and the layout for the thesis.

Chapter 2 Presents a comprehensive literature review of the relevant studies on the fate and transformations of individual and mixtures of ENPs in various aquatic systems. It provides detailed information of the analytical techniques used in the various investigations involving transformation of ENPs in aquatic systems.

Chapter 3 provides information on the materials, experimental procedures, methods, and characterisation techniques employed to achieve the objectives and aims of this study.

Chapter 4 provides findings and comprehensive discussions of the work herein. The influence of water chemistry on the transformation of ENPs and plausible effects of their transformation products to aquatic organisms are discussed.

Chapter 5 presents a summary of findings in the work. The overall conclusions and recommendations for future work on the interactions of ENPs and TCS in natural aquatic systems are presented.

© University of Pretoria

Chapter 2: Literature review

2.1. Nanotechnology

Nanotechnology is defined as the study, imaging, measuring, modelling, or manipulation of matter with dimensions in the range 1–100 nm at least in one dimension where unique phenomena enable novel applications. However, in certain cases the 100 nm limit does not apply as EMNs are defined based on the nanometric-scale and materials possessing characteristics different from their bulk counter parts (Maynard, 2011). The term `nanotechnology` was coined by Taniguchi et al. (1974) who described it as the precision reduction of bulk materials to nanometer range in the film passivation of semiconductors. As such, nanotechnology was viewed to encompass the processing, separation, consolidation, and deformation of materials by one atom or one molecule (Hulla et al., 2015).

2.1.1. Engineered nanoparticles

An ENP may be defined as any intentionally produced particle that has a characteristic dimension ranging from 1 to 100 nm and has properties that are not observed in non-nanoscale particles with the same chemical composition (Auffan et al., 2009). However, other definitions suggest this definition is limiting. One such definition considers an upper limit of 1000 nm and defines ENPs as, any natural, incidental, or manufactured materials in an unbound state, aggregate, or agglomerate where 50% or more of the total number of particles in a given material being in size range 1 to 1000 nm, across all 3 dimensions (Jovanović, 2015). However, among the proposed definitions for ENPs, the most widely accepted definition is by the European Union (EU) Commission which defines ENPs as any natural, incidental or manufactured materials containing particles in an unbound state or as an aggregate or agglomerate and where at least 50 % of the particles in the number distribution, one or more external dimensions are in the size range 1–100 nm (Commission, 2011). In the current study, the definition by EU is upheld. This decision is based on the rationale that ENPs with size range below 30 nm are characterized by an excess of energy at the surface. Hence, these ENPs are thermodynamically unstable which forms the basis of their novelty and yet particles above 30 nm share the same properties as their bulk counter parts (Auffan et al., 2009; Jolivet et al., 2004). The high surface area of ENPs has a great effect on their properties. For example, the

© University of Pretoria

average surface energy of bulk materials is *ca* 0.56 J/g while that of ENPs at nanoscale *ca.* 1 nm is approximately 560 J/g which gives an increase by a factor of one thousand in surface energy (Auffan et al., 2010). Novel properties of ENPs such as surface energy and reactivity make it impossible to apply physicochemical, thermodynamic and toxicological knowledge of materials at micron scale to materials at nanoscale (Auffan et al., 2010). Metal, metal oxide, carbonaceous, fullerenes and quantum dots are among different types of ENMs. Metals and metal oxides are the ENPs most commonly used in commercial and consumer products (Vance et al., 2015).

2.1.2. Production of ENPs

The production of metal oxide based ENPs e.g. TiO_2, ZnO, CeO_2, Al_2O_3, CuO and many more has increased in recent years (Gao et al., 2013; Hou et al., 2017; Kunhikrishnan et al., 2015). For example, in 2014 the worldwide production volume of nCuO was 570 tons and it was projected to increase to 1600 tons by 2025 (Hou et al., 2017); whereas that of nAl_2O_3 was above 1200 tons in China alone (Gao et al., 2013). Currently, it is challenging to predict the exact production volumes of ENPs. This is because most companies involved in their production maintain a high level of confidentiality on the data concerning quantities they produce (Hendren et al., 2011). This lack of accurate data on the production volumes of ENPs has negatively affected the prediction of their environmental concentrations and the subsequent fate and effects on aquatic organisms.

2.1.3. Synthesis and characterisation of ENPs

Nature generates natural nanoparticles through natural processes such as terrestrial dust storms, erosion, forest fires, volcanic eruptions and other geochemical processes (Cupaioli et al., 2014; Lead and Wilkinson, 2007; Nowack and Bucheli, 2007). Advances in technology has led to the manufacturing of ENPs involving various techniques that can be broadly categorised as top-down, bottom-up and hybrid techniques depending on the type of approach (Meyer et al., 2009). These methods include synthesis, purification, characterisation and functionalization of ENPs which determines the intrinsic physicochemical properties that affect the novel properties of ENPs. Top-down technique entails specialised breaking, attrition and milling of bulk materials to nanoscale level (Guo, 2005; Majumder et al., 2007). However, the ENPs produced are heterogeneous, irregular and structurally defective with non-uniform size. Bottom-up technique involves crafting structures atom by atom or molecule by molecule through covalent

© University of Pretoria

or supramolecular interactions (Ochekpe et al., 2009; Teo and Sun, 2006). Despite the random movements of atoms which poses a challenge, bottom-up remains the preferred approach for nanotechnology because it produces homogeneous particles with controlled growth and surface properties (Mansoori, 2002; Ochekpe et al., 2009). ENPs may be functionalized using various types of surface coatings such as citrate, polyethylene glycol (PEG), polyvinylpyrrolidone (PVP), and other types of coatings depending on intended applications (Angel et al., 2013). Functionalization leads to modification of surface chemistry and characteristics of ENPs, which in turn influences their likely transformation in various environmental systems.

Characterization of ENPs is critical in evaluating their suitability for specific application. The specific characteristics of ENPs dictates their transformation, fate, bioavailability, and toxicity in various environmental compartments. Various techniques based on the principles of microscopy, light scattering, photography and imaging, transmitted light and individual particle sensors are now available for characterisation of ENPs. Some of the instruments used for determining various parameters include: Zetasizer (surface charge and size distribution), Scanning electron microscopy (SEM) (particle size, size distribution, morphology and elemental composition), Transmission electron microscopy (TEM) (particle size, size distribution, morphology and elemental composition), Powder X-ray diffraction (PRXD) (crystallite size and crystallinity), Inductively Coupled Plasma Mass (ICP-MS) (mass concentration and elemental composition), Inductively-coupled plasma optical emission spectrometry (ICP–OES) (mass concentration and elemental composition), Single particle inductively coupled plasma mass spectrometry (SP-ICP-MS) (elemental composition, particle size, particle number and mass concentration), Ultra-Violet/ Visible Spectrophotometry (UV-Vis Spec) (composition change), Fourier–transform infrared spectroscopy (FTIR) (surface functionality), etc. In the current study, ICP-MS, PXRD, SEM, TEM and Zetasizer were used to characterize the ENPs. Because of its great sensitivity and low detection limit, ICP–MS was used in this study. The various analytical techniques used are summarised in Table 2.1.

© University of Pretoria

Table 2.1: Analytical techniques widely used for the characterisation of ENPs

Instrument	Measured parameters	Merits	Demerits	References
Zetasizer	• Particle size distribution • Surface charge	• Can analyse a wide range of particle size (4 nm to 6 µm) • Measures both ζ-potential and HDD.	• Requires suspension of the sample in a liquid and it uses DLS technique which focusses on larger particles especially the aggregates in the sample. • Does not provide the size and shape of individual particles • Not able to qualitatively distinguish components of mixture	(Hornyak et al., 2008; Peters et al., 2011; Zhang et al., 2012)
SEM	• Particle shape size and size distribution • Particle morphology • Elemental composition (via EDS) • Agglomeration state	• Surface details of nanoparticles with a wide range of nano-dimensions upto as low as 10 nm • Morphology, size and shape of the nanoparticles can be determined	• Fails to display a true size distribution or population size of the sample, as it has to be done in solid phase • ENPs must first be coated with a conductive material such as carbon or gold before analysis • Time consuming, laborious and costly • Lower resolution compared to TEM	(Hornyak et al., 2008; Mavrocordatos et al., 2004; Peters et al., 2011; Tiede et al., 2008)
TEM	• Particle size, morphology and shape	• It is a single particle technique, which detects in the regions of 5nm to 500µm • Identifies the topology and morphology of the ENPs	• TEM sample must be an ultra-thin layer so that the electron beam can penetrate through the material to give a comprehensive image	(Cao, 2004; Mavrocordatos et al., 2004; Peters et al., 2011)

© University of Pretoria

	• Elemental composition (via EDS) • Particle size distribution • Aggregation state	• Ability to determine particle size from the imaging of the ENPs mixtures observed • Higher resolution compared to SEM		
UV-Vis Spectroscopy	• Compositional change in ENPs, and/or organic compounds in presence of other environmental factors	• Magnitude, peak wavelength and bandwidth of the plasmon resonance are dependent upon the size and shape of the resulting ENPs found in a solvent medium. • Cost effective method to determine change in nanomaterial mixtures when exposed with other chemicals or NOMs	• No topological, or morphological imagery can be observed	(Hornyak et al., 2008)
PXRD	• Particle size • Particle size distribution • Structure/crystallinity	• Crystalline nanoparticle bulk material can be compared to other powder patterns so that the unique fingerprinting of the sample can be used to determine the qualitative nanoparticle material. • Estimating the average size of a single-crystal nanoparticles or crystallites found in nanocrystalline bulk materials by means of applying the Sherrer equation.	• Nanoparticles greater than 10 nm are easily analysed using XRD, however smaller nanoparticles are often not crystalline and therefore XRD is not idea for their analysis • The sample must be in the solid phase, therefore limiting the application of the technique	(Hornyak et al., 2008; Sharma et al., 2012; Uvarov and Popov, 2013)
ICP–MS	• Total mass concentration	• It is very sensitive technique with low detection limit upto ng/L	• Sample preparation procedure is laborious • It is very costly	(Laborda et al., 2016)

© University of Pretoria

	• Elemental composition	• Multiple analysis of sample composition can be achieved simultaneously		
ICP–OES	• Elemental composition • Mass concentration	• Its detection limit is as low as ppb levels • It is less costly compared to ICP–MS	• It is less sensitive than ICP–MS. Therefore, it cannot be used to determine very low concentration.	(Laborda et al., 2016)
SP-ICP-MS	• Elemental composition • Particle size, particle distribution • Particle number concentration and mass concentration	• Utilised for obtaining additional qualitative elemental information about particle or dissolved forms of nanoparticles present in a sample • Provides mass of the nanoparticle, i.e. size of the nanomaterial provided the morphology, size and density is known • Quantitative information may also be provided about either the particle number concentration, and/or the concentration of the dissolved materials present in the medium with high sensitivity at with detection limit upto ng/L	• In the case of the nanoparticles aggregating in the medium, the SP-ICP-MS data obtained is only able to provide shape and size of the combined mixture • Cannot provide information about particle morphology	(Hornyak et al., 2008; Navratilova et al., 2015)
FTIR and Raman Spectroscopy	• Surface functionality	• FTIR is useful for qualitative information about nanomaterials that are modified or capped, provided that the photon absorbed from the IR radiation by the molecule excites the molecule such that a vibrational energy is given off at a frequency in the IR region	• Only gives vibrational and rotational information, on single atom to atom interaction. The complete structure is not able to be observed.	(Hornyak et al., 2008; Jiang et al., 2017)

© University of Pretoria

	• identification of hydrogen bonds and π–π interactions between ENPs and organic pollutants

Abbreviations: DLS: Dynamic Light Scattering, , FTIR: Fourier Transformer Infra-red, HDD: Hydrodynamic diameter, ICP-MS: Inductively Coupled Plasma Mass Spectrometry, ICP–OES: inductively-coupled plasma optical emission spectrometry, SEM: Scanning Electron Microscope, SP-ICP-MS: Single Particle Inductively Coupled Plasma Mass Spectrometry, TEM: Transmission Electron Microscope, UV-Vis Spec: Ultra-Violet/ Visible Spectrophotometry, PXRD: Powder X-ray diffraction

© University of Pretoria

2.1.4. Application of ENPs

The application of ENPs in commercial and industrial products has increased in recent years because of their novel properties which leads to improved product quality (Hansen et al., 2016; Zhang et al., 2015). The production of metal oxide ENPs was estimated to reach 5 x 10^5 tons by 2020 (Robichaud et al., 2009). Among metal oxide ENPs, nAl_2O_3 and nCuO have found application in various commercial and industrial products as summarised in Table 2.2. However, the release of ENPs from a given product category into the environment is dependent on how they are embedded into the holding matrixes (Froggett et al., 2014; Musee, 2011b) and product use (Hansen et al., 2016; Tiede et al., 2015; Wigger et al., 2015). For instance, cosmetics, paints, catalysts, catalyst carriers, and textiles, are likely to readily release ENPs into the aquatic systems as the final sink.

Table 2.2: Applications of nAl_2O_3 and nCuO in different product categories

ENPs	Application	Refs.
nAl_2O_3	Personal care products, catalysts, ceramics	(Zhang et al., 2015)
	printers and toners	(Pirela et al., 2014)
	Fillers and coupling agents in polymers	(Landry et al., 2008)
	Heat transfer fluids	(Wong and Kurma, 2008)
	Ceramics, ultrafiltration membranes	(Defriend et al., 2003)
nCuO	Magnetic storage, solar energy transformation, batteries, catalysis, electronics and sensors	(Applerot et al., 2012)
	Coating, catalysts, textiles	(Anita et al., 2011)
	Catalyst, superconductors, ceramics	(Singh et al., 2016)
	Electronic chips, heat transfer nanofluids, lithium batteries, gas sensors, semiconductors and solar cells	(Ahamed et al., 2015)

2.2. Fate processes and influencing factors

The fate, transformation and bioavailability of ENPs in the environment depends on the physical and chemical transformations that they undergo: Aggregation, dissolution, adsorption,

© University of Pretoria

complexation and dispersion may increases or decreases their toxicity (Hotze et al., 2010; Lowry et al., 2012; Misra et al., 2012; Wang et al., 2016). These physical and chemical transformations are influenced by combined effects of abiotic factors such as pH, IS, and NOM which affects the size and the surface charge of ENPs. The surface charge influences their interactions through repulsive and attractive forces associated with their charge and charges of other components ubiquitous in the environment such as NOM. Processes and abiotic factors which control the fate, transformation and bioavailability of ENPs are discussed in the following sections.

2.2.1. Adsorption

Adsorption is a process by which substances attach to the surface of solids by means of Van der Waals attractions (physisorption), electrostatic interactions (ion exchange), or chemical bonding (chemisorption) (Dąbrowski, 2001; Pan and Xing, 2008; Rabe et al., 2011). In physisorption, the adsorbate is weakly and non-specifically bound to the surface of ENPs. Ion exchange and chemisorption involve either a charged interaction or chemical bonding to specific available surface sites. Adsorption of substances (e.g. NOM) may have two opposing effects on the stabilization of the particles. For example, if the surface coverage is partial, then the dispersion may be destabilized, and aggregation occurs via a bridging effect between the free surface and the non-adsorbed functional groups of the adsorbate. This usually observed in the case of large molecules such as polymers or humic substances. However, if the surfaces of the ENPs are fully covered, the dispersion may be stabilized via electrostatic and steric interactions which impede aggregation (Saleh et al., 2010).

Adsorption of NOM imparts negative charges onto the surface of ENPs. Therefore, if ENPs are positively charged (pH < pH_{ZPC}), electrostatic destabilization/stabilization is initiated (process I in Figure 2.1). For negatively charged ENPs (pH > pH_{ZPC}), electrosteric stabilization via ligand exchange mechanism occurs (process II in Figure 2.1). This impedes aggregation of ENPs unless intramolecular or intermolecular bridging occurs that induces flocculation (Philippe and Schaumann, 2014). Hydrophobic interactions between ENPs and NOM leads to enhanced stability of ENPs (process III in Figure 2.1) (Yang et al., 2009). Surfaces of ENPs have a high affinity for various macromolecules which are components of NOM (Auffan et al., 2010). Adsorption of NOM decreases the bioavailability of ENPs. For example, the toxicity of silver nanoparticles (nAg) was greatly reduced by the adsorption of NOM onto nAg (Fabrega

© University of Pretoria

et al., 2009). Organic macromolecules and inorganic ligands adsorb onto ENPs surfaces. Consequently, they alter their surface chemistry and affect their behaviour in the environment and in biological systems. For example, the mobility of ENPs in the environment is greatly promoted by adsorption of polymer coatings onto surfaces of ENPs (Phenrat et al., 2010). In addition, adsorption of NOM has a significant influence on stability of ENPs in freshwater systems.

2.2.2. Dissolution

Dissolution is an energetically favourable interaction between the dispersed phase and the continuous phase leading to a homogeneous phase (Borm et al., 2006; Mwaanga, 2012). Dissolution entails the release of ions by ENPs into an aqueous media. The toxicity of metal ENPs is partially attributed to the metal ions present following dissolution in aqueous media (Leareng et al., 2020; Mashock et al., 2016; Song et al., 2020). Therefore, ENPs dissolution play an important role on the observed toxicity of ENPs because released ions often are attributed to the cellular responses of ENPs (Levard et al., 2012; Raghupathi et al., 2011; Zheng et al., 2011). Various environmental factors (e.g. pH, IS and NOM) and physicochemical properties of ENPs (e.g. surface energy, surface area, morphology, adsorbing species and aggregation status) can affect their dissolution (Auffan et al., 2009; Borm et al., 2006; Lin et al., 2010; Mwaanga, 2012). In addition, size and morphology have a significant influence on dissolution as it is influenced by differences in surface area to mass ratio. Hence smaller ENPs have higher solubility than larger ones (Mudunkotuwa et al., 2011).

Dissolution has been reported to increase with decreasing pH (Baalousha et al., 2008; Li et al., 2013; Odzak et al., 2017; Omar et al., 2014). For example, the solubility of iron oxide ENPs was reported to be 35% and 10% at pH of 2 and 3 respectively, and below detectable concentrations at pH > 4 (Baalousha et al., 2008). The reason for the increased dissolution were likely due to increased interparticle repulsions observed at low pH which leads to low aggregation. However, this would depend on the point of zero charge of the ENPs. IS compresses the EDL which reduces electrostatic repulsion energy leading to increased aggregation. High aggregation leads to low dissolution because of the decrease in surface area available for dissolution (Li et al., 2013). Hence, at high IS low dissolution was observed whereas at low IS, dissolution was high (Odzak et al., 2015; Son et al., 2015; Yung et al., 2015).

© University of Pretoria

The presence of NOM in the exposure media has been reported to enhance the dissolution of ENPs (Jiang et al., 2015; Li et al., 2013; Xiao et al., 2018).

However, it has also been reported that NOM adsorption onto the active sites of ENPs could impede dissolution (Deonarine et al., 2011; Yu et al., 2017). NOM can lead to a shift in thermodynamic equilibrium towards ions by chelation of released ions as the systems may not violate LeChatelier`s principle (Philippe and Schaumann, 2014). NOM may provide a coating which can act as a significant kinetic barrier for the diffusion of released ions from the surface of ENPs. In addition, NOM plausibly impede the diffusion of reagents necessary to enhance dissolution (Philippe and Schaumann, 2014). Therefore, the net effect of NOM on dissolution of ENPs depends on the nature of NOM itself, nature of ENPs and the characteristic chemistry of the exposure media (Auffan et al., 2009; Mudunkotuwa et al., 2011; Mwaanga et al., 2014; Philippe and Schaumann, 2014). The mechanism of how NOM influences dissolution has not been satisfactorily elucidated despite the chelation and/or complexation of free metal ions having been proposed as the underlining mechanism (Majedi et al., 2014; Omar et al., 2014; Wang et al., 2015).

The dissolved ions may recombine to form ENPs or interact with other species forming complexes as shown in process IV of Figure 2.1. In certain cases, during transformation processes, oxide coating and sulfidation occurs after dissolution as summarised in processes V and VI of Figure 2.1, respectively. The amount of total dissolved metal ions in a given system is the sum of the free ions, metal ions in soluble hydroxo-complexes, and metal ions from soluble metal-ligand complexes. Hydrophobic high-molecular weight ligands like major components of HA consisting of abundant hydroxyl, carboxyl, and phenolic groups in high concentration enhance the dissolution of ENPs (Jiang et al., 2015).

To determine the dissolution of ENPs, various laboratory separation and analytical techniques are used. The techniques involve centrifugation and filtration through micron-sized filters such as the 0.22 µm filters to separate the ions from the particulates in solution. However, owing to likely adsorption of released ions onto possible components of the exposure media and complexation effects in turn may affect the quantitative recovery of released ions through filtration. In addition, possible sorption of ions to the filter membranes may also lead to a reduction in detectable ions. The recovered ions are preserved in acidic solution prior to

© University of Pretoria

analysis via various analytical techniques depending on expected ion concentration such as ICP–MS, AAS, ICP–OES as summarised in Table 2.1.

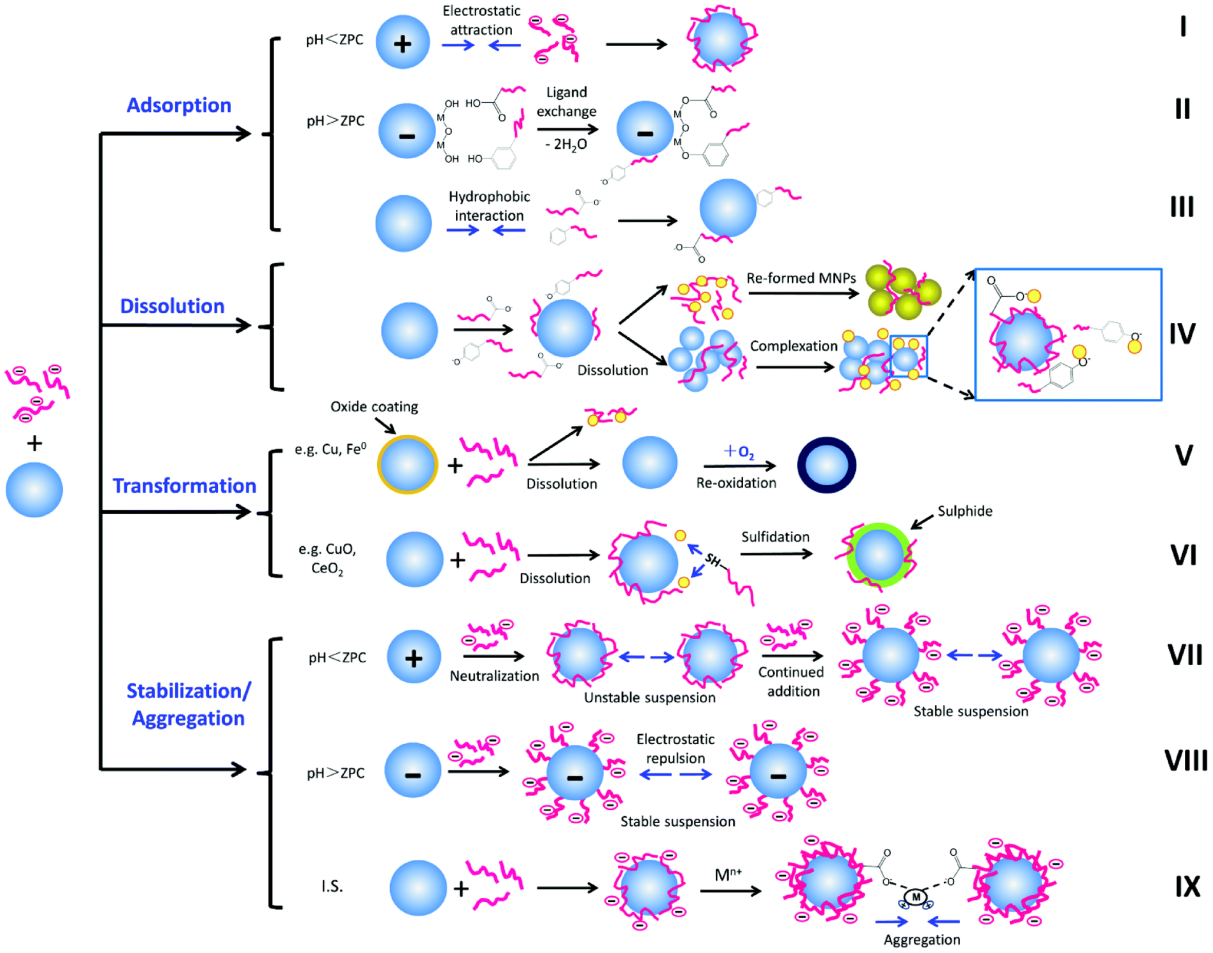

Figure 2.1: Adsorption (processes I–III), dissolution (process IV), transformation (processes V–VI) and stabilization/aggregation (processes VII–IX) behaviours of ENPs in the presence of NOM. (Source: Wang et al 2016: Reproduced with permission from Royal Society of Chemistry)

2.2.3. Aggregation

Aggregation of ENPs may be defined as a process where particles collide and attach with the resultant aggregate strength being dependant on kinetics of the process which is influenced by exposure media chemistry, particle surface chemistry and degree of agitation in the system (Lin et al., 2010; Petosa et al., 2010; Wiesner et al., 2006). The van der Waals and electrostatic attractions govern the formation of clusters of particles (Adamczyk and Weroński, 1999).

© University of Pretoria

Aggregation of ENPs essentially influences their fate, transport, reactivity, mechanical strength, surface energy, solubility, electrical and thermal conductivity, sedimentation bioavailability, and their toxicity (Lowry et al., 2012; Saltiel et al., 2004). There are two types of aggregation, namely homo-aggregation and hetero-aggregation. Homo-aggregation takes place between particles of the same ENPs whereas hetero-aggregation is between ENPs and other types of particles which may be other types of ENPs, or other forms of particles present in the environment. Aggregation leads to a reduction in the surface area to volume ratio which influences the quantum effects (Lowry et al., 2012). The aggregation process and the nature of aggregates formed are governed by collision frequency and attachment efficiency (Amal et al., 1992). Hence, high collision frequency at higher concentration leads to rapid aggregation. Aggregation is a thermodynamically favoured process as formation of aggregates results in reduced overall surface energy of ENPs (Marie et al., 2014; Yung et al., 2015). In addition, the extent of aggregation and deposition are dependent on the surface chemistry of the particles and the porous media as well as the chemistry of the bulk solution (Petosa et al., 2010).

Aggregation of ENPs is largely influenced by abiotic factors: i.e. pH, IS and NOM of the exposure media. The pH of the exposure media affects the surface charge of the ENPs which influences the interparticle repulsion forces, thus affecting the aggregation process. Maximum aggregation is observed around the pH of point of zero charge (pH_{zpc}). At pH_{zpc}, the surface charge of the ENPs is zero whereas far away from pH_{zpc} a stable suspension is observed due to maximum interparticle repulsion as shown in processes VII and VIII in Figure 2.1 (Peng et al., 2017a; Zhou and Keller, 2010). IS, depending on type and concentration of electrolytes, tends to compress the EDL which reduces electrostatic repulsion energy leading to increased aggregation. Furthermore, multivalent cations enhance aggregation via bridging mechanism with NOM components as shown in Process IX in Figure 2.1 (Van Hoecke et al., 2011; Zhou and Keller, 2010). The stabilization effect of NOM on ENPs has two components: The electrostatic component due to negative charges imparted by NOM on the surface of ENPs through adsorption and, the steric component resulting from adsorption of various macromolecules present in NOM. The presence and concentration of NOM influences the aggregation of ENPs by adsorbing onto the surfaces of ENPs providing a surface charge which increases interparticle repulsive energy and initiates steric stabilization (Domingos et al., 2009; Loosli et al., 2014b; Omar et al., 2014; Romanello and De Cortalezzi, 2013). It decreases the probability of homo-aggregation via electrosteric (combination of electrostatic and steric)

© University of Pretoria

repulsions (Diegoli et al., 2008; Quik et al., 2010). The electrostatic stabilization of NOM is due to the interactions of its carboxylic and phenolic functional groups with the surface of ENPs (Arenas-Lago et al., 2019). In addition, biotic factors may also promote aggregation of ENPs through attachment of ENPs to living organisms such as bacteria and algae (Ge et al., 2015; Unrine et al., 2012) and release of biopolymers which may enhance aggregation via bridge formation (Bone et al., 2012; Ferretti et al., 2003; Santschi et al., 1998).

The aggregation of ENPs is controlled by the inter-particle repulsive and attractive energy which are influenced by the electrical double layer (EDL) (Fang et al., 2020; Mahdavi et al., 2019). The formation of EDLs inside an aggregate and the resultant interaction of the double layers of aggregates in close proximity involves the overlap of double layers and correspondingly charge regulation (Schießl et al., 2012). The EDLs around particles of similar chemical composition and crystal structure have the same polarity and strength. Therefore, when two particles are in close proximity, the overlapping EDLs create a repulsive double layer force (Bouhaik et al., 2013; Handy et al., 2008). If ENPs of similar chemical composition, crystal structure and their EDLs have same polarity, a net repulsive energy barrier is created leading to low aggregation. However, if their EDLs have opposite polarity net attractive force result in promoting high aggregation which may lead to sedimentation (Bouhaik et al., 2013; Solovitch et al., 2010).

Aggregation may fundamentally affect the nature of ENPs found in different sinks and receptors. For example, the water column may contain smaller particles whereas the benthic zone may contain larger particles or agglomerates (Römer et al., 2013). It may also enhance bioaccumulation by making ENPs accessible (Ward and Kach, 2009) or by increasing the ingestion rates (Croteau et al., 2014). At concentrations significantly higher than currently environmentally relevant levels, sterically stabilized ENPs are prone to aggregation possibly due to polymer entanglement and bridging mechanisms with divalent cations as shown in process IX in Figure 2.1 (Alabresm et al., 2017; Lead et al., 2018). The physicochemical processes that influence the fate and behaviour of ENPs in aquatic systems are summarised in Figure 2.1. Aggregation of ENPs may be tracked using various instruments such as TEM, Zetasizer based on DLS etc as summarised in Table 2.1.

© University of Pretoria

2.2.4. Exposure medium chemistry

The fate and transformation processes of ENPs in aquatic systems are dependent on exposure media chemistry. The factors that influence exposure media chemistry include pH, IS and the type and concentration of NOM. The following sub-sections discusses how these factors affect the fate and transformation of ENPs in aquatic systems.

2.2.4.1. Potential of hydrogen (pH)

The pH defines the colloidal charge on an ion concentration scale based on the concentration of H^+ and OH^- in a given system (Hunter, 2013). Metal oxide ENPs can possess a positive or a negative charge when dispersed in aqueous media depending on the pH of the exposure medium. The surface hydroxyl groups of metal oxide ENPs get protonated at low pH leading to positive ζ-potential whereas at high pH they are deprotonated hence have a negative ζ-potential. However, a pH exists where a neutral charge point is observed. At this pH the hydroxyls are neither protonated nor deprotonated, and a ζ-potential of zero is observed. This point is called the pH of isoelectric point (pH_{IEP}) or pH of the point of zero charge (pH_{PZC}) (Lowry et al., 2016). Therefore, the pH may affect the protonation or deprotonation of hydrated metal oxide surfaces and various ligands present in the exposure media which influences the aggregation or stabilization of ENPs in the aquatic systems (Yang et al., 2009). Dramatic aggregation of ENPs is observed at the pH_{PZC}, whereas stable suspensions are observed at pH ranges away from the pH_{PZC} (Mui et al., 2016; Sousa and Teixeira, 2013).

2.2.4.2. Ionic Strength (IS)

The electrical conductivity of an aqueous solutions is dependent on the presence of ions which are ubiquitous in the environment. The most common ions which influences the IS of aquatic systems listed in order of decreasing conductivity are H^+, Na^+, Ca^{2+}, Mg^{2+}, NH_4^+, K^+, Cl^-, SO_4^{2-}, HCO_3^-, CO_3^{2-}, F^-, NO_3^-, Al^{3+}, Fe^{2+}, HSO_4^-, Li^+, OH^-, Fe^{3+}, Cu^{2+}, Mn^{2+}, Zn^{2+}, $NaSO_4^-$ and $NaSO_3^-$ (Mccleskey et al., 2012). The influence of other ions, even if they may be present in freshwater, on solution conductivity is usually negligible. The conductivity of an electrolyte solution is calculated using the expression 2.2.

$$K = \Sigma \lambda_i m_i \qquad 2.2$$

© University of Pretoria

where K is conductivity, λ_i is molar ionic conductivity of the i^{th} ion and m_i is the molality of the i^{th} ion in aqueous media. The degree of accuracy in theoretical conductivity depends on how accurately λ_i and m_i are measured (Visconti et al., 2010). For charged species in aqueous media, the activity coefficient decreases with increasing IS but for uncharged species it increases with increasing IS. Hence, dissolution of charged species increase with increasing IS whereas that of uncharged species decrease with increasing IS within the limits of (IS ≤ 1 M), beyond which the reverse process is observed as aggregation becomes highly favoured leading to a reduction in the number of available sites for dissolution (Mwaanga, 2012). The IS of a system is calculated as follows:

$$\mathrm{IS} = \frac{1}{2}\sum_i C_i Z_i^2 \qquad 2.3$$

where IS is the ionic strength in mM, C_i is the concentration of the i^{th} species in mM, and Z_i is the charge of the i^{th} species. The IS of freshwater systems varies widely, but generally it is less than 10 mM. For example, most literature has reported IS of freshwater systems in the range 0.8–7.0 mM (Conway et al., 2015; Heinlaan et al., 2016; Leareng et al., 2020; Tong et al., 2014).

According to the compression theory of the EDL, variations in IS may lead to changes in the potential around the particles (Fang et al., 2020). EDLs result from the spontaneous charging of particle surfaces in a liquid medium due to adsorption or dissociation processes (Schießl et al., 2012). EDLs of neighbouring particles interact with each other due to electrostatic and osmotic forces between the ions and the surfaces (Schießl et al., 2012). The interaction energy is influenced by the concentration of ions. Therefore, increase in IS results in increased number of mobile ions or counter ions in the compact layer which contributes to the decrease in electric potential difference between the particle interface and solution (Fang et al., 2020; Pham and Nguyen, 2014). The reduction in electric potential leads to thinning of the EDL around ENPs surface with resultant enhanced aggregation (Fang et al., 2020; Handy et al., 2008; Solovitch et al., 2010). The counterion association is highly pronounced at high IS such that the effective charge number of ENPs approaches zero. Therefore, the major limiting factor to aggregation becomes diffusion as electrostatic repulsion is at minimum (Kallay and Žalac, 2002; Pham and Nguyen, 2014).

© University of Pretoria

2.2.4.3. Natural Organic matter (NOM)

NOM is formed as a result of microbial decomposition of microorganisms, animal-, and plant residues present in various environmental compartments such as soil and water (freshwater, groundwater, lake water, river water, etc.) (Matilainen et al., 2010; Nebbioso and Piccolo, 2013; Yu et al., 2017). NOM has a wide molecular weight (MW) variation up to about (10 kDa) and it is characterised by the presence of functional groups such as aldehydes, ketones, quinones, thiols, phenols, methoxyls and carboxyls (Aiken et al., 2011a; Nebbioso and Piccolo, 2013). Due to differences in the origins of NOM, its composition exhibits substantial geographical and seasonal viability (Ritson et al., 2014). The concentration of NOM in freshwater systems has been reported to be within the range of (1–10) mg/L (Philippe and Schaumann, 2014; Yu et al., 2017).

The net negative charge on NOM is largely dependent on the degree of protonation and deprotonation of the phenolic and carboxylic functional groups as a function of pH in a given media. At low pH, these groups are largely protonated; hence NOM is less negatively charged whereas at high pH they are deprotonated, and therefore have a high negative charge (Sun and Lee, 2012). In freshwater and at near neutral pH and low IS, NOM molecules undergo structural relaxation to extended shapes. This is due to intramolecular electrostatic repulsive interactions (Stumm and Morgan, 2012).

The interactions of NOM and ENPs are thermodynamically favoured (Loosli et al., 2015b) due to both entropic and enthalpic factors (Loosli et al., 2015a). Therefore, the adsorption of NOM on ENPs is inevitable. Adsorption of NOM on ENPs is MW dependent where ENPs were found to have higher affinity for higher MW NOMs compared to lower MW forms (Chekli et al., 2013; Mwaanga et al., 2014; Yu et al., 2017). The source and composition of NOM determines its influence on the stability of ENPs in aquatic systems (Sikder et al., 2021; Sikder et al., 2020). For example, Sikder et al. 2021 observed that NOM from the Pacific Ocean promoted aggregation of 20 nm Platinum ENPs relative to NOM from Suwannee River where the differences = were associated to elemental composition. NOM with high oxygen to carbon ratio which indicates high presence of oxygen containing functional groups such as carbonyl and carboxylic groups are more likely to impart high negative surface charge on ENPs. This can lead to enhanced electrostatic repulsive forces, which in turn can promote ENPs stability in aqueous media (Deonarine et al., 2011; Sikder et al., 2021). In addition, the interaction of

© University of Pretoria

NOM with ENPs in the lower nano-size range is more significant than with those in the higher nano-size range (Chowdhury et al., 2013; Sikder et al., 2020). For example, Skider et al. 2020 observed that NOM promoted aggregation of polyvinylpyrrolidone coated platinum ENPs of size 20 nm but stabilized larger sized ones of 95 nm.

Ligand exchange, via a three-step mechanism, has been proposed as the dominant mechanism for NOM adsorption onto metal based ENPs. The first step involves surface hydroxyl protonation of ENPs making them more easily exchangeable, and the second step is based on outer-sphere complexation of protonated hydroxyls with NOM carboxylic groups. And, the last step proceeds via inner-sphere complex formation mechanism in which exchange of ligands occur through condensation reaction among the functional groups as summarised in process II in Figure 2-1 (Yang et al., 2009; Yu et al., 2017). NOM adsorption through ligand exchange involves a high binding energy resulting into an irreversible process (Yu et al., 2017).

Due to the adsorption of NOM, ENPs accumulate negative charges on their surfaces which leads to electrostatic stabilization due to repulsive effects (Yang et al., 2009). Hence, NOM is most often associated with the stabilisation effect on ENPs via electrostatic, steric or electro-steric mechanisms. However, it is not always the case that the adsorption of NOM on ENPs will impede aggregation. Under certain conditions it can promote aggregation. For example, higher MW NOM including polysaccharides and peptides may enhance aggregation of ENPs via formation of intramolecular cation-bridges enhanced by presence of divalent cations e.g. Ca^{2+} that facilitates complex formation with NOM functional groups such as carboxylate groups providing multiple cross-linkers among ENPs (Bharti et al., 2011; Koh and Cheng, 2014; Murphy et al., 1994; Yu et al., 2017).

Depending on the type of NOM, charge screening on dissolved NOM may occur at high IS conditions (Chen et al., 2003a; Mwaanga et al., 2014). Moreover, under certain pH and IS conditions, NOM may undergo molecular aggregation or disaggregation (relaxation) (Mwaanga, 2012; Stumm and Morgan, 2012) which may enhance the aggregation of ENPs. At low IS or high pH, the surface charge of NOM increases due to ionization (most function groups are in deprotonated state) and the resultant stabilization effect has a larger contribution from electrostatic effects. Conversely, at high IS or low pH the surface charge on dissolved NOM decreases due to charge screening with the observed stabilization effect largely being due to steric effects (Illés and Tombácz, 2006; Mwaanga, 2012). The stabilization of ENPs is

© University of Pretoria

dependent on the characteristics of NOM such as molecular structure, MW, charge, hydrophobicity and conformation (Mwaanga, 2012; Piccolo, 2001; Stumm and Morgan, 2012). For example, if adsorbed NOM assumes a flat conformation on the ENPs, electrostatic effect dominate stabilization whereas in extended conformations, steric effects become more dominant (Tiller and O'melia, 1993; Yokoyama et al., 1989). NOM broadly can form complexes with many different multivalent cations which may neutralize part of its negative charges and modify molecular conformation (Majzik and Tombácz, 2007a; Majzik and Tombácz, 2007b; Ottofuelling et al., 2011). Hence, multivalent cations have the ability to simultaneously reduce both electrostatic and steric stabilization effects of NOM.

2.3. Fate and transformation of ECs in aqueous media

The fate and transformation of ECs in aquatic systems play a significant role on their effects to aquatic organisms. Various factors influence their fate and transformation in the environment such as molecular properties, polarity, functional groups, ionizability, physical form including dissolved, colloidal or particulate and environmental factors including pH, IS, NOM and temperature (Besha et al., 2019; Schwarzenbach et al., 2006). The following subsections reviews the fate and transformation of TCS and selected ENPs as individual components and as mixtures in various aquatic systems.

2.3.1. TCS a dominant organic EC in PCPs

The widespread use of the polychlorinated, binuclear and aromatic broad-spectrum antimicrobials, such as the organic compound TCS, has raised serious concerns on environmental safety (Carey and Mcnamara, 2015; Halden et al., 2017). TCS is used in more than 2000 products including soaps, deodorants, shampoos, acne creams, detergents, toothpastes, clothing, toys, carpets, plastics and paints (Barghava and Leonard, 1996; Halden, 2014; Smith, 2013). It is worth noting that TCS and ENPs share similar applications in PCPs. Hence, they co-exist in aquatic systems and their interaction is inevitable. It was reported that between 1992 and 1999, the majority of an estimated 700 consumer products with antibacterial properties contained TCS (Schweizer, 2001). Globally, at least 1500 tonnes of TCS are released every year via consumer products, most of which ends up in wastewater treatment plants (WWTPs). Limited removal efficiency of TCS in WWTPs has been reported (Chalew and

© University of Pretoria

Halden, 2009; Singer et al., 2002). Its concentration in freshwater systems ranges from 50 to 2300 ng/L and it is higher in wastewater up to micrograms (0.07–14 000 µg/L) (Singer et al., 2002). Table 2.3 gives a summary of environmental concentrations of TCS in surface water from various parts of the world.

Table 2.3: Environmental concentrations of TCS in surface water from various countries across the globe

Country	TCS (ng/L)	Refs.
Australia	21–75	(Ying and Kookana, 2007)
China	11–478	(Zhao et al., 2010)
Germany	10	(Bester, 2005)
Japan	0.6–5.9	(Coogan and Point, 2008; Dhillon et al., 2015)
United Kingdom (UK)	5–37	(Kasprzyk-Hordern et al., 2008; Sabaliunas et al., 2003)
South Africa	39–8720	(Lehutso et al., 2017; Musee, 2018)
Switzerland	74	(Okumura and Nishikawa, 1996; Xie et al., 2008)
India	944–9650	(Nag et al., 2018; Ramaswamy et al., 2011)
USA	1–2300	(Fair et al., 2009; Katz et al., 2013; Kolpin et al., 2002)

The IUPAC name of TCS is 5-chloro-2-(2,4-dichlorophenoxy) phenol (Figure 2.2). It is available as a white powder with a slight phenolic odour. The MW is 289.54 g/mol and the molecular diameter is about 7.4 Å (Rossner et al., 2009). Its solubility in water is less than 1 ng/L (Du Preez and Yang, 2003; Montaseri and Forbes, 2018). The pKa is in the range 7.9–8.1 (Pemberton and Hart, 1999) and this implies that, depending on pH of the exposure medium, it may exist as partially a dissociated form. At pH < pKa it will exist in protonated form whereas at pH > pKa it will be present in deprotonated form. This is of relevance as anions do not generally adsorb as strongly on organic carbon and clay as their neutral counterparts (Mackay and Boethling, 2000; Montaseri and Forbes, 2016). In aquatic environmental systems, TCS is expected to adsorb onto suspended solids and sediments, posing a potential threat to aquatic organisms (List, 2008; Montaseri and Forbes, 2016). Derivative compounds of TCS

© University of Pretoria

such as methyl triclosan, biphenyl ethers and chlorinated phenols, which are also toxic, have been reported to be present in the aquatic environment (Fiss et al., 2007; Kanetoshi et al., 1987).

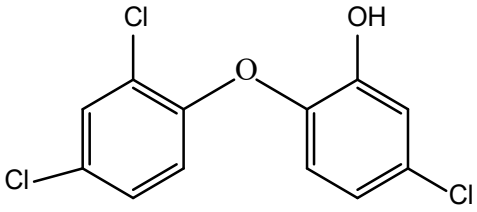

Figure 2.2: structural formula of 5-chloro-2-(2,4-dichlorophenoxy) phenol (Triclosan)

2.3.2. Fate and transformation of individual ENPs in aquatic systems

In aquatic environment, ENPs undergo numerous transformation processes as detailed under subsection 2.2 driven by their inherent intrinsic physicochemical properties (e.g. size, shape, surface chemistry, etc.) (Fabrega et al., 2011; Lowry et al., 2012; Wang et al., 2016), and exposure media chemistry like pH, IS, type of NOM, etc. (Conway et al., 2015; Odzak et al., 2014; Peng et al., 2017a; Sousa and Teixeira, 2013; Yang et al., 2009; Ye et al., 2018a; Zheng et al., 2011). Many studies have documented the fate and transformation of various ENPs in aqueous media (Collin et al., 2014; Fatehah et al., 2014; Luyts et al., 2013). The fate and transformation of nAl_2O_3 and nCuO in aqueous media were mostly conducted in DIW with only a few studies done in freshwater as detailed in subsections 2.2.2.1 and 2.2.2.2.

2.3.2.1. Fate and transformation of nAl_2O_3 in aquatic systems

The fate and transformation of nAl_2O_3 has been studied in DIW (Ghosh et al., 2008; Godymchuk et al., 2015; Mui et al., 2016) and in freshwater (Pakrashi et al., 2012). For studies in DIW, ENPs were observed to undergo maximum aggregation at pH = pH_{IEP} which was in the pH range 7.5–8.0, whereas ENPs were stable away from pH_{IEP} (Ghosh et al., 2008; Mui et al., 2016). Aggregation was also observed to be promoted by IS due to compression of the EDL and the effect was more significant at higher IS with divalent cations having greater influence than monovalent cations (Godymchuk et al., 2015; Mui et al., 2016). Conversely, Godymchuk et al., (2015) reported that the monovalent (NaCl) was more influential on aggregation than the

© University of Pretoria

divalent ($CaCl_2$). However, no rationale was provided for this rare observation. Both HDD and ζ-potential were influenced by the presence of NOM. The ζ-potential becomes more negative due to adsorption of NOM onto surfaces of ENPs and a reduction in size of aggregates is observed because of electrostatic and steric effects (Ghosh et al., 2008; Mui et al., 2016). In freshwater systems, nAl_2O_3 was reported to be stable within the first few hours of exposure but aggregation increased over time and high dissolution (~94%) partly due to prolonged exposure (Pakrashi et al., 2012). However, the characterisation results of the freshwater used in their study were not provided hence no key influencing factors could be identified. A summary of fate and transformation studies of nAl_2O_3 in aqueous media are listed in Table 2.4.

© University of Pretoria

Table 2.4: Summary of fate and transformation studies on nAl_2O_3 and nCuO

Type and Specifications of ENPs used	Exposure media and parameters	Instruments used	Description of fate and transformation findings	Reference
nAl_2O_3 Size: 60 nm Surface area: 230 m^2/g	DIW; pH (4–11) HA concentration: 5–10 mg/L ENPs concentration: 40 mg/L Temperature: 25 ± 0.1 °C	Malvern Zetasizer, AFM	The ζ-potentials was positive at lower pH and and pH_{IEP} was 7.9 beyond which ζ-potentials was negative Maximum aggregation was observed at pH_{IEP} High negative ζ-potentials and low aggregation was observed in presence of NOM	(Ghosh et al., 2008)
γ-nAl_2O_3 Size: 20–30 Shape: equiaxed Surface area: 8.49 m^2/g	DIW; pH: 6.7 ± 0.5 IS: 0–100 mM (NaCl or $CaCl_2$) ENPs concentration: 102 mg/L Temperature: 25 ± 1 °C Time: 48 h	Malvern Zetasizer, TEM, SEM	Electrolytes were observed to enhance aggregation which increased with increase in IS The monovalent electrolyte (NaCl) destabilised ENPs more than the divalent ($CaCl_2$)	(Godymchuk et al., 2015)
γ-nAl_2O_3 Size: 5, 10, 20–30 nm Shape: spheres and rods	DIW; pH range: 3–12	DLS, TEM, XRD, ICP–OES	The ζ-potentials was influenced by pH and positive at lower and negative and higher pH with pH_{IEP} was in the range 7.5–8 where maximum aggregation was observed. Aggregation was enhanced by IS with $CaCl_2$ having a higher effect than NaCl. ζ-potentials decreased with increasing IS.	(Mui et al., 2016)

© University of Pretoria

	IS range: 1–1000 mM (NaCl) and 3–3000 mM ($CaCl_2$) HA concentration: 1–50 mg/L ENPs concentration: 614 mg/L Temperature: not specified Time: 24 h		High negative ζ-potentials and low aggregation were observed in presence of even at the lowest concentration of HA (1 mg/L)	
nAl_2O_3 Size: < 50 nm Shape: spheres Surface area: 35–43 m^2/g	Natural lake water ENPs concentration: 50, 500 and 1000 ng/L Time: 48 h (aggregation) and 6 months (dissolution)	DLS, TEM, XRD, ICP–OES	Aggregation was low in the first 6 h (< 100 nm) but increased after 48 h (> 1000 nm) Dissolution was about 94 % over the experimental time frame	(Pakrashi et al., 2012)
nCuO Size: < 50 nm Shape: Nearly spherical Surface area: 29 m^2/g	Milli-Q water; pH: 3–12 IS range: 0–100 mM ($CaCl_2$) HA concentration: 1–50 mg C/L at pH 8 ENPs concentration: 100 mg/L Time: 12 h	Malvern Zetasizer, TEM, XRD	The ζ-potentials was positive at lower pH and negative at pH > pH_{IEP} and pH_{IEP} was 10. Maximum aggregation was observed at pH_{IEP} Aggregation was enhanced by IS and ζ-potentials decreased with increasing IS NOM imparted high negative ζ-potentials and aggregation was impeded.	(Sousa and Teixeira, 2013)
nCuO Size: 30–50 nm Shape: Spherical	Milli-Q water; pH: 6–9 Water hardness: 0–300 mg/L as $CaCO_3$	DLS, TEM, ICP–MS	The pH more influence on both aggregation and dissolution compared to hardness or NOM Formation of NOM–Ca^{2+} complexes reduced the ability of NOM and hardness to promote aggregation	(Son et al., 2015)

© University of Pretoria

	NOM: 0–10 mg /L ENPs concentration: 4.14 mg/L Temperature: 25 °C Time: 10 days			
nCuO Size: 40 nm Shape: Spherical or elliptical Surface area: 131 m^2/g	Milli-Q water; pH: 3–9 at IS 10 mM NaCl IS range: 1–100 mM (NaCl or $CaCl_2$ at pH 7 NOM: 1–100 mg /L at pH 7 and 10 mM NaCl ENPs concentration: 100 mg/L Temperature: 25 °C Time: 48 h	Malvern Zetasizer, TEM, FAAS	The ζ-potentials was positive at lower pH and negative at pH > pH_{IEP} and pH_{IEP} was 6.21 at which maximum aggregation and sedimentation was observed High dissolution was observed at low pH (3) and it decreased with increasing pH IS promoted aggregation and sedimentation which increased with increase in IS. The divalent electrolyte ($CaCl_2$) influenced aggregation more than the monovalent (NaCl). Increase in IS led to a reduction in ζ-potentials. Dissolution was promoted by NaCl but exhibited by the divalent $CaCl_2$ NOM imparted high negative ζ-potentials and impeded aggregation with various types of NOM exhibiting different degrees of influence	(Peng et al., 2017a)
nCuO Size: 20–100 nm	Natural water from various sources ENPs concentration: 10 mg/L	Malvern Zetasizer, SEM, XRD, ICP–AES	Aggregation was promoted in exposure media with high IS and low NOM concentration Sedimentation was observed to show positive relationship with IS and an inverse relationship with NOM.	(Conway et al., 2015)

© University of Pretoria

Surface area: 12.31±0.05 m^2/g	Time: over 1 h for aggregation, 6 h for sedimentation and 90 days for dissolution studies Temperature: not specified		phosphates PO_4^{3-} inhibited aggregation and imparted negative charge on surfaces of ENPs Dissolution was high in exposure media with low pH but, it was low in exposure media with high NOM concentration due to chelation and coating effects of NOM.	
nCuO Size: 22–25 nm (powder)	Natural lake water and Milli-Q water ENPs concentration: 1–100 mg/L Time: over 24 h (aggregation) and 9 days (dissolution) Temperature: 22 ± 1 °C	Malvern Zetasizer, UV–Vis spec., ICP–MS	High aggregation (>2000 nm) and sedimentation was observed in lake water owing to high IS. Very low dissolution was observed due to high aggregation and sedimentation.	(Heinlaan et al., 2016)

Abbreviations: AFM: Atomic Force Microscopy, DLS: Dynamic light scattering, FAAS: flame atomic absorption spectrometer, ICP–AES: inductively coupled plasma atomic emission spectroscopy, ICP–MS: Inductively Coupled Plasma Mass Spectrometry, ICP–OES: inductively-coupled plasma optical emission spectrometry, SEM: Scanning Electron Microscope, SP-ICP-MS: Single Particle Inductively Coupled Plasma Mass Spectrometry, TEM: Transmission Electron Microscope, UV-Vis Spec.: Ultra-Violet/ Visible Spectrophotometry, XRD: Powder X-ray diffraction.

© University of Pretoria

2.3.2.2. Fate and transformation of nCuO in aquatic systems

Few studies have reported on the fate and transformation of nCuO in various aquatic systems. The studies were conducted in DIW (Peng et al., 2017a; Son et al., 2015; Sousa and Teixeira, 2013), and freshwater systems (Conway et al., 2015; Heinlaan et al., 2016) as exposure media. For studies conducted in DIW, ζ-potential of nCuO has been reported to be greatly influenced by pH, it is positive in acidic pH range and negative at pH > pH_{IEP} (Peng et al., 2017a; Sousa and Teixeira, 2013). Variations in pH_{IEP} have been reported, i.e. pH_{IEP} = 6.21 (Peng et al., 2017a) and pH_{IEP} = 10 (Sousa and Teixeira, 2013). These observations suggest that pH_{IEP} may be influenced by other factors, e.g. such as the presence of a coating on ENPs.

Both aggregation and dissolution have been observed to be influenced by pH. Maximum aggregation was observed at pH = pH_{IEP} (Peng et al., 2017a; Sousa and Teixeira, 2013) whereas maximum dissolution under acidic pH regime and minimal dissolution in basic pH range (Peng et al., 2017a). IS was reported to promote aggregation with divalent cations exhibiting higher influence than monovalent cations; attributed to larger compression of the EDL which in turn led to a reduction in electrostatic repulsive force promoting inter-particle interaction, thus high aggregation and subsequent sedimentation (Peng et al., 2017a; Sousa and Teixeira, 2013). The monovalent electrolyte (NaCl) reportedly enhanced dissolution of nCuO which increased with increasing concentration of NaCl whereas the divalent cation ($CaCl_2$) slightly inhibited dissolution of nCuO (Peng et al., 2017a). These findings indicate that both IS and type of electrolyte influence the aggregation and dissolution of nCuO.

The presence of NOM was observed to increase the ζ-potential (high negative) of nCuO due to the adsorption of NOM by ENPs which imparts negative charge on surfaces of ENPs and enhances their stability via electrostatic and steric stabilization (Peng et al., 2017a; Sousa and Teixeira, 2013). In a study involving a combination of three factors (pH, water hardness and NOM), the pH was reported to have greater influence on both aggregation and dissolution of nCuO (Son et al., 2015). A combination of water hardness and NOM has been reported to cause limited aggregation of ENPs. This was attributed to significant interactions as a consequence of the binding of Ca^{2+} to the carboxyl functional groups of NOM forming NOM–Ca^{2+} complexes reducing the ability of water hardness to compress the EDL and enhance aggregation (Son et al., 2015). However, other studies have reported that the interaction between Ca^{2+} and NOM leads to formation of bridges resulting into enhanced aggregation of

© University of Pretoria

ENPs (Murphy et al., 1994; Yu et al., 2017). In natural water systems, high IS and low concentration of NOM promote aggregation of nCuO (Conway et al., 2015; Heinlaan et al., 2016). Phosphates (PO_4^{3-}) have been reported to form a negatively charged layer of copper phosphate onto the surface of nCuO which in turn increases the negative charge density and promote electrostatic repulsion impeding aggregation (Conway et al., 2015).

NOM impedes dissolution of nCuO in aqueous media. For example, Conway et al. (2015); investigated the dissolution of 1 mg/L nCuO in wastewater and storm runoff with NOM concentrations of 2.38 and 6.49 mg/L where dissolution was found to be < 10% and 0 %, respectively. Miao et al. (2016); reported a dissolution percentage of < 5% in wastewater. However, other findings hold that the presence of NOM enhances the dissolution of ENPs (Jiang et al., 2015; Xiao et al., 2018). Systems with low pH promote dissolution of nCuO (Conway et al., 2015). Ionic species present in natural water matrixes, e.g. Cl^{-1}, SO_4^{2-}, PO_4^{3-}, etc., can form complexes with released Cu^{2+} from dissolution of nCuO. These findings suggest that various water chemistry parameters such as IS, pH, NOM and presences of specific ionic species such as phosphates and oxidation state of ions released by ENPs are key parameters likely to predict the fate and transformation of ENPs in natural aquatic systems. The studies on fate and transformation of nCuO in aqueous media are summarized in Table 2.4.

From Table 2.4, all the studies done in DIW used high exposure concentrations of ENPs (40–614 mg/L) for nAl_2O_3 and (1–100 mg/L) for nCuO. These concentrations are orders of magnitudes beyond environmentally relevant concentrations as evidenced by both field measurements (Donovan et al., 2016; Johnson et al., 2011) and PECs based on modelling (Boxall et al., 2007b; Keller and Lazareva, 2013; Mueller and Nowack, 2008). The IS range used (0–3000 mM) is also far beyond what is environmentally relevant considering the fact that the concentration of common electrolytes in the environment are very low. For example, in freshwater systems, Na^+ concentrations ranges from 0.26 to 0.78 mM (Guo et al., 2001; Jalali and Jalali, 2016), and much lower for K^+ (0.001 to 0.005 mM) (Talling, 2010). The study by Peng et al. (2017) used 10 mM NaCl as background electrolyte during their investigations on influence of pH or NOM on stability of nCuO, a concentration high enough to influence the observed results as a consequence of high IS.

Investigations by Pakrashi et al. (2012) in natural lake water used low concentrations of ENPs close to what is environmentally relevant. However, the physical-chemical properties of the

© University of Pretoria

natural lake water used as exposure media were not reported to aid account for the observed behaviour such as the high dissolution of nAl_2O_3 reported. Hence, all these studies have fundamental limitations and their findings may not be sufficient to fully elucidate the fate and transformation of nAl_2O_3 in freshwater systems. Such data is essential as realistic estimates of ENPs fate in environmentally relevant conditions are largely lacking.

2.3.3. Fate and transformation of binary mixtures of ENPs in aquatic systems

A review on the fate and transformation of binary mixtures of ENPs with respect to aggregation, dissolution, and adsorption is summarised in Table 2.5. Similar to the observations under fate and transformation of individual ENPs in aquatic systems, interactions of mixtures of ENPs in aqueous media are dependent on the exposure media chemistry parameters such as pH, IS, NOM, type of electrolytes, UV radiation among others (Hazeem et al., 2016; Iswarya et al., 2015; Wilke et al., 2019). A limited number of studies have reported on the fate and transformation of mixtures of ENPs in aquatic systems (Azevedo et al., 2017; Benavides et al., 2016; Fang et al., 2017; Hazeem et al., 2016; Huynh et al., 2014; Iswarya et al., 2015; Mansouri et al., 2016; Tong et al., 2014; Wilke et al., 2016). Most of these studies reported hetero-aggregation and adsorption of particulate and ionic species onto surfaces of less soluble component ENPs in the mixture. However, these studies used either environmentally unrealistic concentrations of ENPs or DIW as exposure media. Therefore, the findings may not satisfactorily account for the transformation of ENPs in natural aquatic systems. Hence, this remains a key data knowledge gap in this field.

2.3.3.1. Aggregation of mixtures of ENPs

Aggregation of binary mixtures of ENPs in various aquatic systems, e.g. DIW (Huynh et al., 2014; Mansouri et al., 2016), algal medium under saline conditions (Hazeem et al., 2016), tap water (Benavides et al., 2016) and natural water (Fang et al., 2017; Iswarya et al., 2015; Tong et al., 2014) has been observed. Binary mixtures of ENPs with opposite surface charges in DIW were observed to undergo concentration dependant hetero-aggregation driven by electrostatic interactions. For example, Huynh et al. (2014) reported concentration dependent hetero-aggregation on the interaction of binary mixtures of nAg and hematite nanoparticles (nHem), nAg/nHem in DIW. Hetero-aggregation due to adsorption of one type of ENPs onto another has been observed. For example, studies on the interaction of $nCuO/nTiO_2$ binary mixtures in

© University of Pretoria

DIW revealed adsorption of nCuO onto $nTiO_2$ leading to enhanced hetero-aggregation (Mansouri et al., 2016).

For the $nTiO_2$/nZnO mixtures, maximum aggregation and sedimentation was observed at high pH values in algal medium under saline conditions (Hazeem et al., 2016). The same mixture was studied in natural water in which concentration dependant hetero-aggregation was apparent as the concentration of nZnO increased (Tong et al., 2014). However, mixtures of the same ENPs were observed to be stable in natural water at pH 7.7 where both ENPs had negative ζ-potentials and the stability was linked to interparticle repulsive effects (Fang et al., 2017).

Investigation on the interaction between anatase and rutile forms of $nTiO_2$ in sterile lake water revealed that binary mixtures had negative ζ-potential although the individual components ENPs had positive ζ-potential under the same exposure conditions and hetero-aggregation was also observed (Iswarya et al., 2015). In summary, these findings suggest that several factors including pH, exposure media chemistry, ζ-potential, mixture concentrations, ENPs properties etc, influence the aggregation of binary mixtures of ENPs in aquatic systems. Fate and transformation studies on binary mixtures of ENPs in various aquatic systems are summarised in Table 2.5.

2.3.3.2. Dissolution and adsorption of binary mixtures of ENPs

Interactions of ENPs in terms of dissolution and adsorption in binary mixtures of ENPs are dynamic and of great significance in assessing their ecological safety in aquatic systems. One type of ENPs have been found to enhance dissolution of other ENPs in binary mixtures which would lead to enhanced bioavailability of ionic species to aquatic organisms. For example, $nCeO_2$ enhanced the dissolution of nZnO in cultivation media (Yu et al., 2016). Less soluble ENPs with large surface area exhibited adsorptive effects on ions from soluble ENPs in the mixture. This leads to the possibility of reduced ion bioavailability or induction of Trojan horse effect. Both are critical phenomena in toxicological studies. For example, the interactions of nAg/$nTiO_2$ in Lake Michigan water (LMW) revealed adsorption of dissolved Ag^+ onto the surfaces of $nTiO_2$ (Wilke et al., 2016). In another study, entailing the nZnO/$nTiO_2$ binary mixtures in LMW, adsorption of Zn^{2+} by $nTiO_2$ was observed (Tong et al., 2014). Adsorption of Ag^+ following the dissolution of nAg onto surfaces of nHem was observed during investigations on binary interactions of nAg/nHem in DIW (Huynh et al., 2014). In addition, a

© University of Pretoria

reduction in dissolution of nCuO due to adsorption of Cu^{2+} onto surfaces of $nTiO_2$ was observed following the interactions of nCuO/$nTiO_2$ binary mixtures in DIW (Mansouri et al., 2016).

The foregoing dissolution and adsorption studies suggest that non- or low-dissociating ENPs such as $nTiO_2$ may modify the combined toxicity by competing with the bacterial surface to adsorb the generated ions e.g. Ag^+ and Zn^{2+}. Overall, stable ENPs e.g. $nTiO_2$, nFe_2O_3 and other adsorptive surfaces in the environment may play an important role in mediating other forms of ENPs as well as other ENPs-related metabolites (e.g. ionic species) in terms of bioavailable to the aquatic organisms. A summary of studies on fate and transformation of mixtures of ENPs is provided in Table 2.5.

Notably, most studies used unrealistically high exposure concentrations of ENPs considering the current environmentally measured concentrations (Bhuvaneshwari et al., 2016; Garner and Keller, 2014) and PECS (Boxall et al., 2007b; Gottschalk et al., 2013; Holden et al., 2014; Keller and Lazareva, 2013; Musee, 2011c), which are in the lower µg/L range. The studies which used natural water matrixes employed environmentally unlikely concentrations of ENPs (Tong et al., 2014; Wilke et al., 2016). Studies which used environmentally relevant concentrations of ENPs used synthetic water as exposure media (Azevedo et al., 2017; Benavides et al., 2016). Most of these studies did not investigate aggregation and dissolution kinetics and lack systematic design on fate and transformation of binary mixtures of ENPs. Hence, the reported findings might not adequately reflect the fate and transformation of binary mixtures of ENPs in natural aquatic environmental compartments. Therefore, there is need to study the kinetics of the interactions of binary mixtures of ENPs in natural aquatic systems, and at environmentally relevant concentrations. This will minimize the knowledge gap on fate and transformation of binary mixtures of ENPs in various natural aquatic systems.

© University of Pretoria

Table 2.5: Summary of studies on fate and behaviour of mixtures of ENPs.

Specifications of ENPs in the mixture	Exposure media and parameters	Instruments used	Description of fate and behaviour findings	Reference
$nTiO_2$ (P 25) (80% Anatase and 20% Rutile; size range 15–25 nm) and nZnO (Spheres with radius 63.5 nm and rods with length 156.6 nm and diameter 47.1 nm)	Lake Michigan water (LMW) (pH 8.4 ± 0.1; DOC 1.77 mg/L and IS 4.77 mM). Stock concentrations of 1 g/L of each ENPs concentration range: 1–50 mg/L nZnO and 10–100 mg/L $nTiO_2$. Exposure duration: Over 48 h for dissolution and adsorption	TEM, Zetasizer, HPLC, PXRD, STEM, XRD, XAS, FAAS	Dissolution of nZnO and adsorption of Zn^{2+} onto $nTiO_2$ was observed. Concentration of Zn^{2+} decreased with increasing concentration of $nTiO_2$. Both ENPs had negative ζ-potentials but concentration dependant heteroaggregation which increased with increasing concentration of nZnO was observed and attributed to collisions of ENPs. Aggregation kinetics was not studied only dissolution and adsorption kinetics were investigated	(Tong et al., 2014)
nAg (Size 7.9 ± 2.4 nm, citrate coated) and $nTiO_2$ (P25) (Shape; Spherical, size ~20 nm; 84% Anatase and 16% Rutile)	Lake Michigan water (LMW) (pH 8.2 ± 0.1; DOC 1.77 mg/L and IS 4.68 mM) ENPs concentration ranges: 5–40 µg/L nAg and 0, 1, and 10 mg/L $nTiO_2$). Exposure duration: over 7 days for dissolution and adsorption	TEM, XRD, ICP-MS, UV-Vis	Adsorption of nAg onto $nTiO_2$ was observed as evidenced by the reduction in concentration of Ag^+ in presence of $nTiO_2$ with maximum adsorption capacity for $nTiO_2$ being ~1.81 ± 0.36 µg nAg/mg P25 $nTiO_2$.	(Wilke et al., 2016)

© University of Pretoria

$nTiO_2$ (Anatase and rutile). (Anatase: shape; cubical and spherical, size < 25 nm, Specific surface area 45–55 m^2/g) and Rutile: Shape; rods, size; length < 100 nm and diameter ~ 40 nm, Specific surface area 130–190 m^2/g)	Freshwater (VIT lake) (pH: 7.76 ± 0.16; TOC: 13.89 ± 0.72 mg/L). ENPs concentration range: 0.25–1 mg/L Exposure duration: over 72 h for dissolution and adsorption	TEM, SEM, Zetasizer, UV-Vis, XRD, FT-IR, ICP–OES	Concentration ratio dependant heteroaggregation was observed which increased with time at higher concentration ratio without clear dependence on one type of ENPs. Adsorption of anatase onto surfaces of rutile ENPs was observed owing to the larger specific surface area of rutile compare to the anatase. Dissolution was not observed as it was below detection limit of ICP–OES (0.003 mg/L)	(Iswarya et al., 2015)
$nTiO_2$ (99.9% Anatase), size; 60–80 nm), surface area; 32.5 m^2/g. and nZnO, size; < 100 nm	Natural water (Grand Canal in Hangzhou, China), (pH 7.7 ± 0.1; DOC 4.65 ± 0.25 mg/L). ENPs concentration range: 10–25 mg/L nZnO and 15 mg/L $nTiO_2$ Exposure duration: over 14 days	SEM, Zetasizer, ICP–AES	Heteroaggregation was deduced without any reported influence of concentration ratios of ENPs. No influence of binary interactions of ENPs was reported on dissolution	(Fang et al., 2017)
nAl_2O_3 (Size: 20 nm) and nZnO (Size: 50 nm)	Dechlorinated tap water at pH 7.4 ± 0.02. ENPs concentration range 10–100 µg/L. Exposure duration: over 48 h	TEM, Zetasizer, ICP–AES	Aggregation of both individual and binary mixtures of ENPs was observed without any indication as to which systems had higher aggregation. No dissolution of nAl_2O_3 was observed but for nZnO as Zn^{2+} were detected. No clear influence due to binary interaction of ENPs was reported	(Benavides et al., 2016)
nZnO and nAg (size and shape unspecified)	Artificial hard water ASTM.	TEM, SEM, ICP-MS	Dissolution of both nZnO and nAg decreased in the mixture more so after 48 h. For example, at 0 h, dissolution of nZnO and nZnO/nAg were 100 % and 95%, respectively.	(Azevedo et al., 2017)

© University of Pretoria

	ENPs concentration ranges: 0.25–5 mg/L nZnO and 1–25 µg/L nAg Exposure duration: over 48 h		No clear indication of how ENPs in binary mixtures influenced the dissolution of each other as no trends were provided on concentration ratios	
nAg (spherical, 64.6 nm) and nHem (spherical, 82.4 nm)	Deionized water (Millipore) at pH 5.5. ENPs concentration ranges: 2.2 mg/L nAg and 1–30 mg/L nHem Exposure duration: over 8 h	TEM, Zetasizer, ICP-MS	Heteroaggregation was observed which was dependant on concentration of nHem in the mixture and it was associated to the electrostatic interactions between the positively charged citrate coated nAg and the negatively charged nHem. Dissolution of nAg was observed and the concentration of Ag^+ in the binary mixtures of nAg/nHem decreased with increasing concentration of nHem due to adsorption of Ag^+ on the surface of nHem	(Huynh et al 2014)
nZnO (Size: 28 nm) and $nTiO_2$ (Anatase; 85.4 wt%, size 19 nm and rutile; 14.6%, size 20 nm)	Algal medium at pH 8–8.22 and temperature 8 °C ENPs concentration range: 10–30 mg/L nZnO and 10–30 mg/L $nTiO_2$. Exposure duration: over 35 days	SEM, EDS, XRD	Heteroaggregation and sedimentation of the binary mixture was observed without any reported influence of ENPs on each other Dissolution of nZnO in the mixture decreased with increasing pH and no influence of $nTiO_2$ was reported on dissolution of nZnO	(Hazeem et al., 2015)
nCuO (Size: 40 nm, specific surface area 20 m^2/g) and $nTiO_2$ (Anatase/rutile) (Size: 20 nm, specific surface area 20 m^2/g)	Distilled water with unspecified pH ENPs concentration: 100 mg/L $nTiO_2$ and 2.5–5 mg/L nCuO. Exposure duration: over 48 h	TEM, SEM, Zetasizer, XRD, UV-Vis, ICP–OES	Concentration dependant heteroaggregation and ζ-potential was observed which increased with increasing concentration of nCuO in the binary mixtures and was associated with adsorption of nCuO onto surfaces of $nTiO_2$. Dissolution of nCuO in the mixture was observed to decrease because of adsorption of released Cu^{2+} onto the surfaces of $nTiO_2$ leading to decreased amount of measured concentration of nCu^{2+} in the mixture.	(Mansouri et al., 2016)

© University of Pretoria

Abbreviations: FAAS: flame atomic absorption spectrometry, EDS: Energy Dispersive spectroscopy, SEM: Scanning Electron Microscope, TEM: Transmission Electron Microscope, UV-Vis Spec.: Ultra-Violet/ Visible Spectrophotometry, XRD: Powder X-ray diffraction, SP-ICP-MS: Single Particle Inductively Coupled Plasma Mass Spectrometry. FTIR: Fourier Transformer Infra-red. NMR: Nuclear Magnetic Resonance.

© University of Pretoria

2.3.4. Fate and transformation of mixtures of ENPs and organic MPOs in aquatic systems

The interactions between ENPs and organic pollutants are largely influenced by their specific properties and environmental factors including pH, IS, NOM and temperature (Besha et al., 2019). Sorption is the major mode of interactions between ENPs and organic pollutants in aquatic systems. It is mediated through hydrogen bonding, π–π interactions and hydrophobic interactions (Besha et al., 2017; Chen et al., 2017). ENPs and organic pollutants containing functional groups like –COOH, –OH, –F, –NH_2, –NH– are susceptible to hydrogen bonding with electronegative atoms such as N and O (Chen et al., 2017; Li et al., 2016). Adsorption between ENPs and organic pollutants has also been associated with π–π interactions in presence of π–donors and π–acceptor (Jiang et al., 2017; Li et al., 2016). Hydrophobic interactions between non polar components of organic pollutants and neutral surfaces of ENPs also contribute to adsorption (Chen et al., 2017; Lee et al., 2015).

In addition, electrostatic interaction have also been reported as another mechanism on the interactions between ENP and organic pollutants in systems where charge interactions are very strong (Lan et al., 2016). Pharmaceuticals with low MW have been observed to exhibit higher adsorption capacity than higher MW ones linked to differences in their mobility in aquatic systems. For example, carbamazepine with lower MW had higher adsorption capacity than diclofenac characterised by higher MW (Suriyanon et al., 2013). The interaction of TCS and copper nanoparticles (nCu) as binary mixtures was investigated and the results showed that the concentration of free TCS decreased in the mixture, whereas the dissolution of nCu increased in presence of TCS (Chen et al., 2018). These findings imply that the toxicity of TCS could be mitigated by presence of nCu due to adsorption. However, toxicity of nCu could be enhanced by presence of TCS due to the promoted dissolution as Cu^{2+}, as the latter is largely responsible for the toxicity of nCu. Therefore, interactions between ENPs and organic MPOs has the capacity to alter the fate, transport and bioavailability of both ENPs and organic MPOs with resultant significant implications on environmental safety.

The few studies done on the interactions of ENPs and organic MPOs so far focus largely on the interactions of pharmaceuticals and ENPs and not much on interactions of PCPs and ENPs. TCS and ENPs will co-exist in the aquatic environment due to similar applications e.g. in PCPs and poor removal in WWTPs. Yet, the implication of their interaction as mixtures in aquatic

© University of Pretoria

systems remains poorly investigated. Hence in this thesis the interactions of binary and ternary mixtures of nCuO, nAl_2O_3 and TCS in freshwater systems are investigated. The findings from this study will be critical in increasing the understanding on the impacts of metal oxide ENPs and TCS as a representative organic pollutant among many other aromatic organic MPOs in aquatic systems.

© University of Pretoria

Chapter 3: Methodology

3.1. Materials

The nCuO (nanopowder < 50 nm, CAS No 1317-38-00), nAl_2O_3 (in suspension with size range 30–60 nm; 20 wt% in water, CAS No 1344-28-10), TCS (CAS No. 3380-34-5), humic acid (HA) (CAS No 1415-93-6) (Characterisation details attached in appendix 3.1 as provided by the manufacturer), sodium chloride (NaCl) (CAS No 7647-14-5) as well as the analytical grades of nitric acid (HNO_3), hydrochloric acid (HCl) and sodium hydroxide (NaOH) were all purchased from Sigma-Aldrich (Johannesburg, South Africa). All materials were used as received from the supplier without any further purification. Freshwater samples were collected from two river systems in different hydrological zones with different physicochemical properties, namely: The Elands River (ER) (25°32'58.4"S 28°33'53.4"E) in Gauteng Province (South Africa), and the Bloubank River (BR) (26°01'20.3"S 27°26'31.6"E) in North West Province (South Africa).

3.2. Characterisation of river water and ENPs

3.2.1. Characterisation of river water

The river water samples used in the study were collected from ER and BR in (July 2017) and (October 2017), respectively. All samples were filtered through a 0.2 μm pore size standard filter (Millipore) and stored in the fridge at 4 ℃ prior to use. Samples were sent for characterisation at a certified laboratory, and the results are presented in Table 3.1.

© University of Pretoria

Table 3.1: Characterisation of freshwater samples from ER and BR of South Africa.

Parameter	Unit	ER water	BR water
pH	-	8.1	7.9
K^+	mg/L	4.24	3.13
Na^+	mg/L	15.6	22.4
Ca^{2+}	mg/L	14.0	36.0
Cl^-	mg/L	17.1	12.9
SO_4^{2-}	mg/L	9.03	6.77
Mg^{2+}	mg /L	9.82	31.0
NO_3^-	mg/L	0.33	0.20
PO_4^{3-}	mg/L	0.57	1.23
NH_4^+	mg/L	4.27	3.40
Cu_{tot}	mg/L	<0.002	<0.002
Al_{tot}	mg/L	<0.002	<0.002
Fe_{tot}	mg/L	<0.004	<0.004
Zn_{tot}	mg/L	<0.008	<0.010
DOC	mg /L	5.51	8.25
Alkalinity	mg $CaCO_3$/L	75.6	217
(EC) @ 25 ℃	mS/m	19.6	39.8
IS	mM	2.48	5.35

DOC: dissolved organic carbon; Al_{tot}: total aluminium; Fe_{tot}: total iron; Zn_{tot}: total zinc; Cu_{tot}: total copper EC: Electrical conductivity

3.2.2. Characterisation of ENPs

A summary of techniques used to determine various aspects of the ENPs are presented in this section. Only most salient features of the tools and techniques are highlighted. TEM is used to characterise ENPs for particle size, morphology and size distribution as detailed in Table 2.1. In the current study, TEM (JEM 2010F, JEOL Ltd., Japan) was used to characterise nCuO and nAl_2O_3 for particle size and morphology. Samples were prepared by dispersing 50 mg/L ENPs in DIW. The samples were then placed on carbon-coated copper grids and dried in a desiccator for 24 h before analysis.

© University of Pretoria

Bruker D8 Advance powder X-ray diffractometer (PXRD) with monochromatized Cu Kα radiation with wavelength of 1.54 Å was used to determine the phase structure and purity of nCuO or nAl_2O_3. A dispersion of nAl_2O_3 was dried in an oven at 80 °C for 24 h as PXRD undertakes analysis in solid phase of the sample. 25 mg of dry powder of nCuO or nAl_2O_3 were used for the analysis.

Braunner, Emmett and Teller (BET) theory was applied to determine the specific surface area of nCuO or nAl_2O_3 using the TriStar II 3020 surface area and porosity analyser (Micromeritics, USA) equipped with V3.02 software. A Sample of suspension of nAl_2O_3 was dried on a watch glass in an oven overnight. Then 1.5 g powders of nAl_2O_3 and nCuO were loaded in two independent BET tube sample holders for analysis.

Malvern Zetasizer Nano series (Model ZEN 3600; Malvern Instruments, UK) was used to measure ζ-potential and HDD using dynamic light scattering (DLS) for both individual and mixture samples of ENPs in various exposure media.

Sedimentation kinetics of ENPs was studied using ultraviolet-visible (UV-Vis) spectroscopy over 48 h. Measurements were done using a 1 cm optical path length quartz cuvettes on the Hitachi high technology U–3900 spectrophotometer (USA).

SEM (Zeiss Crossbeam 540 FEG SEM, Zeiss Pty Ltd, Oberkochen, Germany) equipped with an energy dispersive spectroscopy (EDS) was used to characterise pristine ENPs and to study hetero-aggregation of the mixtures of ENPs. Mixtures of ENPs were prepared in river water and sonicated for 30 min at 25 ℃ using ultrasonic bath to achieve homogeneity. The mixtures were then kept at 25 ℃ for 24 h then shaken vigorously by hand to achieve homogeneity before drops were dispensed on silver grid and kept in a desiccator for 24 h to allow for complete drying. The samples were coated with gold before analysis.

ICP–MS (ICPE-9820, Shimadzu, Japan) was used to investigate the dissolution of nCuO and nAl_2O_3 in various exposure media. The samples were filtered to remove particles using Amicon ultra-15 filters (MWCO 3 kDa) via centrifugation at 4000 xg for 45 min. The filtered samples were preserved using 20 µL of concentrated HNO_3 before analysis, and the supernatant was analysed for total dissolved copper and aluminium.

Visual MINTEQ (version 3.1, https://vminteq.lwr.kth.se) was used to predict speciation of copper and aluminium in both river water samples based on the water chemistry parameters

© University of Pretoria

provided in Table 3.1. The Stockholm humic model (SHM) was used with default parameters as model inputs as the actual values from the humic acids in the river water were not established, and hence, will be considered in future works.

3.3. Aggregation kinetics of individual and binary mixtures of ENPs in DIW

Aggregation kinetics of nCuO and nAl_2O_3 with respect to influencing factors that is, pH, IS and NOM were investigated in DIW (ultrapure water, resistivity of 18.2 MΩ cm, Elga PureLab Option System, UK). Stock suspensions of 10 mg/L nAl_2O_3 or nCuO were prepared by adding 5.0 µL of nAl_2O_3 suspension or 1 mg of nCuO powder to 100 mL volumetric flask and diluting with DIW to achieve specified pH, IS, or NOM concentration. The resultant suspensions were sonicated for 30 min at 25 ℃ using ultrasonic bath to achieve homogeneity. From the resultant suspensions, where necessary, further dilutions were done to achieve lower concentrations of 1 and 0.1 mg/L of nAl_2O_3 or nCuO. Binary mixtures of ENPs were investigated at concentrations of (1, 0.1), (1, 1), and (1, 10) mg/L nAl_2O_3 and nCuO, where the values in the parenthesis are for nAl_2O_3 and nCuO, respectively. Another set of samples were investigated at concentrations of (1, 0.1), (1, 1), and (1, 10) mg/L where the values in the parenthesises are concentrations of nCuO and nAl_2O_3, respectively. Notably, the concentrations of ENPs used in this study were lower than most widely employed in numerous previous studies. However, they are still orders of magnitude higher than environmentally relevant concentrations which are in the lower scale of µg/L range. The concentrations used herein were informed by the detection limits of the instruments used in this study such as the Malvern Zetasizer Nano series (Model ZEN 3600; Malvern Instruments, UK). The Malvern Zetasizer was used to track changes in HDD and ζ-potential hourly from 0 to 6, and then at 24 and 48 h. All measurements for the HDD and ζ-potential were done in triplicates, and hence, reported as mean and standard deviation (mean ± SD).

3.3.1. Influence of pH

Stock solutions in the pH range 3 to 9 were prepared by adjusting the pH of DIW using either HCl or NaOH and stored at 4 °C prior to use. The pH stock solutions were used as exposure media to determine the influence of pH on aggregation and ζ-potential as detailed in section 3.3 except for binary mixtures which were only studied at pH 4 and 7. The obtained HDD and ζ-potential results were used to determine the isoelectric point of nAl_2O_3 and nCuO.

© University of Pretoria

3.3.2. Influence of IS

Stock solutions of NaCl were prepared by dissolving 584.5 mg of NaCl in 1000 mL DIW using a volumetric flask. This was diluted to yield a concentration of 10 mM NaCl. The pH of the stock solution was adjusted to pH 7 using NaOH and where necessary further dilutions were done to achieve concentration of 1 mM NaCl and the stock solutions were stored at 4 °C prior to use. The stock solutions of 1 and 10 mM NaCl were used as exposure media to study the influence of IS on aggregation and ζ-potential of the various ENPs concentrations over 48 h.

3.3.3. Influence of NOM

HA was used as a representative of NOM. Stock solutions were prepared by transferring 10 mg of HA powder into a 1000 mL volumetric flask and dissolved it in DIW to achieve concentration of 10 mg/L HA. The solution was stirred using a magnetic stirrer for 2 h to ensure complete dissolution and then the suspension was filtered using a 0.2 μm pore size standard filter (Millipore) to remove insoluble particles. The pH of the stock solution was adjusted to 7 using NaOH and stored under the same conditions as the stocks prepared in in section 3.3.2 prior to use or dilution to 1 mg/L HA where necessary. The stock solutions were used to investigate the influence of NOM on aggregation and ζ-potential of individuals and binary mixtures of ENPs at various concentrations. The samples under the influence of HA were studied following the procedure detailed in the preamble of this section.

3.4. Aggregation kinetics of individual and binary mixtures of ENPs in river water

The influence of river water on aggregation kinetics and ζ-potential of ENPs was studied using river water collected from two rivers, BR and ER both in South Africa. The river water was filtered, characterised and stored as detailed in section 3.2.1. The filtered river water was used as exposure media to investigate aggregation kinetics and ζ-potential of ENPs at concentrations provided in section 3.3. In addition, the concentrations of (0.1, 0.1) mg/L nAl_2O_3 and nCuO, respectively, were investigated since the concentrations of ENPs in the natural aquatic environment are likely to be very low. Where necessary, stock solutions at 10 mg/L ENPs were prepared in DIW at pH 7 in order to limit the influence of river water before exposure experiments were carried out. The procedure provided in section 3.3 was followed during the studies in river water.

© University of Pretoria

3.5. Aggregation Kinetics of binary mixtures of ENPs and TCS in river water

Stock solutions of TCS were prepared by dissolving 1 mg of TCS into 0.5 mL of acetone. This was done to ensure TCS was completely dissolved as it is insoluble in water. The resultant mixture was transferred into a 100 mL volumetric flask and diluted using DIW to achieve a concentration of 10 mg/L TCS and the stock solution was stored at 4 °C before use. Further dilutions were done in river water as exposure media to achieve concentrations of 100 and 1000 ng/L TCS which were used to investigate the influence of TCS on aggregation kinetics and ζ-potential of ENPs in river water. Suspensions of nCuO and nAl_2O_3 were prepared as described in section 3.4. Further dilutions were done to obtain lower concentrations of 1 and 0.1 mg/L of nAl_2O_3 or nCuO. Binary mixtures of ENPs and TCS investigated were at concentration of (0.1 mg/L ENPs, 100 ng/L TCS); (0.1 mg/L ENPs, 1000 ng/L TCS); (1 mg/L ENPs, 100 ng/L TCS); (1 mg/L ENPs, 1000 ng/L TCS) in river water as exposure media. The samples were analysed for ζ-potential and HDD over 48 h.

3.6. Aggregation Kinetics of ternary mixtures of ENPs and TCS in river water

The stock solutions of TCS and suspensions of ENPs prepared in section 3.5 were used to study the aggregation kinetics of the ternary mixtures. Ternary mixtures were prepared at the lower two concentrations of the ENPs (0.1 and 1 mg/L) and the two TCS concentrations (100 and 1000 ng/L). These concentrations of ENPs were chosen as they are close to what is expected in the environment and the chosen concentrations of TCS are within what is expected in freshwater systems as shown in Table 2.3. The concentrations of ternary mixtures are summarised in Table 3.2.

© University of Pretoria

Table 3.2: Mixture concentrations of studied ternary mixtures

Sample number	nCuO (mg/L)	nAl_2O_3 (mg/L)	TCS (ng/L)
1	0.1	0.1	100
2	0.1	1	100
3	1	0.1	100
4	1	1	100
5	0.1	0.1	1000
6	0.1	1	1000
7	1	0.1	1000
8	1	1	1000

3.7. Dissolution of individual and mixtures of ENPs in river water

Samples of individual ENPs as well as binary and ternary mixtures prepared for aggregation kinetics studies as described in sections 3.4, 3.5 and 3.6 were also used for dissolution studies. In addition, samples were collected for dissolution studies after 2 and 48 h, and then filtered to remove particles using Amicon ultra-15 filters (MWCO 3 kDa). The samples were then loaded into 15 mL centrifugal filters and centrifuged at high-speed of 4000 xg for 45 min. Thereafter 10 mL aliquot of the filtrate were collected and preserved using 20 µL of concentrated HNO_3 prior to analysis. For quality control, samples of inorganic salts of copper and aluminium, that is ($CuSO_4$) and ($AlCl_3.6H_2O$), respectively, within the same metal concentration as in samples of ENPs were prepared following the same procedure. All measurements were done in triplicates using inductively coupled plasma mass spectrometer (ICP-MS) (ICPE-9820, Shimadzu, Japan).

3.8. Experimental measurements and statistical analysis

The results are recorded as mean value ± standard deviation (mean ± SD). Two-way analysis of variance (ANOVA) was used for statistical differences. Differences within and between samples were considered statistically significant when at $p < 0.05$. Statistical analysis was done using GraphPad Prism Version 5.04 (GraphPad Prism software Inc., San Diego, CA, USA).

© University of Pretoria

Chapter 4: Results and Discussion

4.1. Characterisation of ENPs

4.1.1. Characterisation of ENPS using TEM

TEM images of both nAl_2O_3 and nCuO (Figure 4.1) show that nCuO had a mixture of hexagonal, rods, and spherical shapes with size range of 18-47 nm (Figure 4.1a). The nAl_2O_3 had both spherical and hexagonal shapes with size range of 35–55 nm (Figure 4.1b). Therefore, TEMs size results were within the manufacturer's specified values for each type of ENPs.

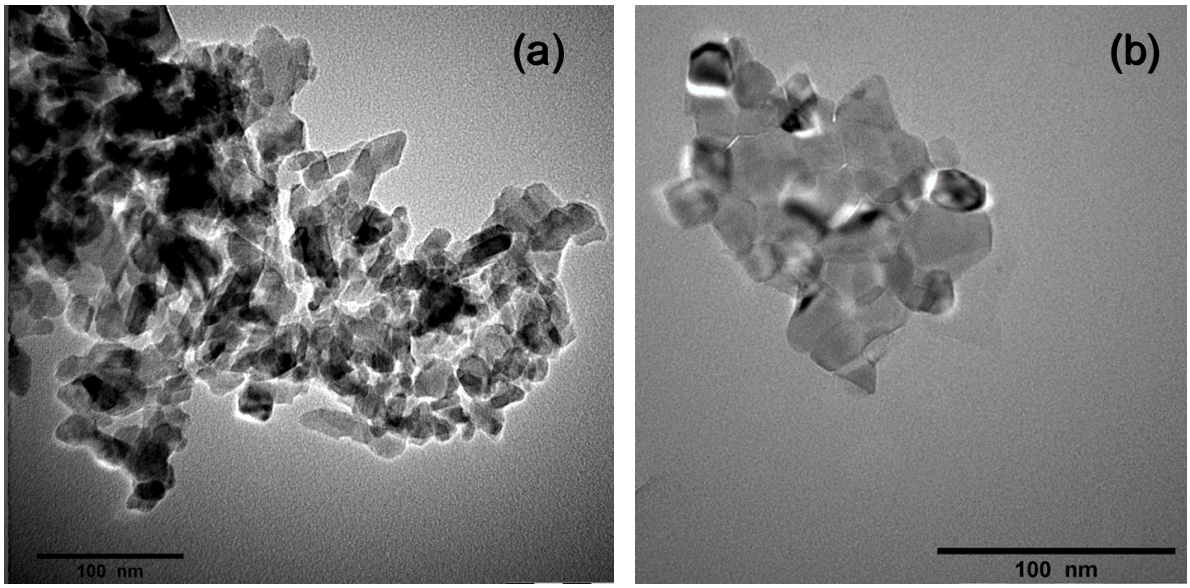

Figure 4.1: TEM images of (a) nCuO and (b) nAl_2O_3. The scale bars correspond to 100 nm.

4.1.2. Characterisation of ENPs using PXRD

The PXRD spectra patterns for the nAl_2O_3 and nCuO are shown in Figure 4.2. Results indicate that the majority of the nAl_2O_3 was the monoclinic alpha phase (Figure 4.2a). Traces of the hexagonal corundum were identified as an impurity phase. The PXRD spectra patterns for nCuO indicate that it was a pure beta phase, i.e. free from impurities (Figure 4.2b).

© University of Pretoria

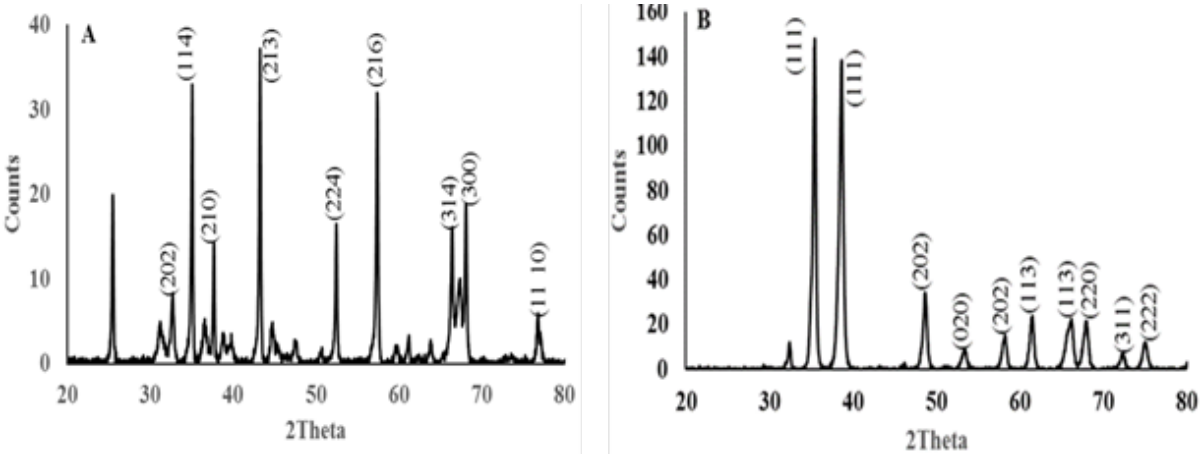

Figure 4.2: PXRD results of nAl_2O_3 (a) and nCuO (b).

4.1.3. Characterisation of ENPs using BET

The BET results showed that the surface area of nAl_2O_3 was 50.5 m^2/g and that of nCuO was 29 m^2/g according to the manufacturer. Therefore, the BET surface area of nAl_2O_3 was about 27-fold higher relative to that of nCuO.

4.2. Aggregation kinetics of Individual ENPs in DIW

4.2.1. Influence of pH

Results on the effects of pH (in the range 3–9) on HDD and ζ -potential at different exposure concentrations indicated the isoelectric point (IEP) for both ENPs was around pH 4 (pH_{IEP}). The observed IEP of 4 is not out of the norm as it is influenced by numerous factors including size distribution, morphology and coating material of the ENPs (Egerton, 2013). Previous studies on nAl_2O_3 have reported pH_{IEP} of 7.7 (Mahdavi et al., 2015) and 7.5 to 8 (Mui et al., 2016). At pH < pH_{IEP}, ζ-potential was positive but changed to negative at pH > pH_{IEP} in agreement with earlier studies (Ghosh et al., 2008; Griffitt et al., 2008). The 0.1 mg/L nAl_2O_3, at pH < pH_{IEP}, and highest pH of 9 had the highest HDD (1339 ± 321) relative to those of 1 mg/L (1293 ± 277) and 10 mg/L (753 ± 139) (Figure 4.3b); but no clear trend was observed at pH range 4 < pH < 9. The observed low HDD at high concentration of ENPs was attributed to enhanced aggregation leading to the sedimentation of larger aggregates. This, in turn, led to smaller aggregate sizes in the suspension as evidenced by lower HDD at the high exposure concentration. High mass concentrations of ENPs results in higher particle number

© University of Pretoria

concentration which results in higher collision frequency between particles with resultant increase in aggregate size and sedimentation as observed previously (Chekli et al., 2015; Fang et al., 2017; Peng et al., 2017b). The reason for random HDD changes was due to aggregation and disaggregation of ENPs at low concentration of 0.1 mg/L. Further, ζ-potential results suggest that higher concentrations may hold higher surface charge (Figure 4.3a). Previously, it has been reported that low particle number concentration at infinite dilution of ENPs can lead to reduction in ζ-potentials (Tantra et al., 2010; Wang et al., 2013). Hence, this may plausibly account at pH > pH_{IEP}, why 10 mg/L had the highest ζ-potential, and in turn, was more stable based on limited HDD changes. Results indicated that at circumneutral pH (pH 7) irrespective of ENPs exposure concentration, HDD values were < 1 000 nm; implying their likelihood to be stable in the aquatic systems generally within pH range 6 to 9 (Carlson, 2002).

Similarly, for nCuO the highest HDD was observed at pH_{IEP} of about 4 which compares well with pH 5.42 reported by (El-Trass et al., 2012). The lowest concentration of 0.1 mg/L exhibited the highest HDD value (1 552 ± 513 nm) (Figure 4.3d), and the least at 10 mg/L (804 ± 73 nm), and plausibly due to rapid aggregation of ENPs at high concentration resulted to formation for larger aggregates leading to sedimentation, and therefore, lower HDD at 10 mg/L. However, although at 10 mg/L nCuO had the least HDD, ζ-potential results were similar for all concentrations (Figure 4.3c) over pH range 3 to 9. This suggests that ζ-potential is unlikely to be the only factor influencing aggregation in DIW under the conditions considered (Figure 4.3d). Similar trends in the effect of concentration on aggregation of nCuO have been reported (Heinlaan et al., 2016; Sousa and Teixeira, 2013) where measured aggregate size increased as the exposure concentration decreased. Sedimentation at high concentration may be the underpinning mechanism to this phenomenon exhibited by nCuO. Other soluble ENPs such as nAg and nZnO in aqueous media exhibit increasing aggregation with increase in concentration (Thwala et al., 2016). Hence, the stability of ENPs in aquatic environment are not only pH dependent (Bian et al., 2011; Loosli et al., 2013), but on the type of ENPs as well, as the results for nCuO indicate.

To understand the aggregation kinetics of ENPs over time, and at relevant pH in the environment; further investigations were done on the effect of the ζ-potential on aggregation at circumneutral pH (Figure 4.4). The results show that, although nAl_2O_3 had negative ζ-potential (-13 and -19 mV) over 48 h at 0.1 mg/L (Figure 4.4a), changes in HDD were within a narrow range of 664 to 794 nm (< 1 000 nm) over 48 h (Figure 4.4b). The polydispersity

© University of Pretoria

index (PDI) was in the range 0.4 to 1.0 implying the system had a wide distribution of particle sizes due to dynamic aggregation and disaggregation processes (Donini et al., 2002; Lowry et al., 2016; Nidhin et al., 2008; Sreeram et al., 2006). At 1 and 10 mg/L, higher ζ-potential in the range of -20 to -25 mV was observed over 48 h. Consequently, concentration-dependent HDD values were observed (Figure 4.4b). Hence, nAl_2O_3 is likely to be stable at higher concentrations in aqueous media compared to lower concentrations where the later are likely to be found in the environment.

In addition, because of higher solubility of nCuO (Adeleye et al., 2014; Studer et al., 2010) than nAl_2O_3 (Wang et al., 2010), results show that the released positively charged Cu^{2+} species may have contributed to the reduction of negative charges on nCuO ζ-potential. This is due to increasing positive surface charge as concentration of Cu^{2+} increases in the system as a result of dissolution of nCuO. This, in turn, leads to screening of the negative charge on nCuO, thus lowering the ζ-potential (Brown et al., 2016; Degen and Kosec, 2000; Thwala et al., 2013). Conversely, where the ζ-potential (Figure 4.4c) were similar for the three exposure concentrations at pH 7, results in Figure 4.4 indicate HDD decreased with increase in exposure concentration.

© University of Pretoria

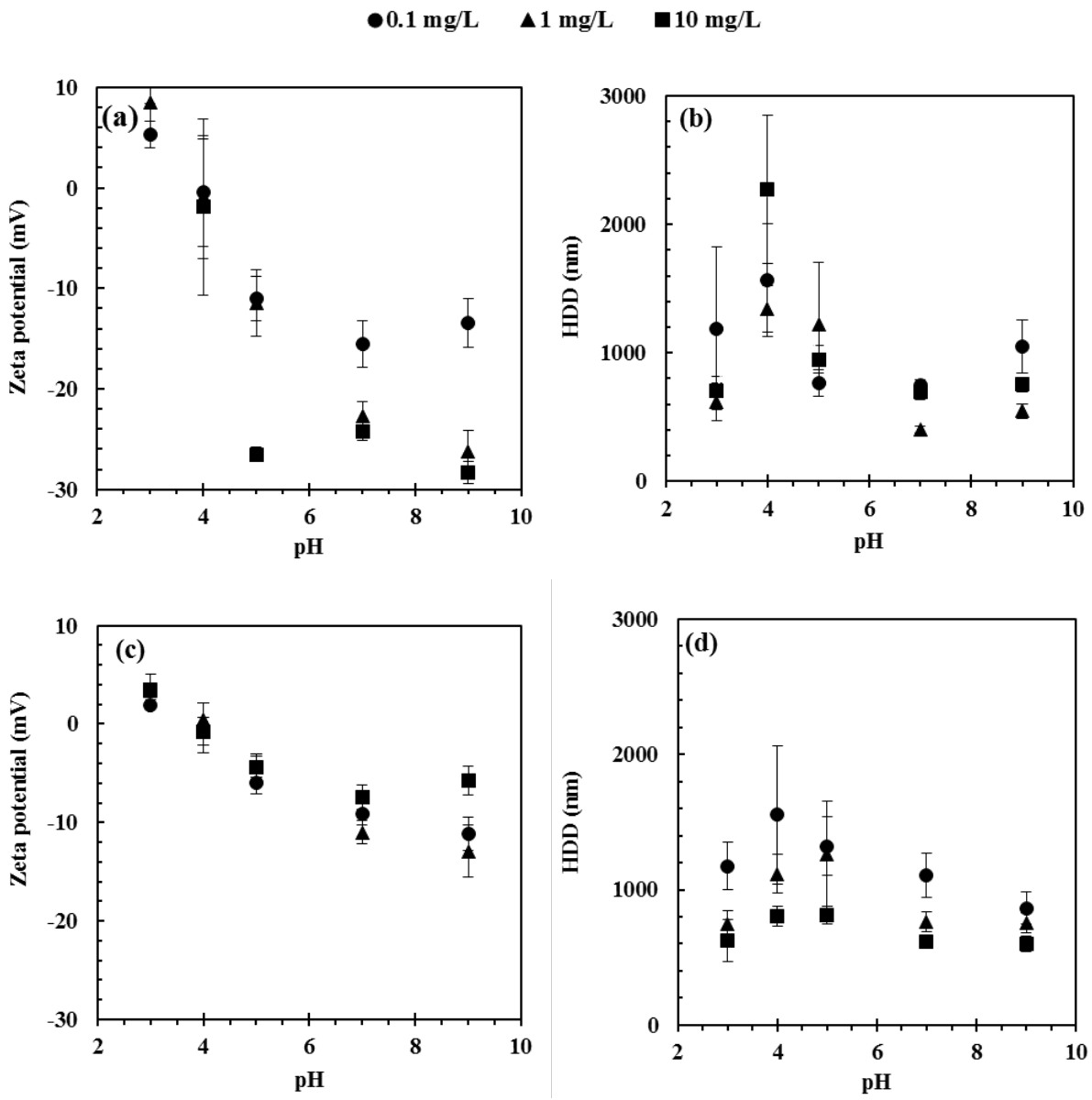

Figure 4.3: ζ-potential and HDD for nAl_2O_3 (a and b, respectively), and nCuO (c and d, respectively) in DIW after 2 h. Error bars represent standard deviations (SD) for three replicates.

The higher HDD observed at lower concentration of 0.1 mg/L plausibly were due to other factors besides the surface charge of ENPs and it warrants further investigation. The low HDD observed at higher concentrations of ENPs are plausibly due to high aggregation and sedimentation processes leaving only smaller particles in the suspension. Depending on ENPs type, aggregation may vary considerably even at the same pH (pH 7), and exposure time (48 h) (Figure 4.4). For example, irrespective of exposure concentration, HDD for nAl_2O_3 was lower compared to nCuO. The difference in aggregation was attributed to lower sizes range of

© University of Pretoria

nCuO (18–48 nm); hence rendering them more reactive compared to those of nAl_2O_3 (35–47 nm) (Auffan et al., 2009; Rusanov, 2005). This is because the novel properties of ENPs are greater at lower nano-size range than at higher size range (Auffan et al., 2009). These observations are in agreement with the predictions of the classical Derjaguin-Landau-Verwey-Overbeek (DLVO) theory as reported elsewhere on studies involving hematite ENPs where 12 nm exhibited higher aggregation than 32 nm under identical exposure conditions (He et al., 2008).

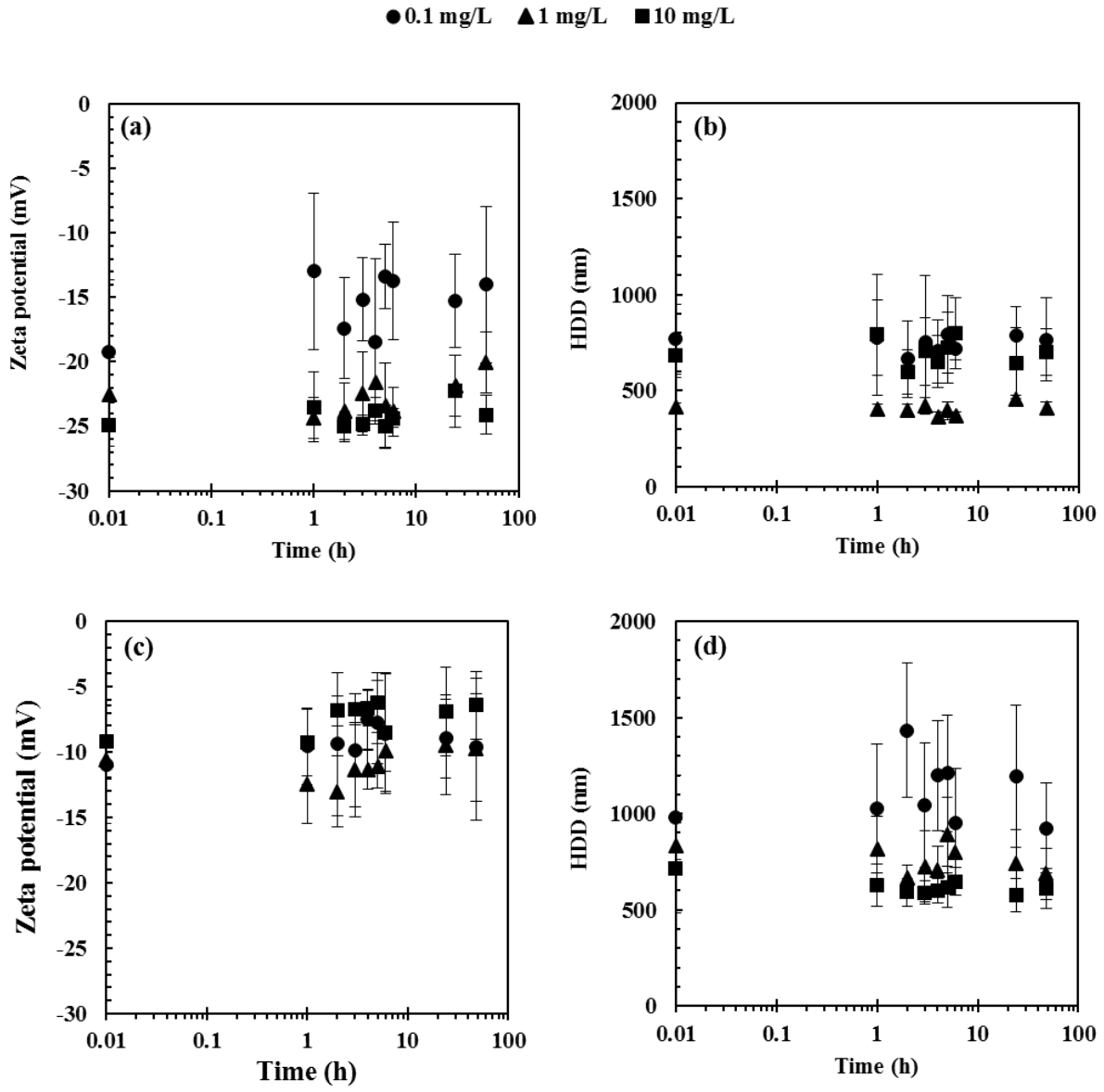

Figure 4.4: ζ-potential and HDD for nAl_2O_3 (a and b, respectively), and nCuO (c and d, respectively) in DIW over 48 h at pH **7.** Error bars represent standard deviations (SD) for three replicates.

© University of Pretoria

The influence of pH on aggregation of ENPs over 48 h at 0.1 mg/L was investigated. The results indicate that, irrespective of pH, both ζ-potential and HDD do not vary significantly (Figure 4.5). pH values away from the pH_{IEP} show comparable HDDs within the experimental time frame considered in this study. In addition, the influence of pH was investigated at higher concentrations of 1 and 10 mg/L. The higher concentrations of nAl_2O_3 had higher ζ-potential compared to the lower concentration of 0.1 mg/L whereas that of nCuO was comparable across all the concentrations (Appendices. 4.1 and 4.2). The lower ζ-potential observed at lower concentrations of nAl_2O_3 may be attributed to a high dissolution of nAl_2O_3 at lower concentration (Table 4.2) where the released Al^{3+} may have had screening effect on the negative charges of nAl_2O_3 with resultant reduction in ζ-potential.

© University of Pretoria

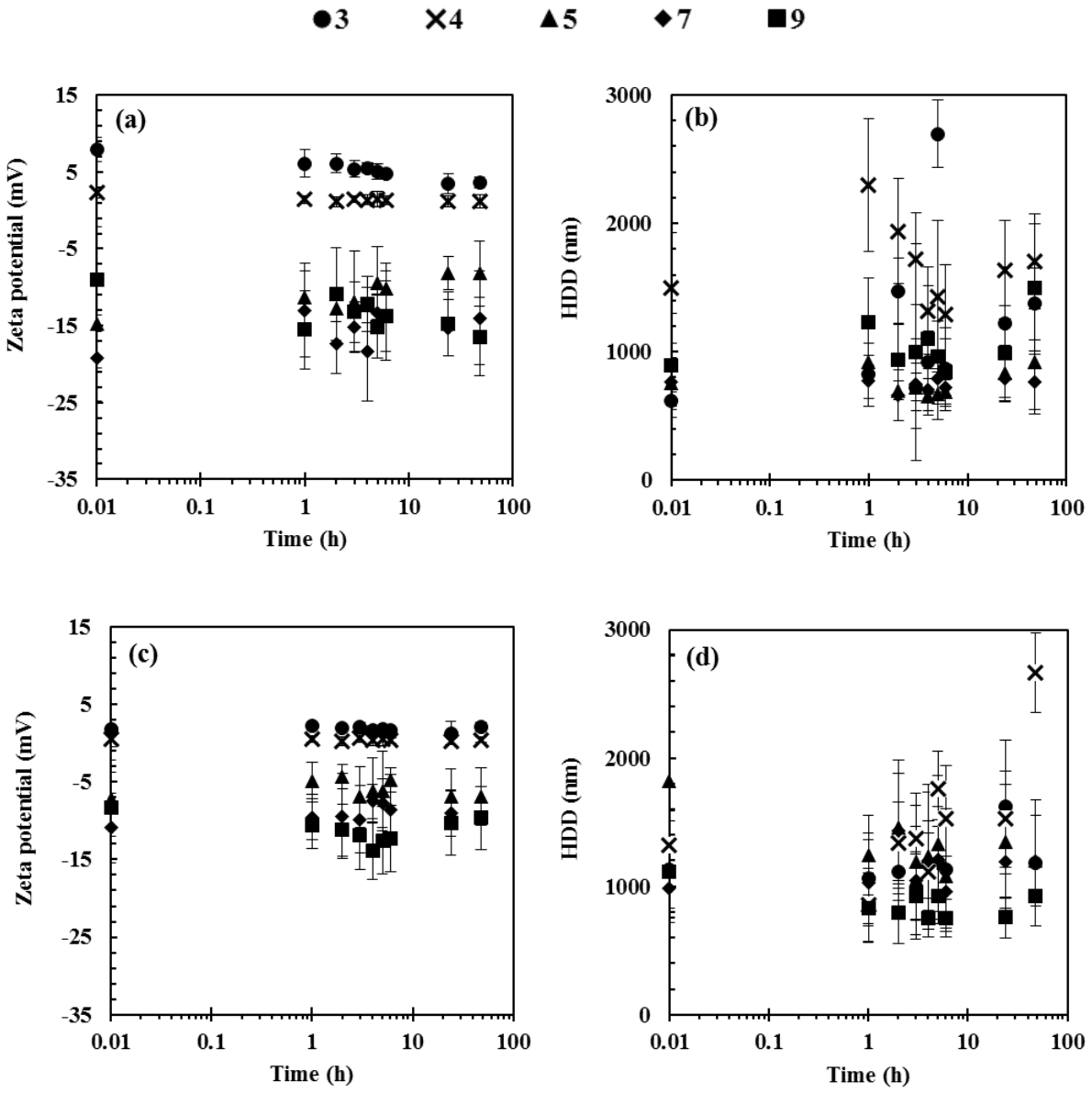

Figure 4.5: The ζ-potential and HDD for nAl_2O_3 (a and b, respectively), and nCuO (c and d, respectively) in DIW within pH range of 3 to 9 over 48 h at 0.1 mg/L. Error bars represent standard deviations (SD) for three replicates.

Sedimentation kinetics of ENPs was studied using ultraviolet-visible (UV-Vis) spectroscopy over 48 h. No peaks were observed in the wavelength range 200 to 800 nm for both nAl_2O_3 and nCuO at the concentrations used in the study except water absorption peak as shown for nCuO (Figure 4.6). Similar observation have been reported at variant concentrations of 25 to 100 mg/L nCuO used for exposure (Heinlaan et al., 2016). However, this technique was

© University of Pretoria

nevertheless successfully applied for the characterisation of ENPs during synthesis where absorption maximum wavelength for nAl_2O_3 is within the range 200 to 250 nm (Piriyawong et al., 2012; Prashanth et al., 2015), whereas for nCuO it is 250 to 400 nm (El-Trass et al., 2012; Naika et al., 2015; Son et al., 2009). Based on these results, UV-vis may not be a suitable technique for studies involving sedimentation kinetics of the considered ENPs because of their low absorption at low concentration. However, the technique is effective for ENPs that absorb strongly in the UV-vis region such as nAg and gold nanoparticles (Haiss et al., 2007; Sikder et al., 2018; Zook et al., 2011).

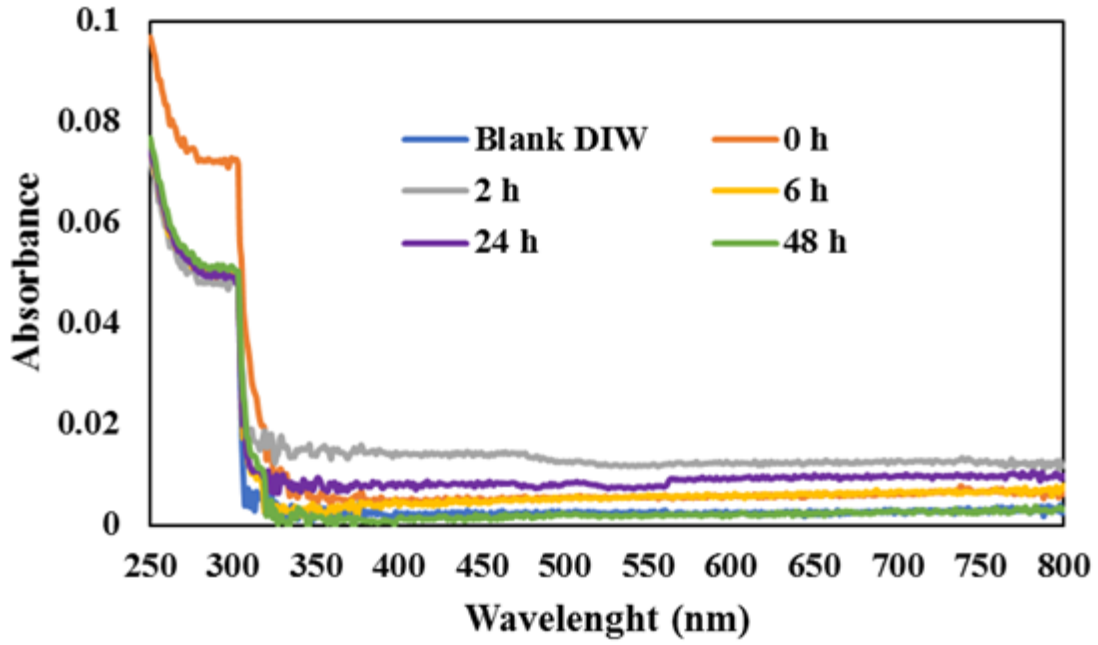

Figure 4.6: UV-visible spectra of 1 mg/L nCuO in DIW at pH 7 over 48 h.

4.2.2. Influence of IS

Effect of IS on the stability of ENPs in aqueous media where an increase in electrolytes concentration resulted in a reduction of ζ-potential, and in turn, an increase in ENPs aggregation has been reported (Badawy et al., 2010; French et al., 2009; Wang et al., 2017). Herein, the effect of IS on aggregation of nAl_2O_3 and nCuO was investigated using monovalent electrolyte NaCl at circumneutral pH (pH ≈ 7) at two concentrations of 1 and 10 mM in DIW. Lower ζ-potentials were observed at higher IS (10 mM) over 48 h (Figures 4.7a and c) for both ENPs, but it was more apparent for nCuO (Figure 4.7c). The effect was independent of exposure concentration. At low IS (1 mM), no change in ζ-potentials was observed at exposure

© University of Pretoria

concentrations of 0.1 and 1 mg/L (Figures 4.7a and c) relative to the control (Figures 4.4a and c). Compared to the control (Figures 4.4b and d), the changes in ζ-potential observed as IS was increased from 1 to 10 mM had an insignificant effect on HDD, as shown in Figures 4.7b and d. The exception was nAl_2O_3 after 24 h (Figure 4.7b) at 10 mg/L. For both ENPs, the PDI ranged from 0.4 to 1 indicating wide size variations between smaller and larger aggregates in each system. However, Godymchuk et al. (2015); reported a significant influence of IS on ζ-potential and HDD from 0 to100 mM NaCl at circumneutral pH on nAl_2O_3 as described in Section 2.3.2.1.

Results in Figure 4.7c indicate no considerable change in ζ-potential (< 5 mV) as IS increased from 1 to 10 mM for nCuO at all concentrations of ENPs because Na^+ has low charge screening effect on the EDL. Therefore, it exerts weak influence on aggregation (Peng et al., 2017a). In studies, where significant ζ-potential reduction and corresponding increase in HDD were observed for nCuO, both very high exposure concentrations of ENPs (e.g. > 100 mg/L) and IS (up to 100 mM) were used as discussed in Section 2.3.2. For example, Peng et al. (2017) investigated up to 100 mM NaCl on 100 mg/L nCuO. Consequently, a decline in ζ-potential, and high HDD were observed. The lower IS (1 mM) used in this study sought to mimic those widely found in the natural environment (Guo et al., 2001; Jalali and Jalali, 2016), although it was still much higher than the actual ones.

In freshwater systems, the concentration of Na^+ is in the range of 0.26 to 0.78 mM (Guo et al., 2001; Jalali and Jalali, 2016); whereas K^+ is much lower at 0.001 to 0.005 mM (Talling, 2010). This points to the likelihood that metal oxide ENPs are unlikely to be destabilized in freshwater systems by monovalent electrolytes at the concentrations found in the environment. Khan et al. (2018b) found that low IS, from the presence of monovalent electrolyte (NaCl), had at most a very limited effect on the aggregation and sedimentation efficiency of nZnO. Overall, monovalent electrolytes like Na^+ are unlikely to induce a change in the aggregation of metal-based ENPs. This is indicated by the results for nAl_2O_3 and nCuO in Figures 4.7b and d.

© University of Pretoria

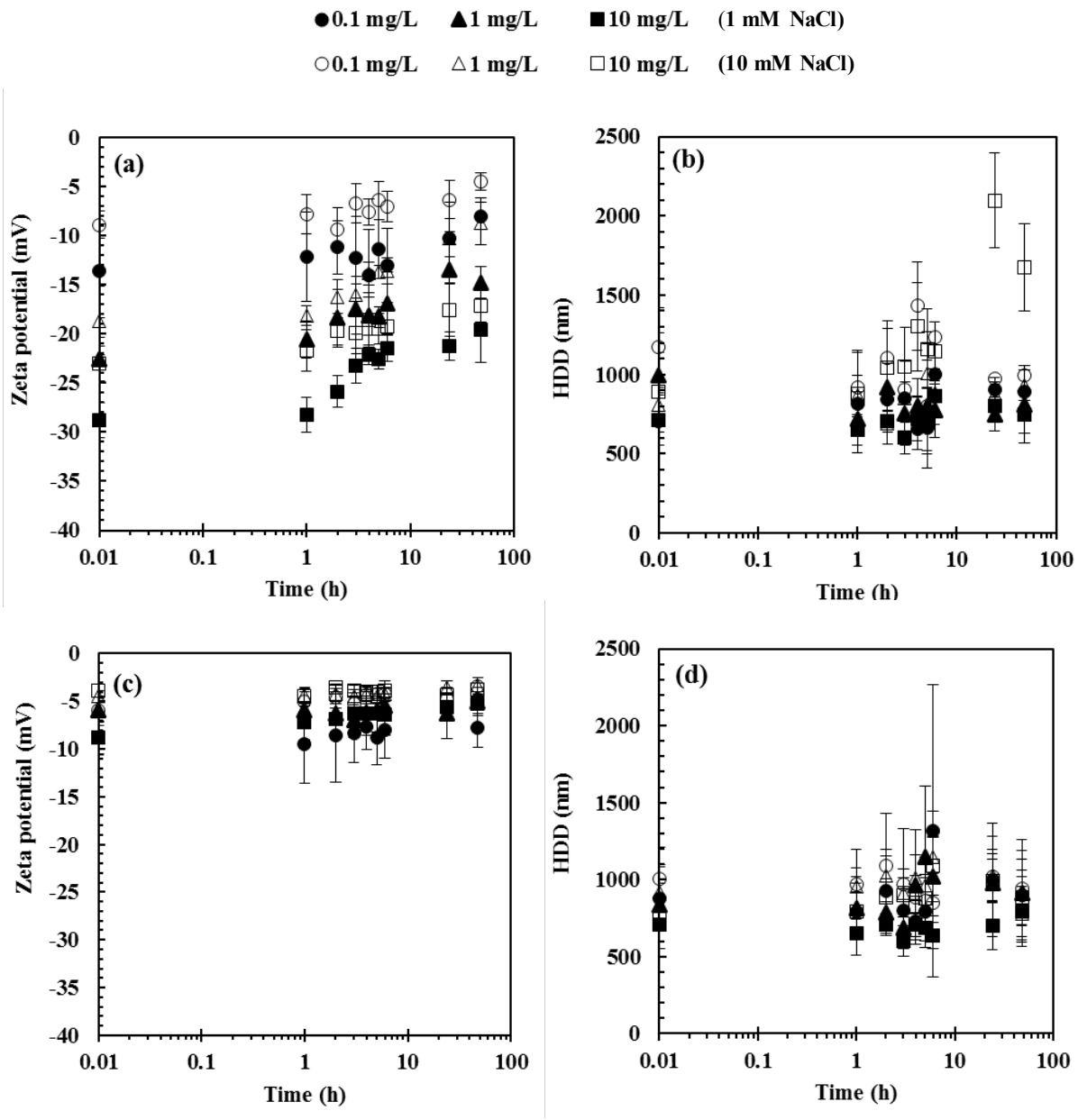

Figure 4.7: ζ-potential and HDD for nAl_2O_3 (a and b, respectively), and nCuO (c and d, respectively) in DIW at 1 and 10 mM NaCl (pH 7) over 48 h. Error bars represent standard deviations (SD) for three replicates.

4.2.3. Influence of HA

Numerous studies have reported the ability of NOM to stabilize ENPs via various mechanisms (e.g. surface hydroxyl protonation, outer-sphere complexation, inner-sphere complexation etc.) as discussed in Section 2.2.4.3. Results of ζ-potential and aggregation shown in Figure 4.8 indicate that, as HA concentration is increased from 1 to 10 mg/L, HA imparted higher negative

© University of Pretoria

charge on the ENPs (increase in ζ-potentials) as shown in Figures 4.8a and c, for nAl_2O_3 and nCuO, respectively.

As a result of the high negative charge imparted by NOM on ENPs, the interparticle repulsive energy increased, thus inhibiting aggregation (Delay et al., 2011; Thio et al., 2011; Yang et al., 2009; Zhang et al., 2009). In the absence of NOM (0 mg/L NOM) at circumneutral pH and 0.1 mg/L of ENPs, negative ζ-potentials of < -24 and < -10 mV were observed for nAl_2O_3 and nCuO, respectively (Figures 4.4a and c). In contrast, after introducing 10 mg/L NOM, ζ-potentials of less than -25 mV were observed as shown in Figures 4.8a (nAl_2O_3) and 4.7c (nCuO). Consequently, lower aggregation was evident (Figure 4.8b for nAl_2O_3 < 700 nm, and Figure 4.8d for nCuO <800 nm). In addition, marginal variations in HDD were apparent for both ENPs over the 48 h (Figures 4.8b and d) because HA-coated ENPs were less aggregated compared to ENPs without the NOM coating. For example, for nCuO at 0.1 mg/L, HDD increased to approximately 1400 nm in the absence of HA (Figure 4.4d). Thus, these results offer antecedent evidence of adsorption of HA (although adsorption was not tracked in this study because of poor absorption of the studied ENPs in the UV-Vis region) onto ENPs where they enhanced their electrostatic repulsion; thus, leading to increased stability.

© University of Pretoria

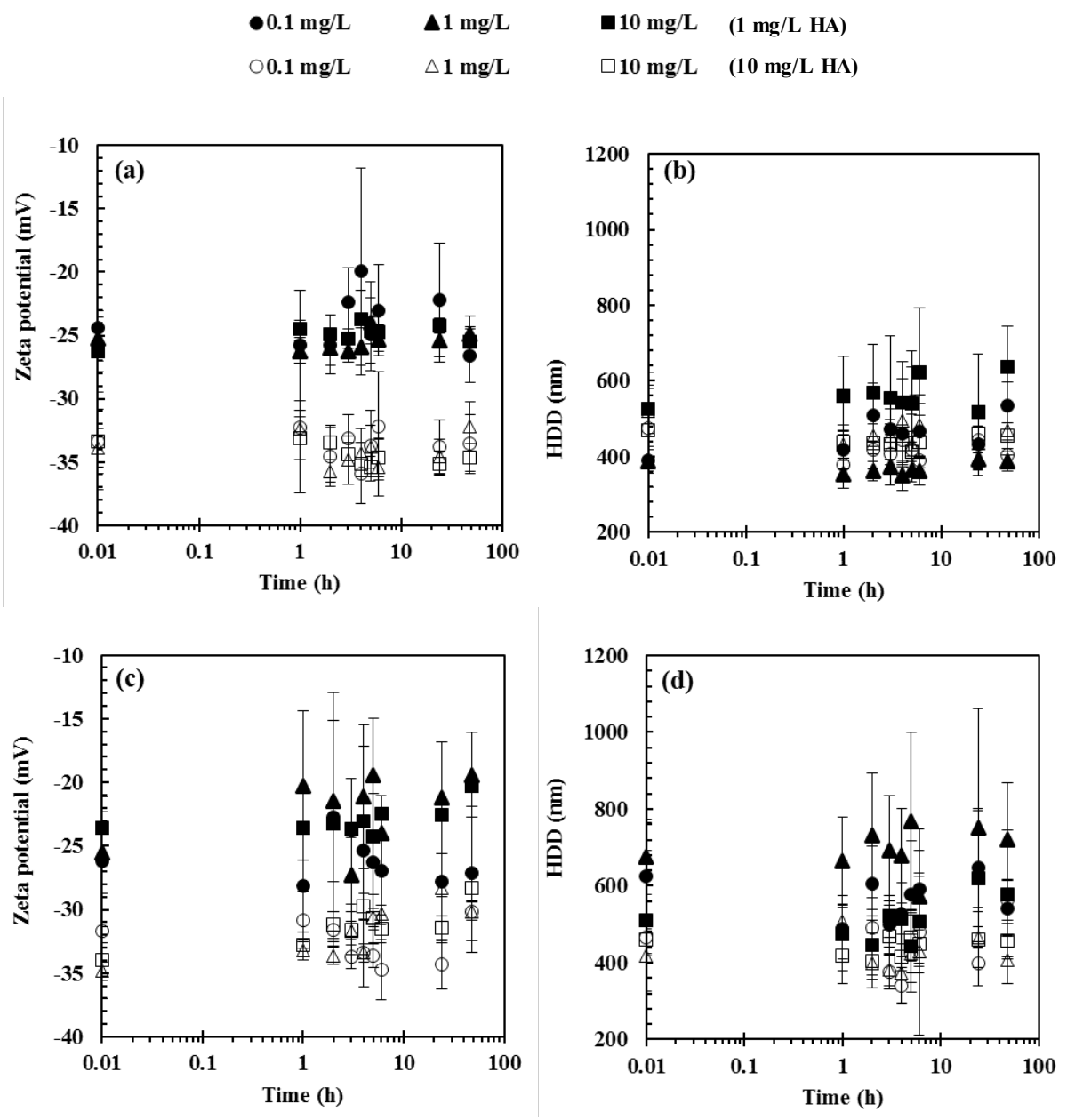

Figure 4.8: ζ-potential and HDD for nAl_2O_3 (a and b, respectively), and nCuO (c and d, respectively) in DIW at 1 and 10 mg/L HA (pH 7) over 48 h. Error bars represent standard deviations (SD) for three replicates.

The increase in negative charge on the ENPs was due to the negatively charged adsorbed HA molecules on the surfaces of nAl_2O_3 and nCuO at pH 7 via mechanisms discussed in section 2.2.4.3. Three plausible processes may account for the lower ζ-potential observed on nCuO in the presence of HA. The larger surface area of nAl_2O_3 (50.5 m^2/g) compared to that of nCuO (29 m^2/g) may have enhanced higher adsorption of HA on the former. This is because ENPs

© University of Pretoria

with larger surface area exhibit higher adsorption capacity for NOM (Monikh et al., 2018). For instance, nFe_2O_3 was shown to adsorb more NOM with resultant higher ζ-potential than $nTiO_2$ due to a larger surface area, irrespective of exposure media (e.g. groundwater, lake water, etc.) (Chekli et al., 2015). Further, ligand exchange between HA and metal oxide ENPs may have occurred (Yang et al., 2009), for example, the hydroxyl groups on metal oxide surfaces with NOM may provide fewer hydroxyl groups for protonation which can partly be responsible for the decrease in the measured ζ-potential (Bian et al., 2011).

In addition, organic anions in HA may have increased the negative charge density adjacent to the particle surface. This causes a shift in the position of the shear plane further away from the surface resulting in a decrease in ζ-potential (Bian et al., 2011; Zhang et al., 2009). This phenomenon may likely have been the dominant one for nCuO. Other studies have reported that HA promotes electrostatic stabilization at low concentrations (in this study 1 mg/L). However, at higher concentrations, both steric and electrostatic stabilization processes enhance the stability of ENPs (10 mg/L) (Chen et al., 2012). This may account for lower HDD at higher HA concentration (10 mg/L) as shown in Figures 4.8b and d. Due to the complexity of the interactions between ENPs and HA, plausibly the three processes may have occurred concurrently which accounts for the differences in the aggregation of nAl_2O_3 and nCuO in the presence of HA.

4.3. Aggregation kinetics of binary mixtures of ENPs in DIW

4.3.1. Influence of nCuO on aggregation of nAl_2O_3 at pH 4 and 7

The influence of pH on aggregation of binary mixtures at pH 4 and 7 was studied. At pH 4, concentration independent effect of adding various concentrations of nCuO to 1 mg/L nAl_2O_3 was observed on ζ-potential. The ζ-potential increased from *ca.* 0 mV in the absence of nCuO to *ca.* +17 mV in the presence of 10 mg/L nCuO as shown in Figure 4.9a. HDD decreased at lower concentrations of nCuO (0.1 and 1 mg/L). However, at the higher concentration of 10 mg/L nCuO, HDD was comparable to that observed from 1 mg/L nAl_2O_3 at its pH_{IEP} as shown in Figure 4.9b. The results indicate that pH_{IEP} values of the mixtures are different from that of the respective pure components. The lower HDD observed from mixtures may be attributed to

© University of Pretoria

the higher ζ-potential of the mixtures. The increase in ζ-potential at pH away from pH_{IEP} promotes interparticle repulsion which impedes aggregation as discussed in section 2.2.5.1.

At circumneutral pH, concentration dependent effect of nCuO was observed on ζ-potential which decreased from *ca.* -25 mV in the absence of nCuO to *ca.* -5 mV in presence of 10 mg/L nCuO (Figure 4.9c). The reason for the reduction in ζ-potential at higher concentration of nCuO in the mixture could be associated to the hetero-aggregation which could have led to the reduction in particles number concentration with the resultant decrease in ζ-potential (Tantra et al., 2010; Wang et al., 2013). In addition, the charge screening effect of released Cu^{2+} from the dissolution of nCuO may have reduced the observed ζ-potential. However, no meaningful difference was observed during the first 5 h for HDD irrespective of mixture composition. However, from 6 to 48 h the mixture of 1 mg/L nAl_2O_3 and 10 mg/L nCuO exhibited the highest HDD (Figure 4.9d). The increase in HDD at high concentration of ENPs may be attributed to increased particle collision frequency leading to enhanced aggregation (Amal et al., 1992). The HDDs from the mixtures at 0.1 and 1 mg/L nCuO at both pH 4 and 7 are comparable.

4.3.2. Influence of nAl_2O_3 on aggregation of nCuO at pH 4 and 7

Introduction of 0.1 mg/L nAl_2O_3 to 1 mg/L nCuO in DIW at pH 4 led to negative ζ-potential up to a maximum of -8 mV. However, increasing the concentration of nAl_2O_3 from 0.1 to 1 or 10 mg/L in the mixtures resulted in positive ζ-potentials up to a maximum of +17 mV at 10 mg/L nAl_2O_3 as shown in Figure 4.10a. The low ζ-potentials observed at lower concentration of nAl_2O_3 may be due to the reduction in particle number concentration at infinite dilution of ENPs which leads to the reduction in ζ-potentials (Bhattacharjee, 2016; Tantra et al., 2010; Wang et al., 2013). For example, Wang et al. (2013), observed that increasing the concentration of bare TiO_2 from 0.5 to 5 mg/L at pH 6 resulted in an increase in ζ-potentials from -6.7 to 8.2 mV. During the first 6 h, HDD for nCuO was higher than that of any mixture concentrations studied, but at 24 and 48 h there is no significant difference in HDD (Figure 4.10b). The influence of nAl_2O_3 and nCuO on each other under various mixture concentrations was non-uniform as attested by results of ζ-potential and HDD shown in Figures 4.9a and b, and Figures 4.10a and b.

© University of Pretoria

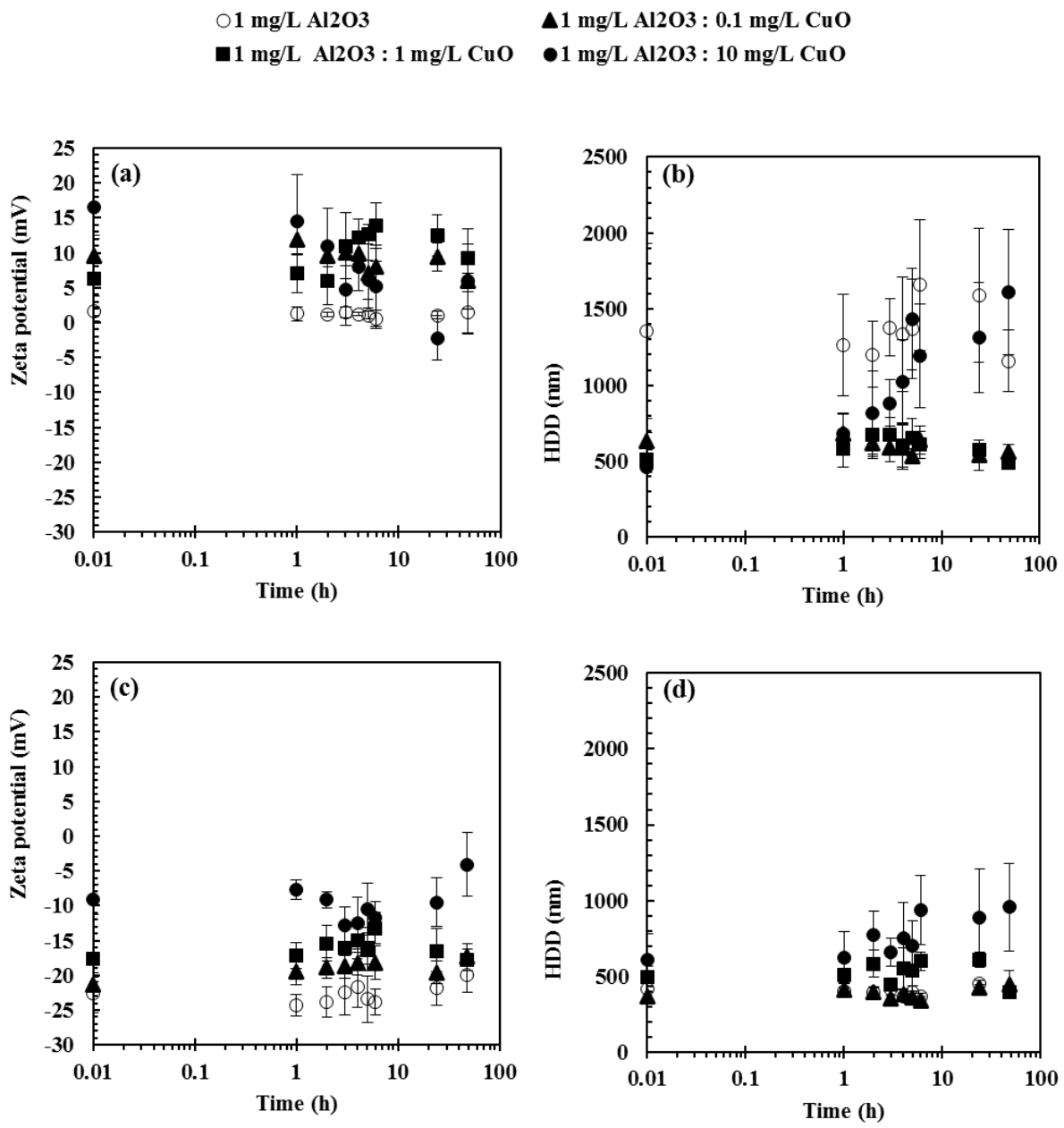

Figure 4.9: ζ-potential and HDD for pH 4 (a and b, respectively), and for pH 7 (c and d, respectively) in DIW at 1 mg/L nAl_2O_3 with varying concentrations of nCuO over 48 h. Error bars represent standard deviations (SD) for three replicates.

At higher pH of 7, concentration dependent increase in ζ-potential of the mixture was observed. ζ-potential increased with increasing concentration of nAl_2O_3 in the mixture from < -10 mV at 0.1 mg/L to *ca* -20 mV at 10 mg/L nAl_2O_3 in the mixture. Notably, the ζ-potential for 1 mg/L nCuO at pH 7 was in the range -9 to -13 mV (Figure 4.4c). Results showed marginal changes in ζ-potential by adding low concentration (0.1 mg/L) nAl_2O_3 to 1 mg/L nCuO. However, increasing the concentration of nAl_2O_3 to 1 or 10 mg/L, observed ζ-potential was higher than

© University of Pretoria

for individual nCuO (Figure 4.10c). Addition of various amounts of nCuO to a fixed concentration of nAl_2O_3 resulted in concentration-dependent ζ-potential and hetero-aggregation. Both increased with increasing concentration of nCuO in the mixture linked to adsorption of nCuO onto surfaces of nAl_2O_3 owing to its large surface area. This is apparent from the trend seen after 6 h of exposure (Figures 4.9c and d). A similar trend was observed by Monsouri et al., 2016 in their study involving nCuO and $nTiO_2$. However, the variation of nAl_2O_3 concentrations at a fixed concentration of nCuO yielded an increase in ζ-potential. A plausible mechanism for the variations in surface charge imparted on the surface of ENPs could be the selective sorption of NOM to surfaces of the ENPs. It is also plausible that nCuO adsorb different NOM molecules compared to Al_2O_3. The adsorbed NOM molecules on surfaces of the two ENPs might possess different surface functional groups and thus might impart different surface charges as observed elsewhere (Louie et al., 2015; Yin et al., 2015). In part this could be because the system had excess nAl_2O_3 uncoated by nCuO through adsorption (Figure 4.10c). However, increasing concentration of nAl_2O_3 had no significant influence on HDD which may be attributed to limited hetero-aggregation (Figure 4.10d).

© University of Pretoria

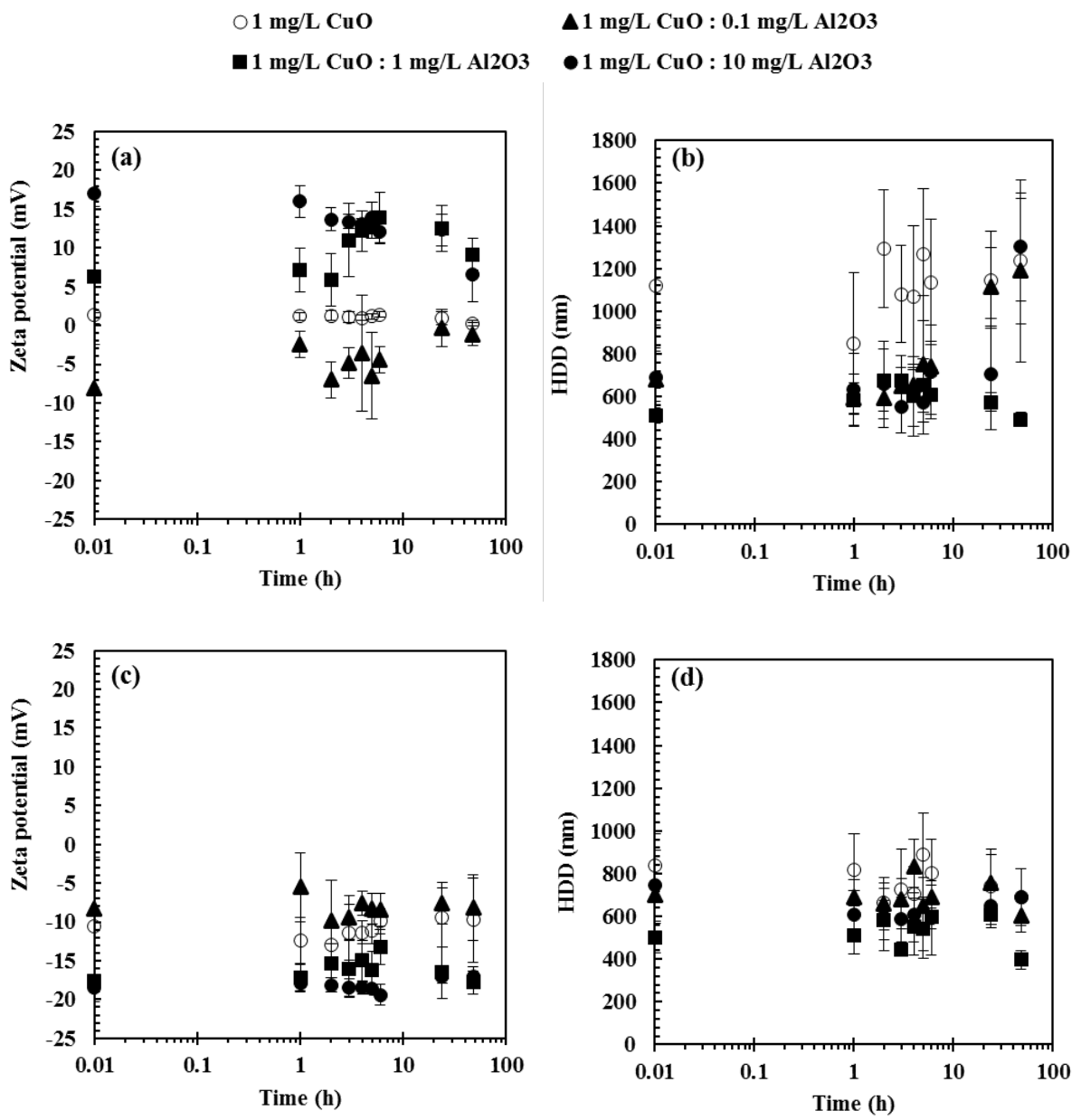

Figure 4.10: ζ-potential and HDD for pH 4 (a and b, respectively), and for pH 7 (c and d, respectively) in DIW at 1 mg/L nCuO with varying concentrations of nAl_2O_3 over 48 h. Error bars represent standard deviations (SD) for three replicates.

4.3.3. Influence of nCuO on aggregation of nAl_2O_3 in presence of electrolyte

The influence of IS on aggregation of binary mixtures of nAl_2O_3 and nCuO in DIW at pH 7 was studied. The ζ-potential decreased with increasing concentration of nCuO in the mixture. For example, at 0.1 mg/L nCuO in the mixture and 1 mM NaCl, ζ-potential was in the range of -16 to -18 mV. Increasing the concentration of nCuO in the mixture to 10 mg/L resulted in a decrease in ζ-potential to the range -10 to -14 mV as shown in Figure 4.11a. This range is

© University of Pretoria

higher than what was observed for individual 10 mg/L nCuO but less than what was observed for individual nAl_2O_3 at 1 mg/L (Figures 4.4a and c). The released ions from the dissolution of nCuO may have screened the charges on surfaces of mixture ENPs leading to the intermediate ζ-potential. In addition, at 10 mM NaCl, higher ζ-potential was observed for all mixture concentrations compared to 1 mM NaCl (Figures 4.11a and c). These observations are contrary to the predictions based on charge screening effect leading to compression of the EDL at higher IS. However, for individual ENPs, ζ-potential decreased with increasing IS under identical exposure media (Figures 4.7a and c). In the first 6 h, no significant differences in HDD were observed despite variability in ζ-potential because ENPs undergo rapid aggregation and disaggregation processes (Baalousha, 2009). The rapid aggregation and disaggregation processes were also confirmed by the PDI which was in the range 0.3 to 1.0 suggesting wide size distribution of particles in the system (Donini et al., 2002; Lowry et al., 2016; Nidhin et al., 2008). However, after 48 h, the HDD increased with increasing concentration of nCuO in the mixture as shown in Figures 4.11b and d. HDD was comparable at both 1 and 10 mM NaCl except at 24 and 48 h where the 10 mM NaCl showed higher HDD (Figures 4.11b and d).

4.3.4. Influence of nAl_2O_3 on aggregation of nCuO in presence of electrolyte

The ζ-potential increased with increasing concentration of nAl_2O_3 in the mixture. For example, at 10 mM NaCl and mixture concentrations of (1, 0.1) mg/L nCuO and nAl_2O_3, respectively, ζ-potential was in the range of -6 to -11 mV. However, after increasing the concentration of nAl_2O_3 in the mixture to the ratio (1, 10) mg/L nCuO and nAl_2O_3, respectively, ζ-potential increased from -22 to -26 mV and the range for individual nCuO was 0 to -4 mV as shown in Figure 4.12c. These results indicate that at high concentration of nAl_2O_3 in the mixture, there are more particles in the system (higher particle concentration) leading to higher ζ-potential beyond infinite dilution (Tantra et al., 2010; Wang et al., 2013). At high concentrations of nAl_2O_3 the released Cu^{2+} from nCuO was insufficient to screen the charge, leading to the observed increase in ζ-potential. Despite hetero-aggregation, the system had a wide particle size distribution as evidenced by the PDI (0.4 to 1). This shows huge discrepancies between smaller and larger aggregates of nanoparticles mixtures in a colloidal system. During the first 6 h, insignificant differences in HDD were observed. However, at 24 and 48 h, nAl_2O_3 concentration dependent increase in HDD was observed as shown in Figures 4.12b and d. The increase in HDD at higher concentration of nAl_2O_3 could be associated to hetero-aggregation and low dissolution of nAl_2O_3. This is contrary to observations regarding the influence of IS

© University of Pretoria

on aggregation of individual components where ζ-potential decreased with increase in IS (Figures 4.7a and c). Higher ζ-potential was observed for all mixture concentrations at 10 mM compared to 1 mM NaCl. For example, at the mixture concentrations of (1, 10) mg/L nCuO and nAl_2O_3, respectively, had ζ-potential in the range -17 to -18 mV and -22 to -26 mV at 1 mM and 10 mM NaCl, respectively, as shown in Figures 4.12a and c. A similar observation has been reported (Godymchuk et al., 2015). Godymchuk et al. 2015 studied the influence of IS due to NaCl on ζ-potential of aluminium nanoparticles and observed that ζ-potential increased with increasing IS. For example, it was 2.1 ± 0.3 mV at IS of 0.01 mM but increased to 11.9 ± 8.6 mV at higher IS of 10 mM.

© University of Pretoria

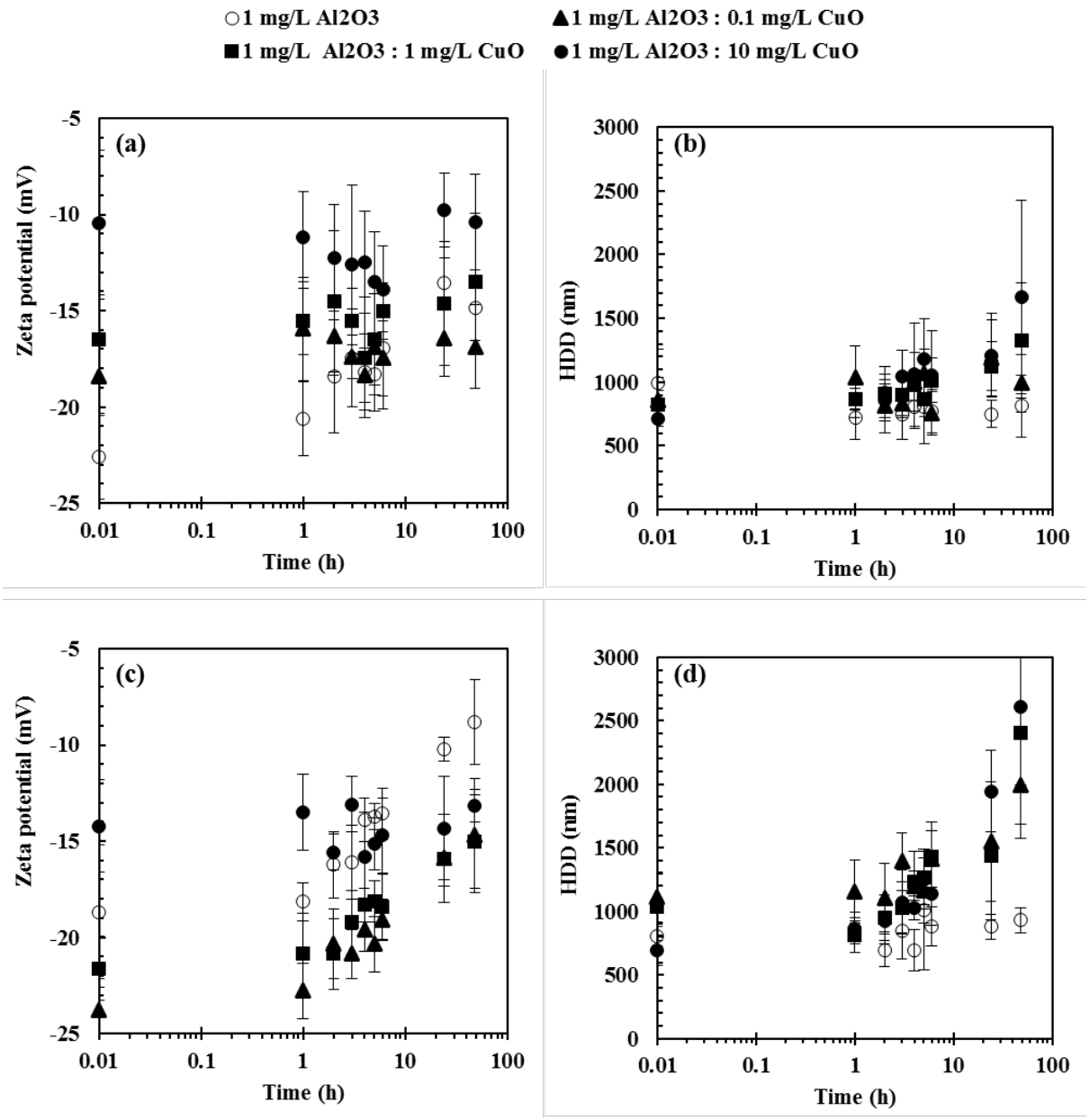

Figure 4.11: ζ-potential and HDD for 1 mM NaCl (a and b, respectively), and for 10 mM NaCl (c and d, respectively) in DIW at pH 7 for 1 mg/L nAl_2O_3 with varying concentrations of nCuO over 48 h. Error bars represent standard deviations (SD) for three replicates.

However, the increase in ζ-potential at higher IS for mixtures did not result in a decrease in HDD. For example, at 48 h, the HDD increased from 1719 ± 386 nm at 1 mM NaCl to 2934 ± 879 nm at 10 mM NaCl as shown in Figures 4.12b and d. These results suggest that aggregation does not depend on ζ-potential alone but, other factors may outweigh the interparticle repulsive forces. In the current case hetero-aggregation was favoured based on the increased HDD observed for mixtures compared to individual ENPs. This was most apparent at 24 and 48 h.

© University of Pretoria

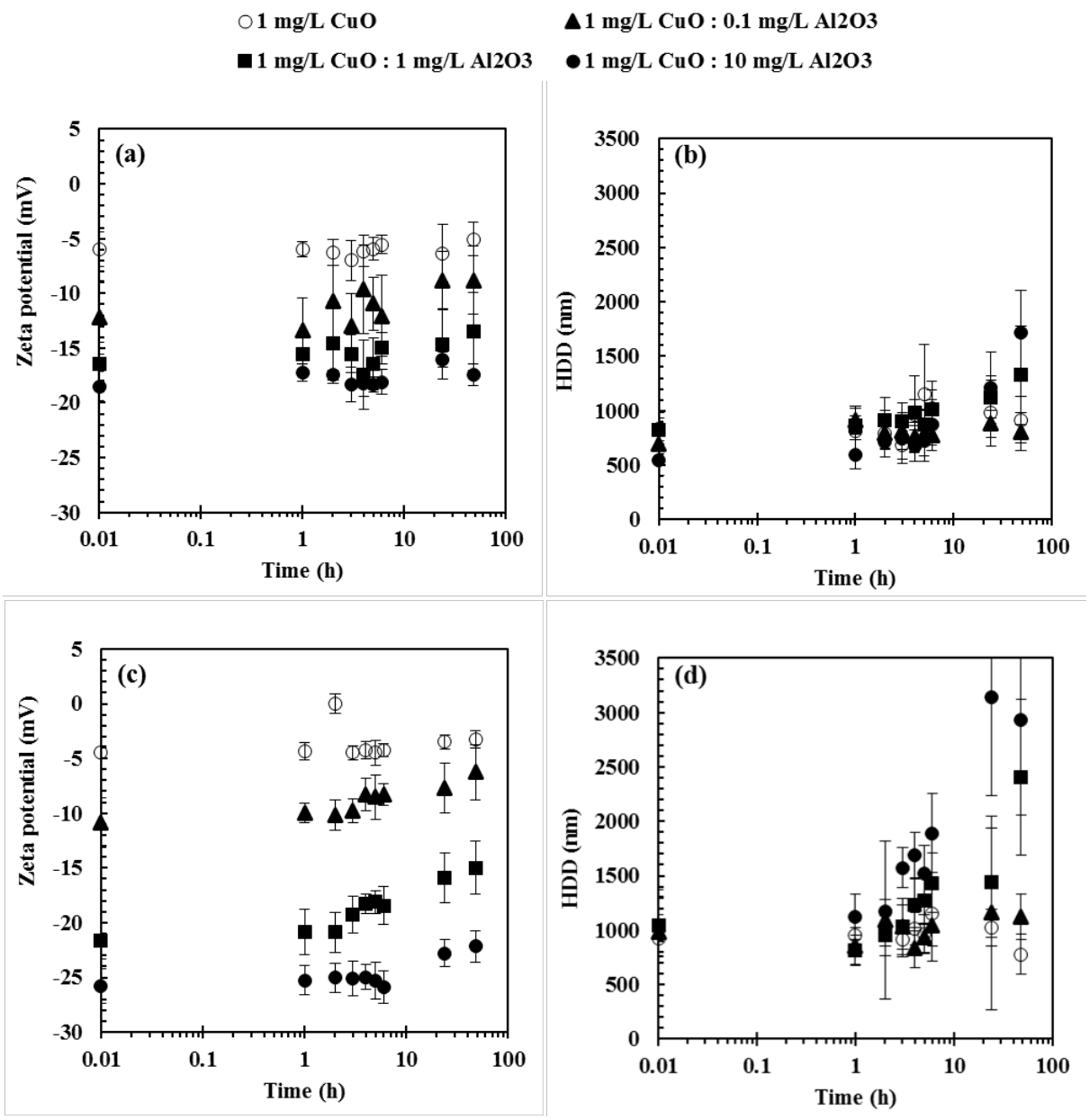

Figure 4.12: ζ-potential and HDD for 1 mM NaCl (a and b, respectively), and for 10 mM NaCl (c and d, respectively) in DIW at pH 7 for 1 mg/L nCuO with varying concentrations of nAl_2O_3 over 48 h. Error bars represent standard deviations (SD) for three replicates.

In part, this could be because of enhanced collision frequencies at higher concentrations leading to rapid hetero-aggregation which is a thermodynamically favoured process in which particles reduce their surface energy by forming aggregates (Marie et al., 2014; Nanda et al., 2003; Yung et al., 2015). For example, the surface energy of embedded nAg is in the range 1.3–5.9 Jm^{-2}, whereas that of the bulk Ag is in the range 1.065–1.54 Jm^{-2} (Nanda et al., 2003).

© University of Pretoria

Further investigations on the influence of IS on binary mixtures were conducted to establish the trend between ζ-potential and IS on the mixtures. Samples for the mixtures of 1 mg/L nAl_2O_3 and 1 mg/L nCuO were prepared in DIW at pH 7 with IS in the range 0.1 to 100 mM. The samples were analysed at 24 and 48 h. It was observed that ζ-potential increased with IS up to the limit of 25 mM, above which ζ-potential decreased with resultant increase in HDD. However, even at 100 mM the HDD was < 1000 nm which implies the mixture aggregates are still in the nano range and would still induce toxic effects to both pelagic and benthic aquatic organisms (Deng et al., 2017; Gomes et al., 2012; Mansano et al., 2018; Vidya and Chitra, 2017). The reason for the reduction in ζ-potential at IS (>25 mM) is attributed to increased aggregation leading to the reduction in particle number concentration which results in reduced charge density (Tantra et al., 2010; Wang et al., 2013). The results are summarised in Table 4.1.

Table 4.1: Influence of IS on aggregation of mixture of (1,1) mg/L nAl_2O_3 and nCuO, respectively in DIW at pH 7

Concentration of NaCl (mM)	24 h		48 h	
	ζ-potential (mV)	HDD (nm)	ζ-potential (mV)	HDD (nm)
0.1	-27 ± 2	361 ± 41	-32 ± 1	434 ± 65
1.0	-31 ± 2	472 ± 28	-30 ± 1	402 ± 29
10.0	-36 ± 1	402 ± 30	-35 ± 1	383 ± 14
25.0	-37 ± 3	461 ± 71	-37 ± 3	410 ± 62
50.0	-28 ± 2	469 ± 24	-28 ± 1	532 ± 43
100.0	-24 ± 1	908 ± 46	-26 ± 2	840 ± 72

4.3.5. Influence of nCuO on aggregation of nAl_2O_3 in presence of HA

The influence of HA (surrogate for NOM) on aggregation of binary mixtures of nCuO and nAl_2O_3 in DIW at pH 7 was studied. The interaction of NOM and ENPs are known to be thermodynamically favoured, both entropically and enthalpically (Loosli et al., 2015a) (Loosli et al., 2015b). Broadly, NOMs are negatively charged because of the presence of numerous

© University of Pretoria

carboxyl and phenolic groups as discussed in section 2.2.4.3. Regardless of mixture concentrations, ζ-potential varied within a narrow range at a fixed concentration of HA that is, -23 to -28 mV and -30 to -37 mV at 1 mg/L and 10 mg/L HA, respectively (Figures 4.13a and c). The concentration dependent increase in negative charge on ENPs in presence of HA was due to the adsorption of HA which imparts negative charge on the surfaces of ENPs by providing a coating (Stumm and Morgan, 2012; Yang et al., 2009). There was no significant difference in ζ-potential among mixtures of various concentration. The HDD observed for mixture concentrations of (1, 0.1) mg/L nAl_2O_3 and nCuO, respectively, was higher than that observed for both individuals at the respective concentrations under same exposure conditions. This was attributed to hetero-aggregation and increased collision frequency at higher particle number concentration in the mixture. At lower concentration of HA (1 mg/L), HDD increased with decreasing concentration of nCuO in the mixture. For example, at concentrations of (1, 0.1) and (1, 10) mg/L nAl_2O_3 and nCuO, respectively, HDD ranged from 800 to 906 nm and 554 to 600 nm, respectively (Figure 4.13b). Similar trend was observed at 10 mg/L HA; but the difference in HDD among various mixture concentrations was much smaller as shown in Figure 4.13d. The lower HDD observed at higher concentration of HA was due to the increased surface charge of ENPs with ζ-potential less than –30 mV (Figure 4.13c) leading to electrostatic stabilization (Jiang et al., 2015; Khan et al., 2018). The reduction in HDD at higher concentration of nCuO in the mixture may be because of enhanced dissolution of nCuO in presence of HA and adsorption of the resultant Cu^{2+} by nAl_2O_3 due to its large surface area.

4.3.6. Influence of nAl_2O_3 on aggregation of nCuO in presence of HA

The ζ-potential increased slightly from the range of -19 to -26 mV for 1 mg/L individual nCuO to -24 to -29 mV for various mixture concentrations at 1 mg/L HA (Figure 4.14b). This is evidenced by comparable HDD values irrespective of mixture concentration ratios (Figure 4.14b). The ζ-potential was slightly higher at higher concentration of HA, but had no significant effect on the observed HDD. For example, for the mixture concentrations of (1, 0.1) mg/L nCuO and nAl_2O_3, respectively, ζ-potential were in the range of -24 to -29 mV and -31 to -36 mV at 1 mg/L and 10 mg/L HA, respectively (Figures 4.14a and c). At higher nAl_2O_3 concentration, more active sites are available due to its large surface area (50.5 m^2/g) leading to enhanced adsorption of NOM. This led to higher negative charge as NOM is negatively charged (Aiken et al., 2011b; Baalousha et al., 2008; Philippe and Schaumann, 2014). The slight increase in ζ-potential at higher HA concentration resulted in a marginal decrease in

© University of Pretoria

HDD from 530 to 630 nm at 1 mg/L and to 426 to 570 nm at 10 mg/L HA for the mixture concentrations (1, 0.1) mg/L nCuO and nAl_2O_3, respectively (Figures 4.14b and d). Contrary to concentration-dependent influence of nCuO on the aggregation of nAl_2O_3 at lower concentration of HA (Figure 4.13b), nAl_2O_3 had no significant concentration dependent effect on the aggregation of nCuO at 1 mg/L HA (Figure 4.14b). These observations indicate that the influence of ENPs on each other in mixtures is not uniform as it is dependent on mixture concentrations.

© University of Pretoria

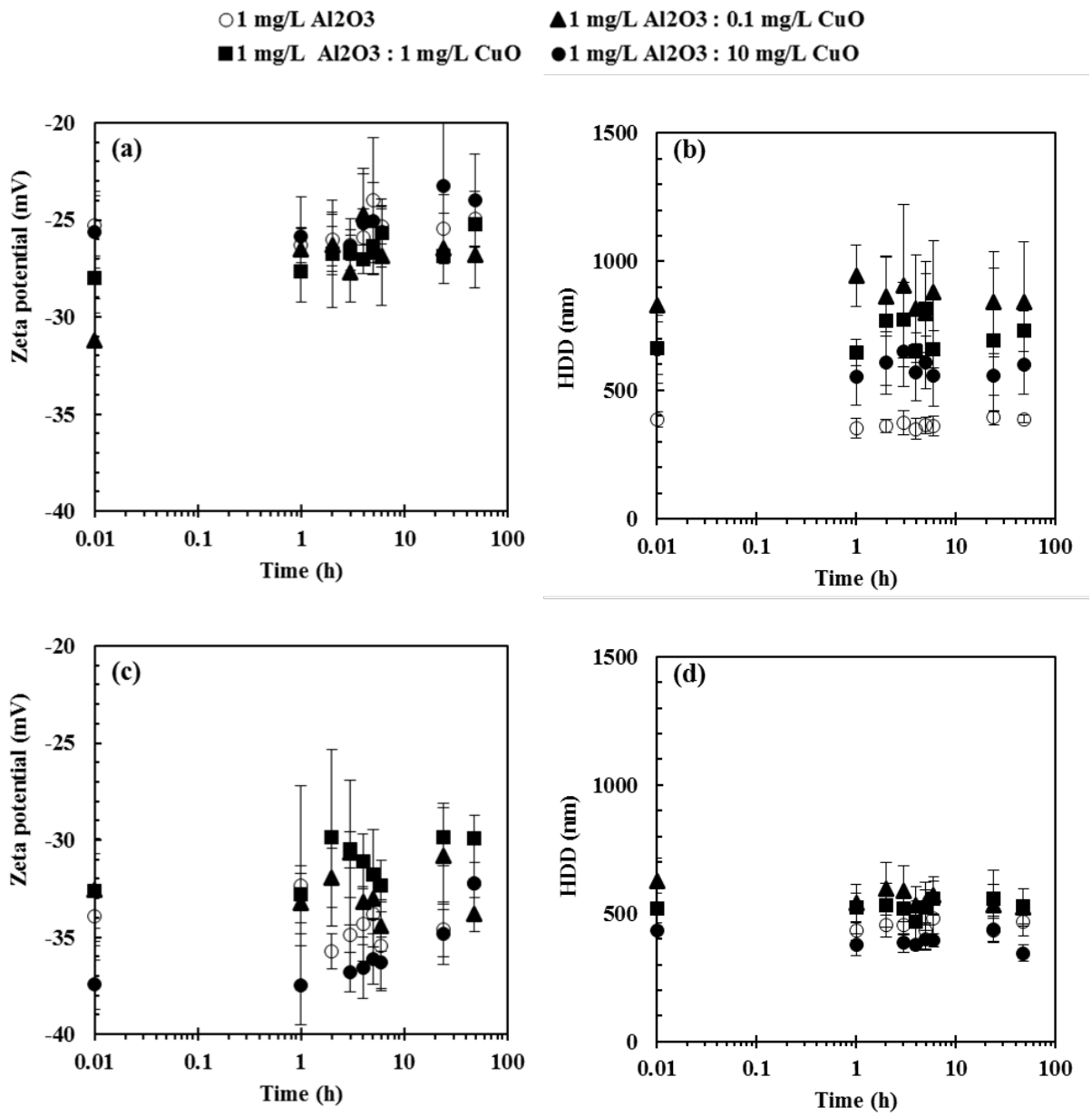

Figure 4.13: ζ-potential and HDD for 1 mg/L HA (a and b, respectively), and for 10 mg/L HA (c and d, respectively) in DIW at pH 7 for 1 mg/L nAl_2O_3 with varying concentrations of nCuO over 48 h. Error bars represent standard deviations (SD) for three replicates.

Interactions of individuals and binary mixtures of ENPs in DIW as influenced by pH, IS and HA herein indicate similarity on the influence of pH on both individual ENPs, and their mixtures. The ζ-potential decreased with increasing IS for the individual ENPs whereas for the mixtures it increased with increasing IS. The reason for this observation may be attributed to higher particle number concentration in mixtures whose charge density outweighed the charge

© University of Pretoria

screening effect of IS. This finding is fundamental as it implies that the degree of influence of IS on the fate and transformation of individual and mixtures of ENPs is not the same. At low IS, monovalent electrolytes may have marginal influence on stability of mixtures of ENPs. The lower concentration of HA (1 mg/L) imparted similar ranges of ζ-potential on both individuals and mixtures. However, the individual ENPs were more highly stabilised than the mixtures. This implies that 1 mg/L of HA coated more particles for individual ENPs than for mixtures and therefore impeded aggregation. Higher concentration of HA (10 mg/L) imparted comparable range of surface charge on both individual and mixtures of ENPs with ζ-potential less than –30 mV. Hence, due to the high interparticle repulsive effects at higher ζ-potential, no significant differences in HDD between singles and mixtures were observed (Loosli et al., 2014a; Omar et al., 2014; Zhang et al., 2009).

© University of Pretoria

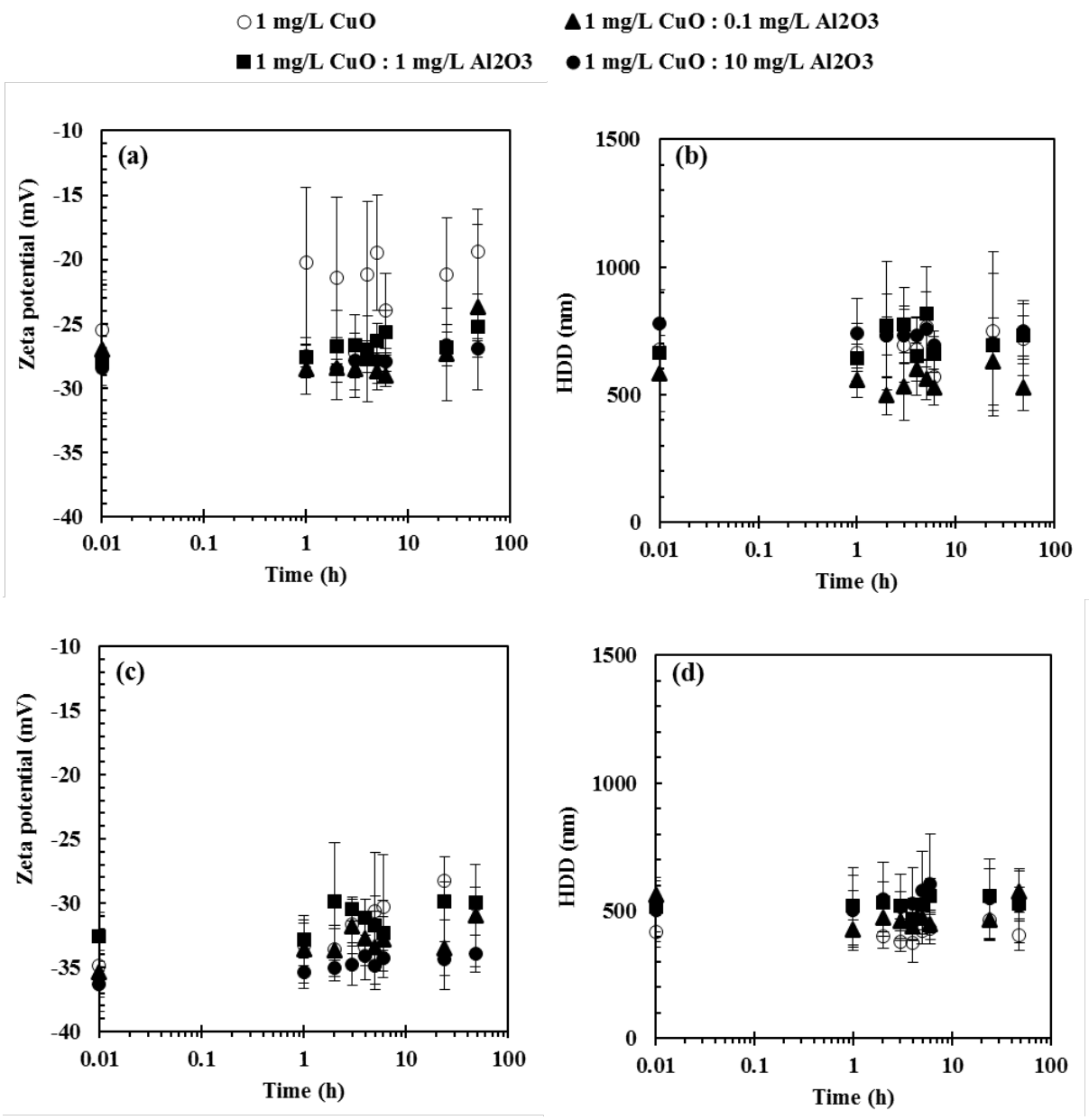

Figure 4.14: ζ-potential and HDD for 1 mg/L HA (a and b, respectively), and for 10 mg/L HA (c and d, respectively) in DIW at pH 7 for 1 mg/L nCuO with varying concentrations of nAl_2O_3 over 48 h. Error bars represent standard deviations (SD) for three replicates.

4.4. Aggregation kinetics of individual ENPs in freshwater

The aggregation kinetics of individual ENPs was studied in river water collected from ER and BR. The characterisation results of the water samples from the two river systems are listed in Table 3.1.

© University of Pretoria

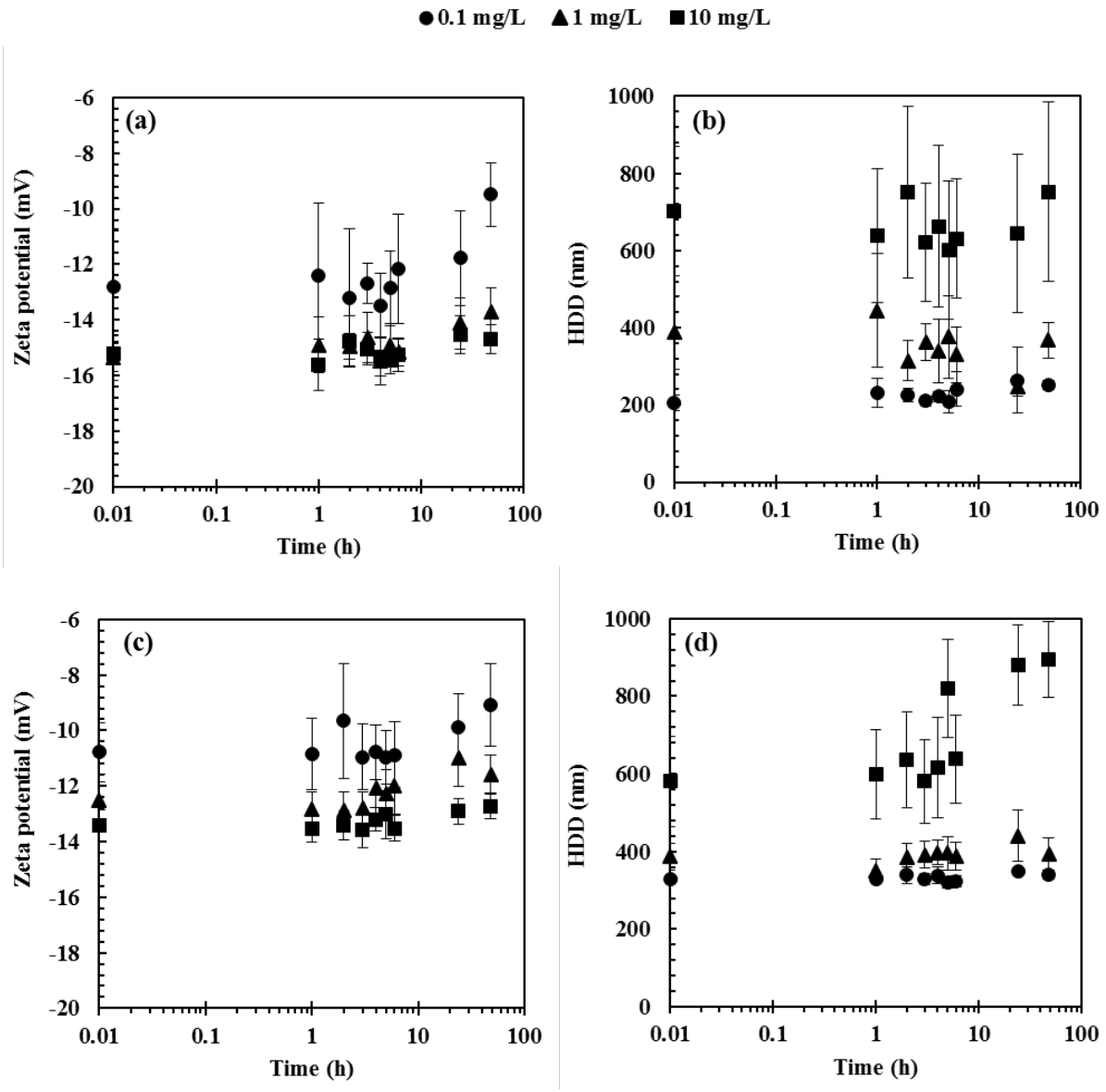

Figure 4.15: ζ-potential and HDD (a and b, respectively) in ER, and (c and d, respectively) in BR for nAl_2O_3 over 48 h. Error bars represent standard deviations (SD) for three replicates.

Aggregation of ENPs was found to be concentration dependent contrary to observations from investigations conducted in DIW. This is because at high concentration in DIW, rapid aggregation occurred leading to sedimentation whereas in river water ENPs were more stable. The sample with 10 mg/L showing the highest HDD and the one with 0.1 mg/L the least as summarised in Figures 4.15 and 4.16 for nAl_2O_3 and nCuO, respectively. At higher exposure concentrations of ENPs (1 and 10 mg/L), rapid aggregation was observed during the first 6 h except for nAl_2O_3 in BR, although the difference was insignificant (Figures 4.15 and 4.16). At

© University of Pretoria

0.1 mg/L, for both ENPs, HDD remained stable < 350 nm over 48 h in river water (Figures 4.15b and d, and Figures 4.16b and d). The DOC (surrogate for NOM) (Table 3.1) can adsorb onto surfaces of ENPs, and in turn provide a barrier against aggregation (Delay et al., 2011; Stankus et al., 2011; Vindedahl et al., 2016). This led to stabilization of ENPs in the river waters. The adsorption of NOM on ENPs has been confirmed using size exclusion chromatography in which ENPs were observed to have a higher affinity for higher MW compared to lower MW components of NOM initiating higher electrostatic and steric stabilization of ENPs (Mwaanga, 2012; Yin et al., 2015).

For example, a study by Yin et al., (2015) reported that NOM with higher MW (>30 kDa) enhanced aggregation whereas NOM with lower MW (< 30 kDa) impeded aggregation of PVP–coated nAg. Increasing the concentration of ENPs from 1 to 10 mg/L, led to rapid aggregation and disaggregation (especially during the first 6 h until ENPs attained stability after 24 h). This raises the possibility of ENPs concurrently having residence between the water, and sediment columns. However, based on ζ-potential and HDD results in Figures 4.15 and 4.16, ENPs concentrations had limited or no influence on aggregation in river water. After 48 h, the ENPs formed larger aggregates at 10 mg/L, an indication that at higher exposure concentrations the ENPs were likely to partly sediment and settle at the bottom.

Results in Table 3.1 show that both river systems had NOM concentrations within the reported range of values in the literature (1–10) mg/L (Conway et al., 2015; Heinlaan et al., 2016; Leareng et al., 2020; Tong et al., 2014). The nature, type and concentration of NOM dictate its net effect on stability of ENPs (Li et al., 2011; Wang et al., 2011). Studies have reported that the adsorption of different components of NOM onto ENPs surfaces is dependent on NOM type (linked to their MW and chemical functionality) and higher adsorption affinity is apparent in NOMs with higher MW (Chekli et al., 2013; Mwaanga et al., 2014; Yu et al., 2017). Therefore, although in this study the distribution of different NOM components (HA, FA, etc.) in each river water were not determined, they may provide a partial account for the observed differences in aggregation of the ENPs linked to differences in MW.

The HDD (< 700 nm) for both ENPs (Figures 4.15b and d, and Figures 4.16b and d) changed insignificantly over 48 h due to the stabilizing effect as a result of water chemistry parameters. This suggest their likely longer residence in the water column and interaction with pelagic organisms. High concentrations of electrolytes (monovalent and divalent cations) shown in Table 3.1 giving net IS of 5.35 mM in BR and 2.48 mM in ER may account for the higher

© University of Pretoria

ENPs aggregates observed at lower concentration (0.1 mg/L) in BR (Figures 4.15d and 4.16d), despite the high concentration of DOC (8.25 mg/L) compared to ER with lower concentration of DOC (5.51 mg/L) which would have countered the effect of IS by inducing stabilization effects on the particles. These findings are in agreement with the literature in natural water (Heinlaan et al., 2016; Romanello and De Cortalezzi, 2013). For example, Heinlaan et al. (2016), studied the aggregation of nCuO in lake water collected from lakes Greifen and Lucerne. The DOC concentrations were 3.4 and 1.1 mg/L with IS of 6 and 4 mM and pH 8.18 and 8.29, respectively. The authors observed that nominal concentration of 25 mg/L nCuO had higher HDD (3358 ± 1037) nm in lake Greifen water with higher concentration of DOC and IS compared to lake Lucerne water with lower concentration of both DOC and IS which had HDD of 2795 ± 1148 nm. As a result, possible strong coagulation due to high concentration of divalent ions e.g. Ca^{2+} and Mg^{2+} may have promoted aggregation in the presence of NOM via formation of intramolecular cation-bridges (Koh and Cheng, 2014; Murphy et al., 1994; Yu et al., 2017). This may account for the low stability of ENPs in BR due to high IS despite high concentration of NOM. As such, stable and unstable dispersions of ENPs may likely remain in water column or sediment, respectively. Therefore, under such scenarios, aquatic organisms within the water column (e.g. filter-feeders like *Daphnia magna*, and fish) as well as benthic filter-feeding invertebrates may concurrently be exposed to ENPs over extended period as observed by Liu et al. (2013); under freshwater conditions.

Current and expected future concentrations of ENPs in freshwater systems are several orders of magnitude lower than the 0.1 mg/L used in this study based on modelled (Boxall et al., 2007b; Gottschalk et al., 2013; Keller and Lazareva, 2013; Musee, 2011c) and detected concentrations (Donovan et al., 2016; Johnson et al., 2011; Peng et al., 2017a; Yang et al., 2016). Hence, findings herein indicate that ENPs may be stable in natural water systems. This implies the stabilized ENPs can interact with water-column or sediment dwelling organisms. This may result in deleterious toxic effects to aquatic life.

© University of Pretoria

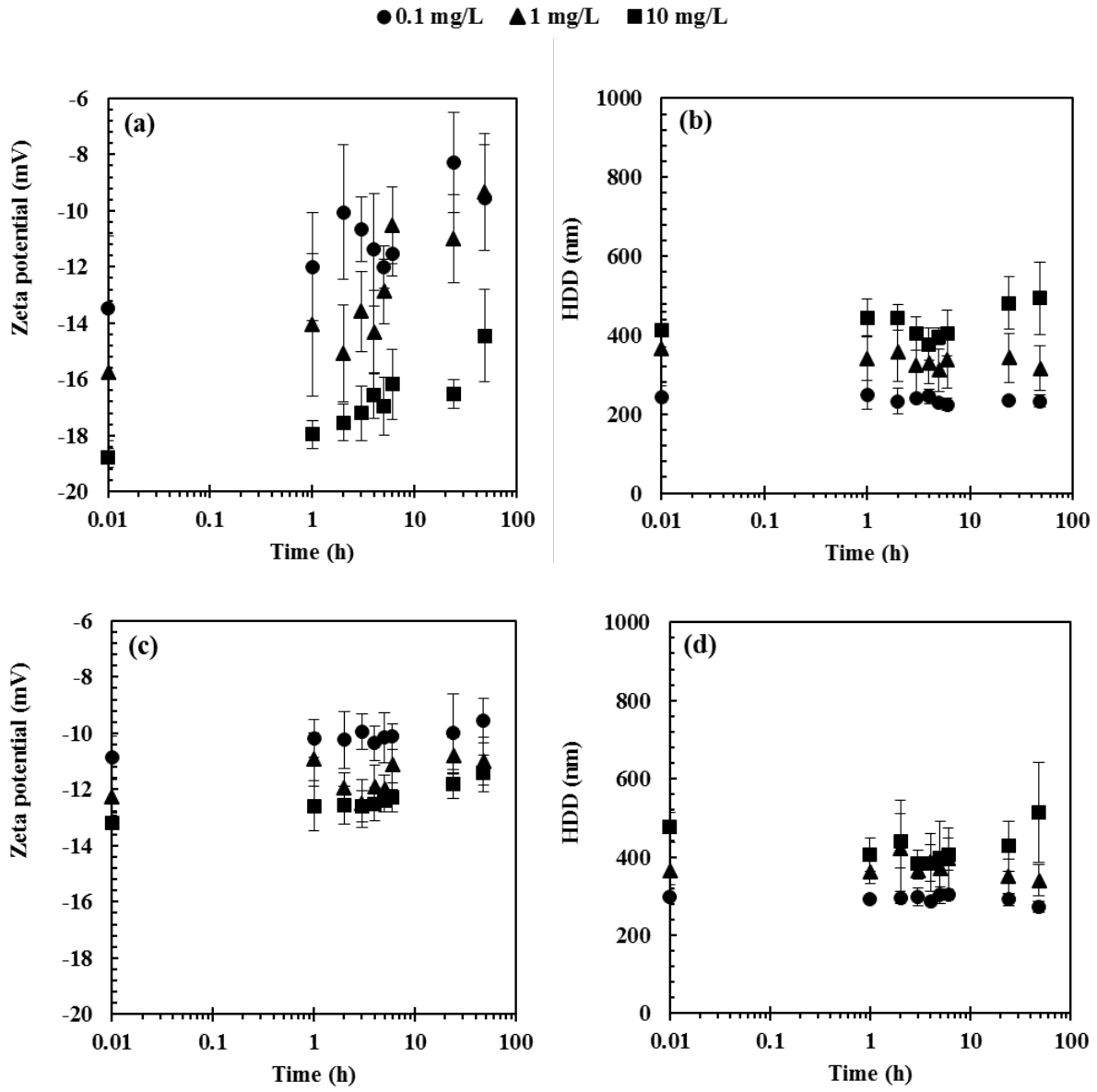

Figure 4.16: ζ-potential and HDD (a and b, respectively) in ER, and (c and d, respectively) in BR for nCuO over 48 h. Error bars represent standard deviations (SD) for three replicates.

4.5. Aggregation kinetics of binary mixtures of ENPs in freshwater

4.5.1. Influence of nCuO on aggregation of nAl_2O_3

The interactions of nAl_2O_3 and nCuO in natural water from BR and ER were investigated under various mixture concentrations. In ER, ζ-potential increased with increasing concentration of nCuO in the mixture at fixed concentration of 0.1 and 1 mg/L of nAl_2O_3; but the differences

© University of Pretoria

were marginal (Figures 4.17a and 4.18a). However, in BR no considerable effect of increasing nCuO concentration in the mixture was observed on ζ-potential (Figures 4.17c and 4.18c). Despite the slight increase in ζ-potential in ER, no meaningful differences were observed in HDD among the various mixture concentrations (Figures 4.17b and 4.18b). However, in BR, HDD increased in the presence of nCuO as shown in Figures 4.17d and 4.18d. Previous studies have reported high aggregation in binary mixtures due to hetero-aggregation (Iswarya et al., 2015; Mansouri et al., 2016; Tong et al., 2014). In freshwater systems, ζ-potential had limited influence on aggregation of ENPs because other factors originating from the complexity of freshwater chemistry came into play. For example, higher MW components of NOM such as polysaccharides and peptides may enhance aggregation of ENPs via formation of intramolecular cation-bridges in presence of divalent cations. For example, Ca^{2+} may facilitate complex formation with NOM functional groups such as carboxylate groups providing multiple cross-linkers among ENPs leading to enhanced aggregation (Bharti et al., 2011; Koh and Cheng, 2014; Murphy et al., 1994; Yu et al., 2017).

Higher HDD was observed for mixtures compared to individual components in BR as summarised in Figures 4.15d and 4.16d. For example, the HDD for 0.1 mg/L nAl_2O_3 ranged from 321 to 349 nm whereas for 0.1 nCuO ranged from 273 to 302 nm in BR. However, for the mixture at concentrations of (0.1, 0.1) mg/L nAl_2O_3 and nCuO, respectively, HDD ranged from 477 to 651 nm (Figure 4.17d). The increase in HDD was attributed to hetero-aggregation (Mansouri et al., 2016; Tong et al., 2014). Similar trends were observed for mixtures involving 1 mg/L nAl_2O_3 and various concentrations of nCuO (Figure 4.17d).

© University of Pretoria

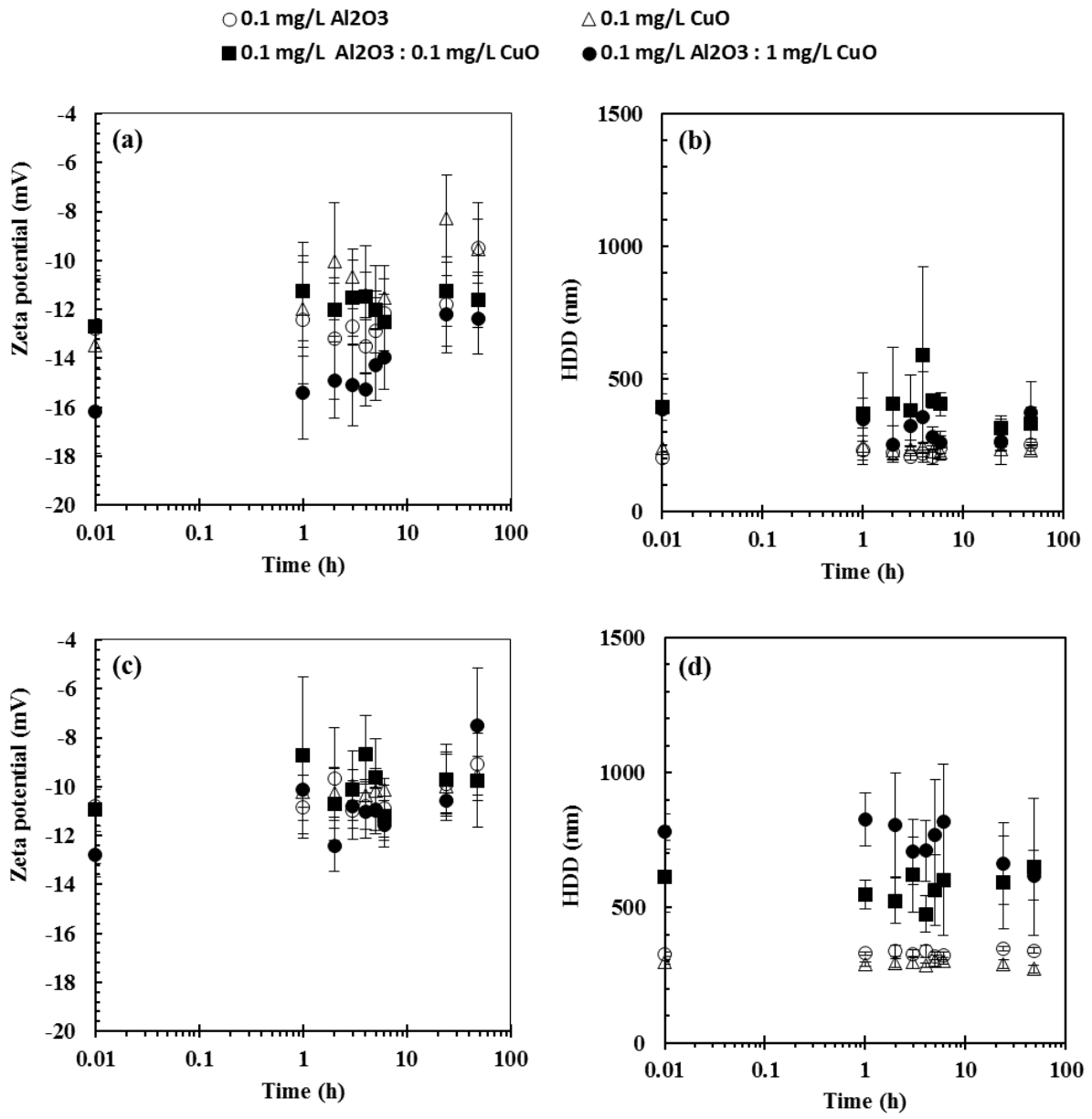

Figure 4.17: ζ-potential and HDD (a and b, respectively) in ER, and (c and d, respectively) in BR for 0.1 mg/L nAl_2O_3 with varying concentrations of nCuO over 48 h. Error bars represent standard deviations (SD) for three replicates.

At pH 7.9, which was the pH of BR water sample, both ENPs were negatively charged with ζ-potential in the range (-10 to -13) mV for 1 mg/L nAl_2O_3 (Figure 4.15c) and for 0.1 mg/L nCuO (-9 to -11) mV (Figure 4.16c). Ideally, similar size range to that observed for individuals should have been observed in the mixtures due to electrostatic repulsion between like charges. However, larger aggregate sizes were observed in mixtures most likely because of higher

© University of Pretoria

collision frequency per unit volume resulting from increased particle number concentration. The higher HDD may have been promoted by ENPs-ENPs hetero-aggregation which is thermodynamically favoured despite both ENPs having negative ζ-potentials. Similar observations have been reported previously (Iswarya et al., 2015; Tong et al., 2014). Tong et al, (2014) studied the interaction of nZnO and $nTiO_2$ in Lake Michigan water (LMW) as exposure media. Both ENPs had negative ζ-potentials, but concentration dependant hetero-aggregation which increased with increasing concentration of nZnO was observed. Iswarya et al. (2015) studied mixtures of crystalline phases (anatase and rutile) $nTiO_2$ in sterile lake water. This revealed mixture concentration- and time dependent hetero-aggregation which increased at higher mixture concentrations without clear dependence on one type of ENPs. The enhanced aggregation in binary mixtures was attributed to the interacting forces acting between the two different nanoparticles, natural colloids present in the lake water and water chemistry of the lake water. In the current study, the composition of river water (Table 3.1) must have influenced the aggregation of binary mixtures of the ENPs.

In addition, the results indicate that HDD increased with decreasing concentration of nCuO at fixed concentration of 1 mg/L nAl_2O_3 over 48 h. For example, maximum HDD was observed from the (1, 0.1) mg/L mixture concentration and least from (1, 10) mg/L of nAl_2O_3 and nCuO, respectively as summarised in (Figure 4.18d). The higher aggregation at low concentration of nCuO in the mixture may have been driven by nCuO as it exhibits enhanced aggregation at lower- compared to higher concentration (Heinlaan et al., 2016). No substantial differences were observed in either ζ-potential or HDD for all the mixture concentrations in ER (Figure 4.18b). This may be attributed to the stabilisation effect of NOM which provides a coating imparting negative charge on ENPs resulting in enhanced electrostatic stabilization. This may have screened out the likely effect due to IS known to promote aggregation of ENPs. Higher aggregation was observed in BR with high concentration of both NOM and ionic species such as divalent cations of Ca^{2+} and Mg^{2+} as shown in Table 3.1. These electrolytes may have formed complexes with NOM via formation of cation-bridges leading to enhanced aggregation (Murphy et al., 1994; Yu et al., 2017). These results indicate that the variations in water chemistry play a significant role on aggregation of ENPs in freshwater systems.

© University of Pretoria

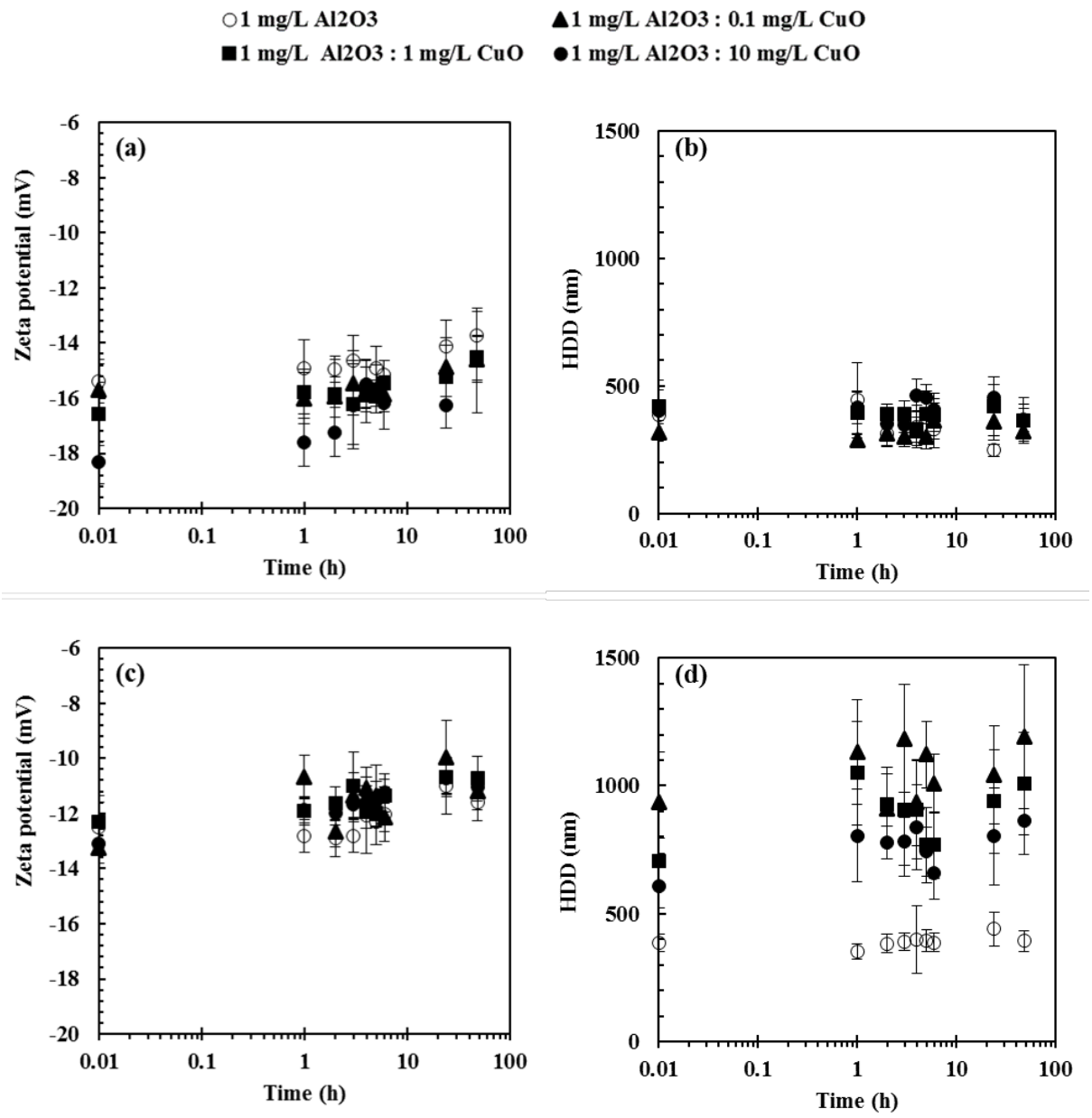

Figure 4.18: ζ-potential and HDD (a and b, respectively) in ER, and (c and d, respectively) in BR for 1 mg/L nAl_2O_3 with varying concentrations of nCuO over 48 h. Error bars represent standard deviations (SD) for three replicates.

4.5.2. Influence of nAl_2O_3 on aggregation of nCuO

The influence of various concentrations of nAl_2O_3 on a fixed concentration of nCuO in BR and ER water samples was studied. For individual ENPs, both ζ-potential and HDD increased with increasing concentration of ENPs without meaningful differences over 48 h (Figures 4.15 and 4.16). In both river water samples, HDD for the lower concentrations of ENPs (0.1 and 1 mg/L) were < 500 nm over 48 h, as discussed in section 4.4. For mixtures in BR, HDD was higher

© University of Pretoria

than that observed for individual ENPs and increased with increasing concentration of nAl_2O_3. For example, HDD of the mixture consisting of 0.1 mg/L nCuO and 0.1 mg/L nAl_2O_3 was in the range of 525 to 651 nm whereas that of the mixture consisting of 0.1 mg/LnCuO and 1 mg/L nAl_2O_3 was in the range of 908 to 1190 nm (Figure 4.19d). Enhanced hetero-aggregation in the mixture may have been due to adsorption of nCuO onto nAl_2O_3 which was less soluble and had larger surface area (Mansouri et al., 2016; Wilke et al., 2016). In ER river, HDD for all mixtures was in the range 200 to 550 nm irrespective of mixture concentration. Increasing the concentration of nAl_2O_3 on 0.1 or 1 mg/L nCuO had no significant influence on HDD (Figures 4.19b and 4.20b). Depending on the type of ENPs present at higher concentration in the mixture, different aggregate sizes may be observed under the same exposure media. For example, HDD in the range of 707 to 827 nm was observed in BR from the mixture concentrations of 0.1 and 1 mg/L nAl_2O_3 and nCuO, respectively (Figure 4.17d). However, HDD increased to a range of 908 to 1190 nm under mixture concentrations of 1 and 0.1 mg/L nAl_2O_3 and nCuO, respectively (Figure 4.19d). However, in ER no significant differences were observed in HDD of the mixtures (Figures 4.17b and 4.19b). These results indicate that both mixture concentrations and water chemistry have significant influence on the aggregation of mixtures of ENPs in natural water systems. Hence, it is impossible to make generalised statements on fate and transformation of mixtures of ENPs in river water.

© University of Pretoria

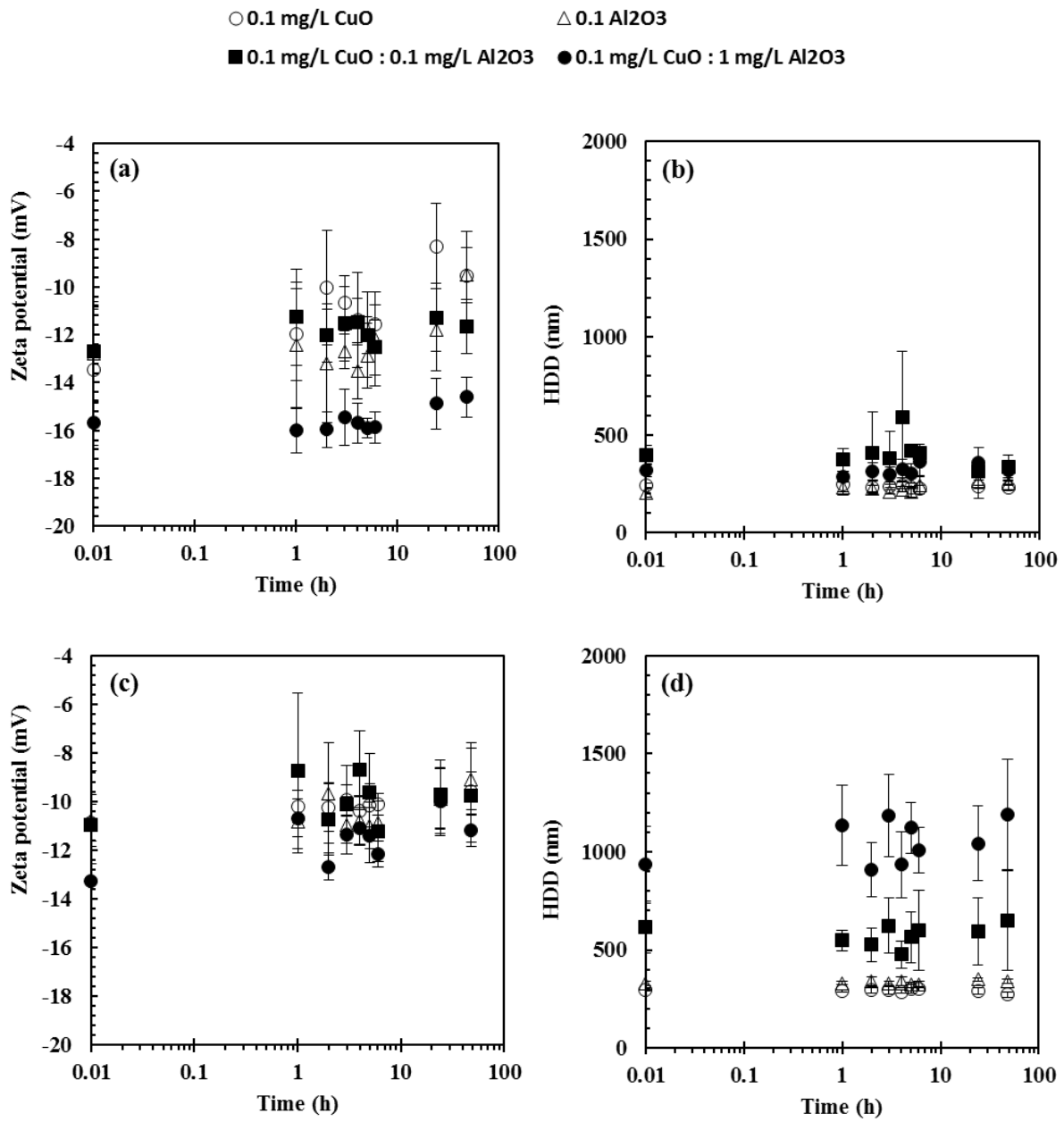

Figure 4.19: ζ-potential and HDD (a and b, respectively) in ER, and (c and d, respectively) in BR for 0.1 mg/L nCuO with varying concentrations of nAl_2O_3 over 48 h. Error bars represent standard deviations (SD) for three replicates.

In BR, For the mixture at (1, 0.1) mg/L nCuO and nAl_2O_3, respectively. HDD decreased over 48 h from 783 nm at 0 h to 620 nm at 48 h. However, that of (1,1) and (1, 10) mg/L nCuO and nAl_2O_3, respectively, increased with the (1, 10) mg/L yielding maximum HDD of 1682 nm at 48 h as shown in (Figure 4.20d). These results are consistent with previous studies on the aggregation of mixtures in freshwater systems where concentration dependent aggregation was observed (Iswarya et al., 2015; Tong et al., 2014). For example, Tong et al. (2014) observed

© University of Pretoria

that the mixture of 1 mg/L nZnO and 10 mg/L $nTiO_2$ had HDD of 765 ± 51 nm whereas the mixture of 20 mg/L nZnO and 10 mg/L $nTiO_2$ had HDD of 887 ± 82 nm. The trend, in which aggregation was increasing with increasing concentration of nAl_2O_3 in the mixture, is opposite to the influence of nCuO on nAl_2O_3 where aggregation decreased with increasing concentration of nCuO in the mixture as shown in Figures 4.18d and 4.20d. In ER, HDD of the mixture was comparable to that of individual nCuO as shown in Figure 4.20b. There was no significant difference in ζ-potential with increasing concentration of nAl_2O_3 in the mixture at 1 mg/L nCuO in both river systems as shown in (Figures 4.20a and c). These results show that the aggregation of mixtures of ENPs is influenced by both mixture concentrations and the chemistry of the exposure media.

© University of Pretoria

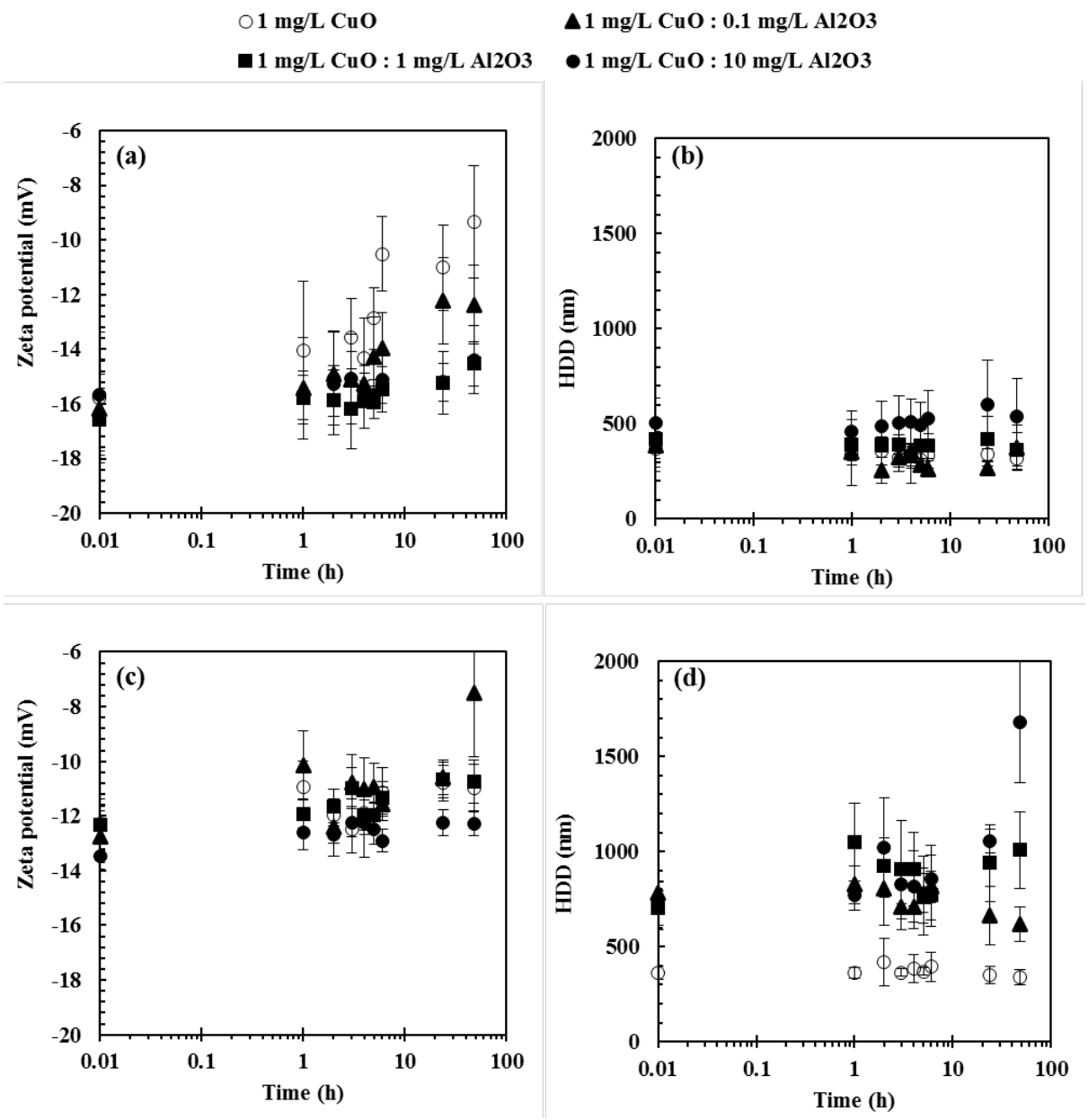

Figure 4-20: ζ-potential and HDD (a and b, respectively) in ER, and (c and d, respectively) in BR for 1 mg/L nCuO with varying concentrations of nAl_2O_3 over 48 h. Error bars represent standard deviations (SD) for three replicates.

Hetero-aggregation of nCuO and nAl_2O_3 was investigated using EDS in SEM and the results are shown in Figure 4.21. The aggregates showed the presence of nCuO (Figure 4.21a) and nAl_2O_3) (Figure 4.21b). Combined analysis by mapping showed random distribution of both nCuO and n Al_2O_3 in the aggregates confirming hetero-aggregation of the ENPs (Figure 4.21d). The regions with high concentration of nCuO showed high contrast on the spectra for the heavy

© University of Pretoria

metal copper and lower contrast for aluminium as shown in (Figure 4.21c). The results provide evidence of the existence of hetero-aggregation in the mixture. Notably, this imaging technique can only show external distribution of ENPs on aggregates and not the internal composition of aggregates. Hence supplementary analytical techniques which can give details on internal composition of aggregates are necessary to confirm the hetero-aggregation.

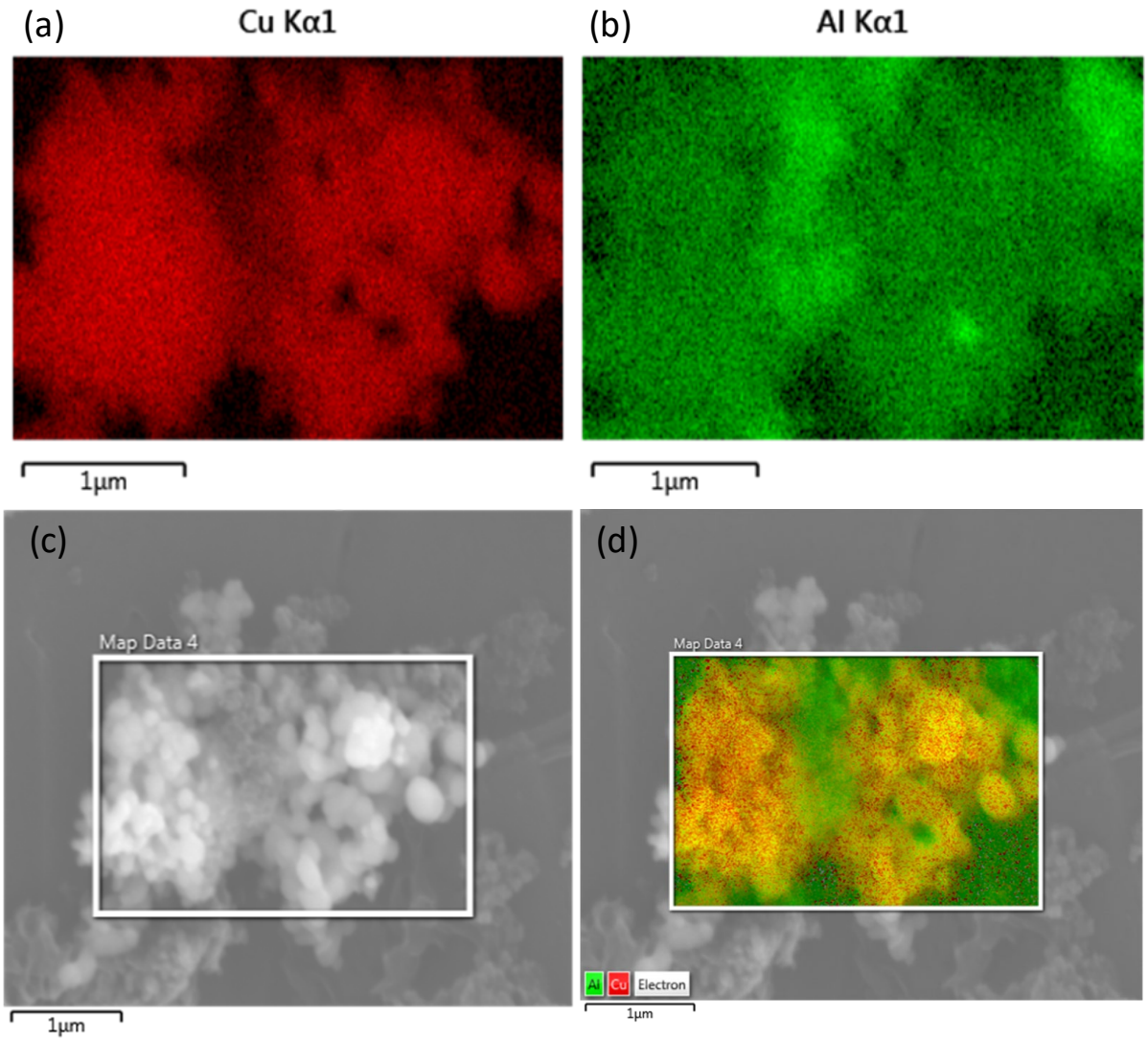

Figure 4-21: EDS in SEM images of hetero-aggregation of mixture of 1 mg/L nCuO and 1 mg/L nAl_2O_3 in BR water sample (a) regions of nCuO in the aggregate, (b) regions of nAl_2O_3 in the aggregate, (c) high contrast regions of nCuO and low contrast regions of nAl_2O_3, (d) hetero-aggregation of nCuO and nAl_2O_3 in the mixture

© University of Pretoria

Considerable variations in HDD and ζ-potential of singles and binary mixtures of ENPs were observed in synthetic and natural water systems. The individual influences of water chemistry parameters (pH, IS and NOM) on aggregation and ζ-potential of ENPs are different from influence of natural water with complex physicochemical composition where counteracting factors are responsible for the net effect observed. The findings reported herein indicate that ENPs are more stable in natural river water than in synthetic water. Hence their behaviour and transformation in natural water is different from that observed in synthetic water. Therefore, this work contributes to the limited but growing knowledge on the influence of water chemistry on fate and transformation of ENPs at environmentally relevant concentrations. However, more studies are necessary on mixtures of ENPs in natural water systems at even lower concentrations so as to generate more realistic data and aid risk assessment of ENPs in the natural aquatic environment.

4.6. Aggregation kinetics of binary mixtures of ENPs and TCS in freshwater

4.6.1. Influence of TCS on aggregation of nAl_2O_3

The influence of TCS on aggregation of nAl_2O_3 in ER and BR water samples was investigated and the results are summarised in Figures 4.22 and 4.23. Because of it is highly hydrophobic nature, even in the deprotonated form, and its relatively high octanol-water partition coefficient, TCS undergoes sorption with particles (Nghiem and Coleman, 2008; Trenholm et al., 2006). The ENPs were stabilised by TCS in ER water. The stabilization was independent of concentration of both nAl_2O_3 and TCS as shown in Figures 4.22b and 4.23b. Since environmental concentrations of ENPs are still orders of magnitudes lower than 0.1 mg/L, TCS plausibly can stabilise ENPs in freshwater systems. This implies that, in the presence of TCS, ENPs may have longer residence in the water column, interact with pelagic organisms and exert toxicological effects. The nAl_2O_3 have been reported to be toxic to various aquatic organisms (Benavides et al., 2016; Pakrashi et al., 2013; Ye et al., 2018b).

However, in BR, TCS exhibited a concentration dependant destabilization effect on nAl_2O_3. The effect was relatively higher at lower concentration of nAl_2O_3 (0.1 mg/L) as shown in Figure 4.22d. No significant influence of TCS was observed on ζ-potential (Figures 4.22c and 4.23c). These findings suggest that, depending on water chemistry, TCS may enhance aggregation of

© University of Pretoria

ENPs. Despite the enhanced aggregation, ENPs are still in the nano-scale range and may still pose toxicological effects to aquatic organisms.

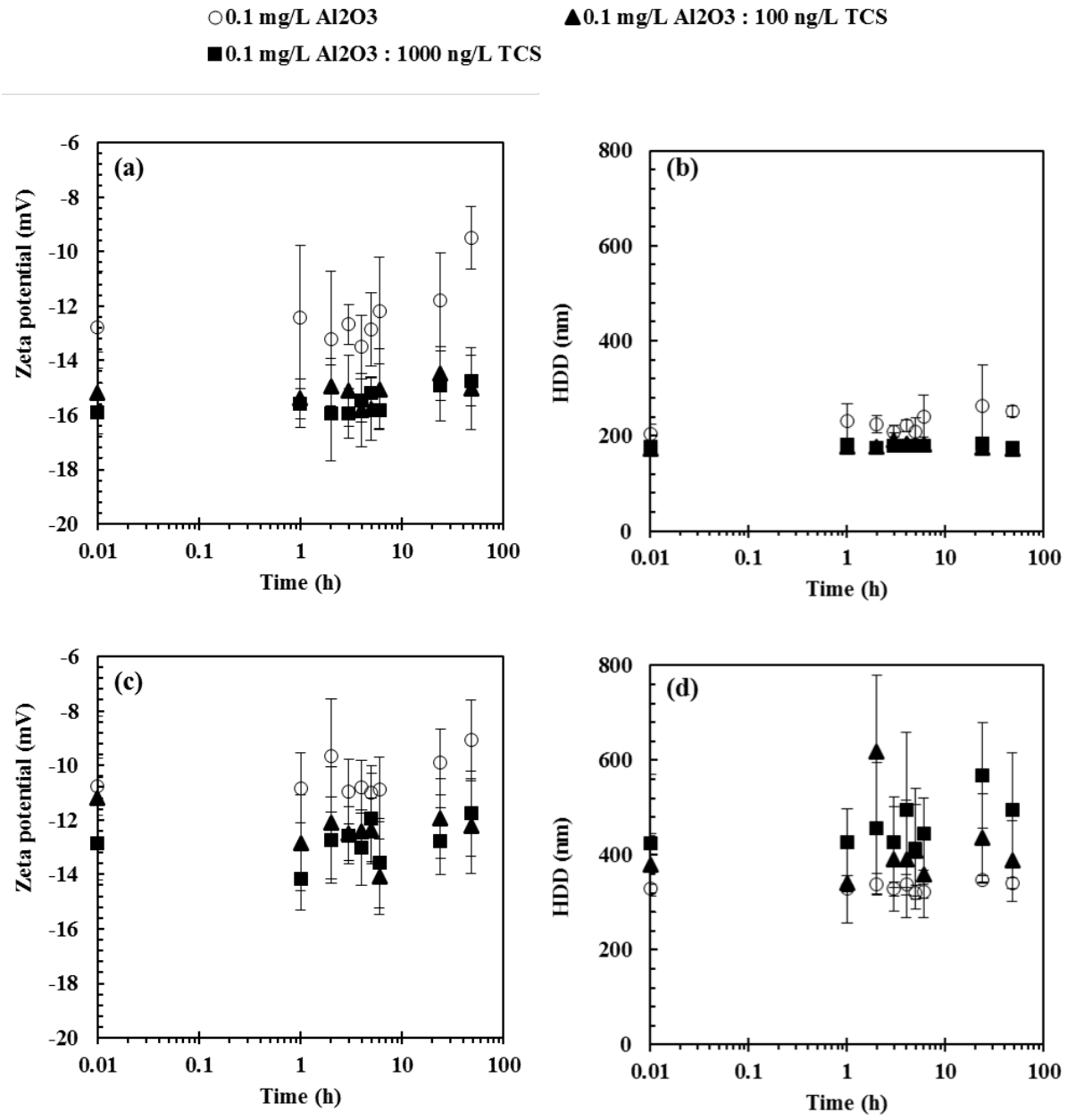

Figure 4.22: ζ-potential and HDD (a and b, respectively) in ER and ζ-potential and HDD (c and d, respectively) in BR at 0.1 mg/L nAl_2O_3 with varying concentrations of TCS over 48 h. Error bars represent standard deviations (SD) for three replicates.

© University of Pretoria

These results point to either stabilization or destabilization of ENPs by TCS, and the extent of these effects are dependent on the water chemistry. In ER, for example, nAl_2O_3 was stabilised by TCS. However, the stabilization effect was independent of the concentration of TCS as shown in Figures 4.22b and 4.23b. Nevertheless, the destabilization effect of TCS in BR was concentration dependent but the difference was insignificant (Figures 4.22d and 4.23d). Adsorption of TCS onto surfaces of ENPs was evidenced by the slight increase in ζ-potential (Figures 4.22a and c, and 4.23a and c). Overall, the stabilization of TCS on ENPs was observed in ER water whereas destabilization effect was observed in BR water. The reason for these observations is attributed, in part, to the interaction of NOM with the organic pollutant TCS (Pignatello, 2012). Pignatello (2012) reported that the interaction of NOM with other organic pollutants is controlled by many factors. This includes a preference for micro-domains within NOM that segregates interactions based on function groups such as aromatic or carbohydrate domains. In addition, the interaction is also controlled by the presence of functional groups that promote hydrogen bonding and a preference based on the configuration and conformation of the molecules and strands at the microstructure level. The sorption of TCS on other particles is influenced by the presence of NOM (Behera et al., 2010; Ferreira et al., 2002; Gu et al., 2007). Hence the stabilization effect of TCS on ENPs was higher in ER with low concentration of NOM (5.51 mg/L) than BR with a higher NOM concentration (8.25 mg/L). Therefore, depending on the nature and concentration of NOM, strong or weak interactions may exist with organic pollutants. This may influence the stabilization effect of organic pollutants on ENPs as attested by the differences observed between ER and BR water samples.

© University of Pretoria

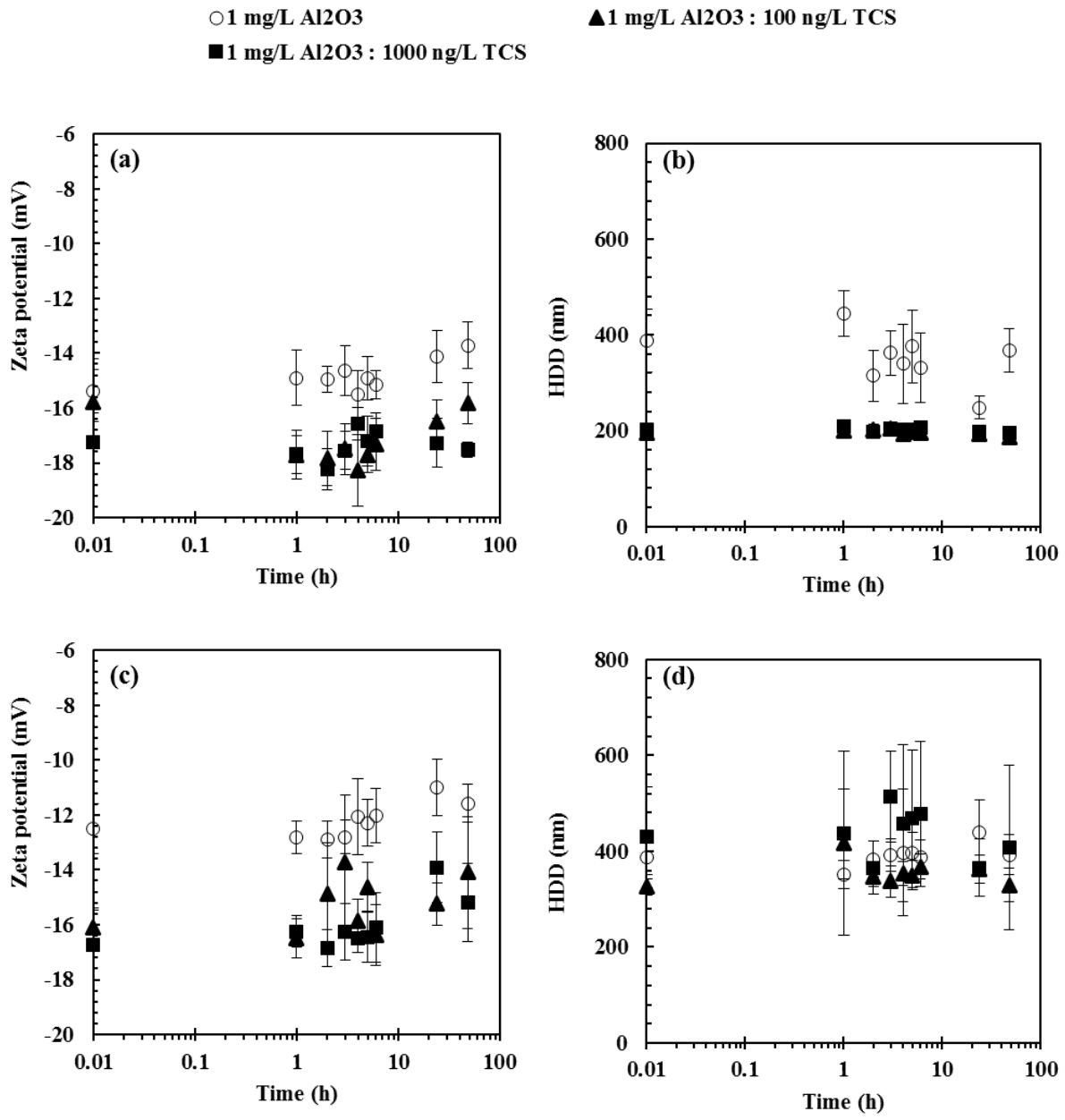

Figure 4.23: ζ-potential and HDD (a and b, respectively) in ER and ζ-potential and HDD (c and d, respectively) in BR at 1 mg/L nAl_2O_3 with varying concentrations of TCS over 48 h. Error bars represent standard deviations (SD) for three replicates.

4.6.2. Influence of TCS on the aggregation of nCuO

The influence of TCS on aggregation of nCuO in ER and BR water samples was studied and the results are shown in Figures 4.24 and 4.25. In ER, TCS had a concentration independent stabilization effect on nCuO and HDD was < 250 nm (Figures 4.24b and 4.25b). The adsorption

© University of Pretoria

of TCS onto ENPs provides a coating which minimizes ENP-ENP interactions leading the observed stabilization effect (Chen et al., 2018). Despite TCS having high ζ-potential of *ca.* -30 mV, it had no significant influence on ζ-potential of nCuO in river water (Figures 4.24a and c, and Figures 4.25a and c). Complex interactions between NOM and TCS in presence of monovalent and multivalent ions in river water may have compromised the influence of TCS on ζ-potential (Behera et al., 2010). These results indicate that in presence of TCS, ENPs will be stabilised in ER water (HDD < 250 nm) as their environmental concentrations are orders of magnitude lower than 0.1 mg/L (Donovan et al., 2016; Johnson et al., 2011). This implies they will have a longer residence time in the water column and interact with pelagic organisms leading to plausible toxicological effects.

However, in BR a destabilization effect of TCS on ENPs was observed (Figures 4.24d and 4.25d). For example, in presence of either 100 or 1000 ng/L TCS, HDD for 0.1 mg/L nCuO ranged from 300 to700 nm (Figure 4.24d). The reason for the destabilization may be attributed to the higher concentration of NOM in BR (8.25 mg/L) which might have impeded the adsorption of TCS on surfaces of ENPs (Behera et al., 2010). In addition, the destabilisation may also be attributed to specific interactions between NOM and TCS which are dependent on the type and nature of NOM (Pignatello, 2011; Pignatello, 2012). TCS had marginal influence on ζ-potential despite its significant influence on HDD compared to the reference ($p < 0.05$) (Figures 4.24c and 4.25c). The destabilisation effect of TCS was independent of the concentration of both nCuO and TCS as summarised in Figures 4.24d and 4.25d. Therefore, despite the enhanced aggregation in presence of TCS, the aggregates are still in the nano-scale range (≤ 1000 nm) Therefore, the ENPs may still induce toxic effect to pelagic organisms. According to colloidal science, dispersed particles within the size range of 1 to 1000 nm will be stable in the continuous phase while particles above this size range will undergo sedimentation (Hotze et al., 2010).

© University of Pretoria

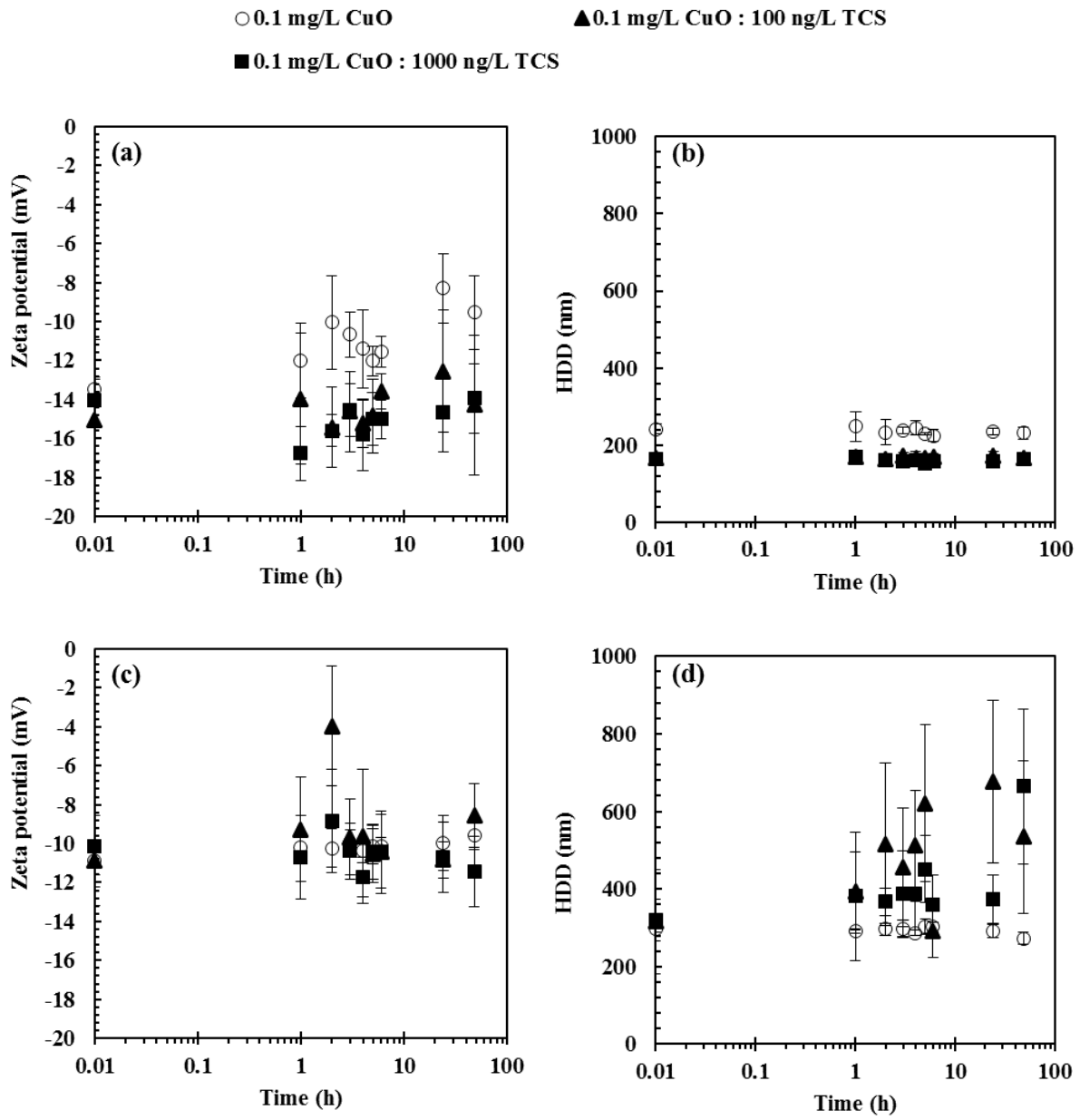

Figure 4.24: ζ-potential and HDD (a and b, respectively) in ER and ζ-potential and HDD (c and d, respectively) in BR at 0.1 mg/L nCuO with varying concentrations of TCS over 48 h. Error bars represent standard deviations (SD) for three replicates.

The stabilization of nCuO in ER was most likely due to adsorption of TCS onto ENPs as evidenced by the slight increase in ζ-potential. Similar observations have been reported during investigations on the interaction of TCS and copper nanoparticles (nCu) (Chen et al., 2018). Chen et al. (2018) investigated adsorption of TCS on nCu using UV-Vis technique by mixing 10 mg TCS and 50 mg nCu in 1 litre of either DIW or synthetic wastewater with resultant concentrations of 10 and 50 mg/L, TCS and nCu, respectively. They observed that 4.5 and 5.3

© University of Pretoria

mg of TCS were adsorbed on 50 mg of nCu in DIW and synthetic wastewater after 24 h, respectively. Hence, in the current study adsorption of TCS may have been responsible for the stabilization of ENPs in ER water samples. The reasons for the destabilisation of ENPs by TCS in BR could be associated to the nature of interactions between NOM and TCS which could have been strong and reduced the availability of TCS to stabilise ENPs.

The influence of TCS on stability of different types of ENPs in identical exposure media was very similar. For example, both nAl_2O_3 and nCuO were stabilised to within a narrow range of 150–250 nm at various concentrations of ENPs and TCS in ER. The stabilisation effect of TCS was more significant at lower concentration of ENPs. In the current study, 0.1 mg/L (HDD ≤ 180 nm) was more stabilised than 1 mg/L (HDD, 160 to 250 nm) ENPs under identical concentrations of TCS and exposure media. However, differences in degree of aggregation at the two concentrations were not significant. These findings suggest that the stabilising effect of TCS on ENPs in the environment will be very significant since environmental concentrations of ENPs are orders of magnitude lower than the lowest concentration used in this study (Boxall et al., 2007a; Donovan et al., 2016; Gottschalk et al., 2013). In addition, the stabilising effect of TCS was concentration independent. For example, the 100 and 1000 ng/L TCS stabilised ENPs in ER to the same extent. These results suggest that even at lower concentrations (Table 2.3) in the environment, TCS may still stabilise ENPs. Based on the current experimental results, the effects of TCS on stability of ENPs in freshwater are more distinctive under low concentration of NOM (nature and type) in the exposure media. This is because the concentration and type of NOM influences the interaction of TCS and NOM (Behera et al., 2010; Pignatello, 2011). For example, the effect of TCS was more apparent in ER with lower concentration of NOM than BR despite the various components of NOM not determined in the two river systems. However, it is worth noting that the stabilization or destabilization effect observed on ENPs as a result of TCS are dependent on the water chemistry of the exposure medium. Due to the complexity of freshwater, the net effect observed on stability of ENPs is the result of various influencing factors within the complex exposure matrix.

© University of Pretoria

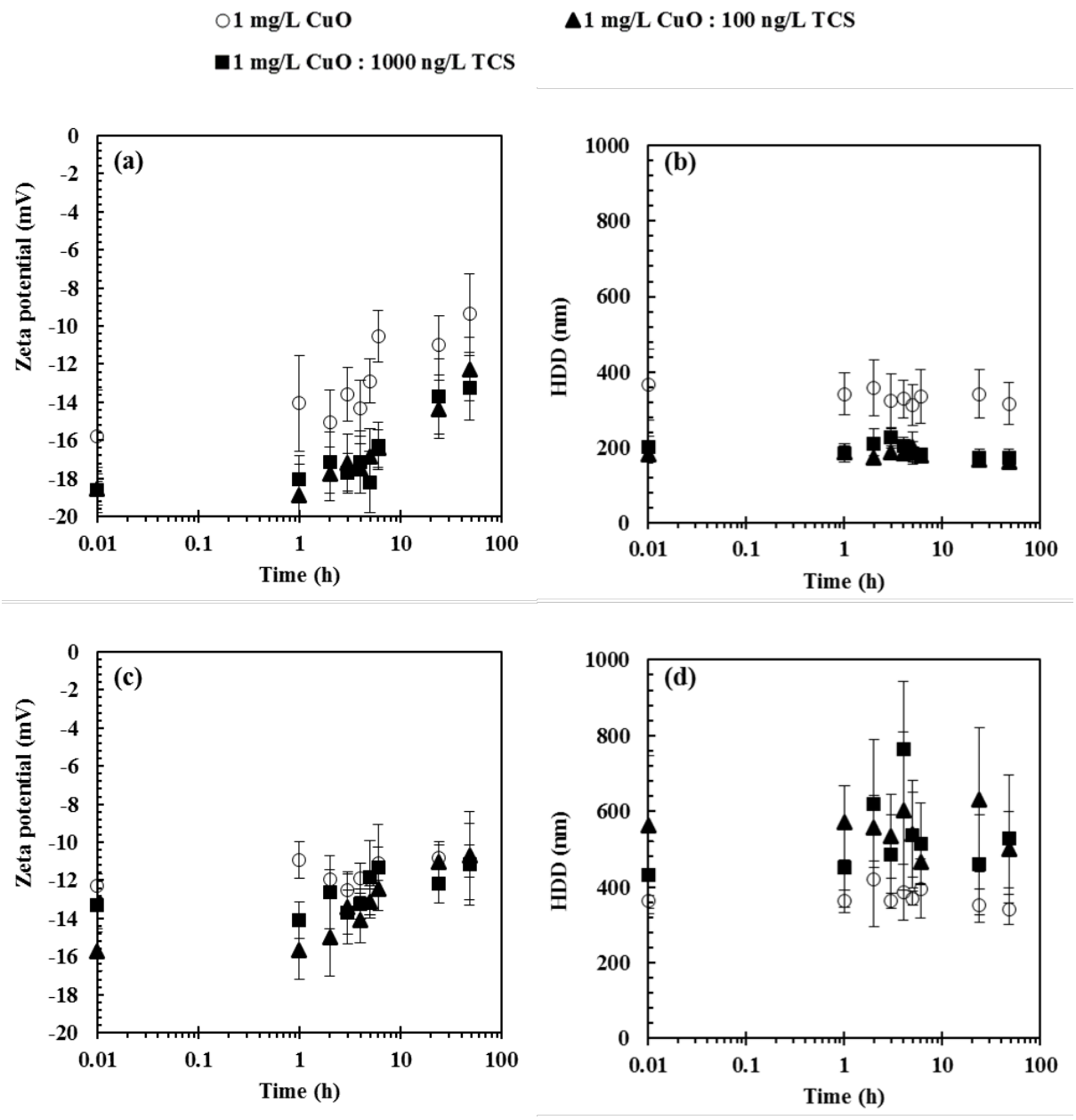

Figure 4.25: ζ-potential and HDD (a and b, respectively) in ER and ζ-potential and HDD (c and d, respectively) in BR at 1 mg/L nCuO with varying concentrations of TCS over 48 h. Error bars represent standard deviations (SD) for three replicates.

4.7. Aggregation in ternary mixtures of ENPs and TCS in freshwater

The interaction of ternary mixtures of ENPs and TCS in river water samples was investigated. In both river systems, the presence of TCS stabilised the ENPs with the effect being greater in ER than BR water samples as shown in Figures 4.26 and 4.27. For example, in the absence of

© University of Pretoria

TCS, the HDD for binary mixtures of nAl_2O_3 and nCuO was in the range 250 to 590 nm (Figures 4.17b and 4.20b) and 470 to 1200 nm (Figures 4.17d and 4.20d) in ER and BR water samples, respectively. In the presence of TCS (100 ng/L), the HDDs decreased to the range of 180 to 400 nm (Figure 4.26b) and 440 to 820 nm (Figure 4.26d) in ER and BR, respectively. The reduction in aggregation was likely due to the adsorption of TCS onto surfaces of ENPs inhibiting aggregation (Chen et al., 2018). The stabilization effect of TCS was lower in BR water with higher concentration of NOM than in ER water with lower concentration of NOM (Table 3.1). This is because of the complex interactions that exist between organic pollutants and NOM which may have minimised the interaction of TCS with ENPs at high concentration of NOM (Behera et al., 2010; Ferreira et al., 2002; Gu et al., 2007). In both river system waters, TCS had no significant effect on the ζ–potential of ternary mixtures as summarised (Figures 4.26a and 4.26c). The ζ–potential was lower in BR than in ER and this may be attributed to the screening effect resulting from both mono and divalent ions present at higher concentration in BR water samples (Table 3.1). The adsorption of TCS on ENPs implies that TCS may enhance the toxicity of ENPs by stabilising and enabling them to have a longer residence time in the water column. In addition, ENPs may also enhance the toxicity of TCS to aquatic organisms via the Trojan horse effect (Naasz et al., 2018; Tong et al., 2014).

© University of Pretoria

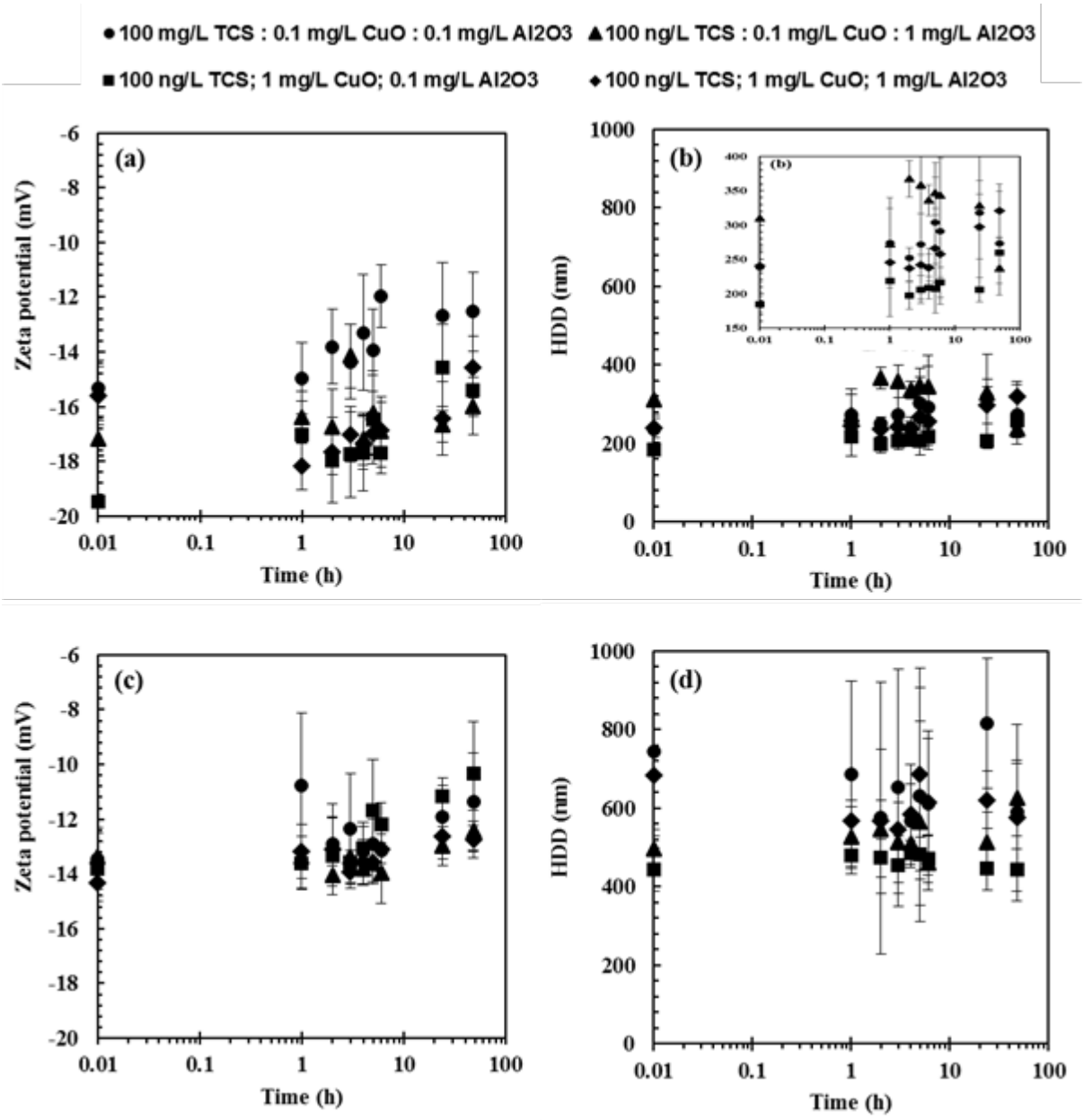

Figure 4.26: ζ-potential and HDD (a and b, respectively) in ER water in presence of TCS, and ζ-potential and HDD (c and d, respectively) in BR water in presence of TCS over 48 h. Error bars represent standard deviations (SD) for three replicates.

Notably, ternary mixtures with higher concentration of nAl_2O_3 had higher aggregation than those with higher concentration of nCuO in the same exposure media. For example, the ternary mixtures with mixture concentrations (100 ng/L TCS: 1 mg/L nCuO: 0.1 mg/L nAl_2O_3) had HDD in the range of 180 to 220 nm and 440 to 490 nm in ER and BR water samples, respectively. However, ternary mixtures with mixture concentrations (100 ng/L TCS: 0.1 mg/L nCuO: 1 mg/L nAl_2O_3) had HDD in the range 240 to 370 nm and 460 to 630 nm in ER and BR

© University of Pretoria

water samples respectively. Hence, higher concentration of nAl_2O_3 enhanced aggregation. The reasons for this trend may be attributed to the low dissolution and larger surface area of nAl_2O_3 (50.5 m^2/g) compared to nCuO (29 m^2/g) making it more reactive (Auffan et al., 2009; Lei et al., 2018)

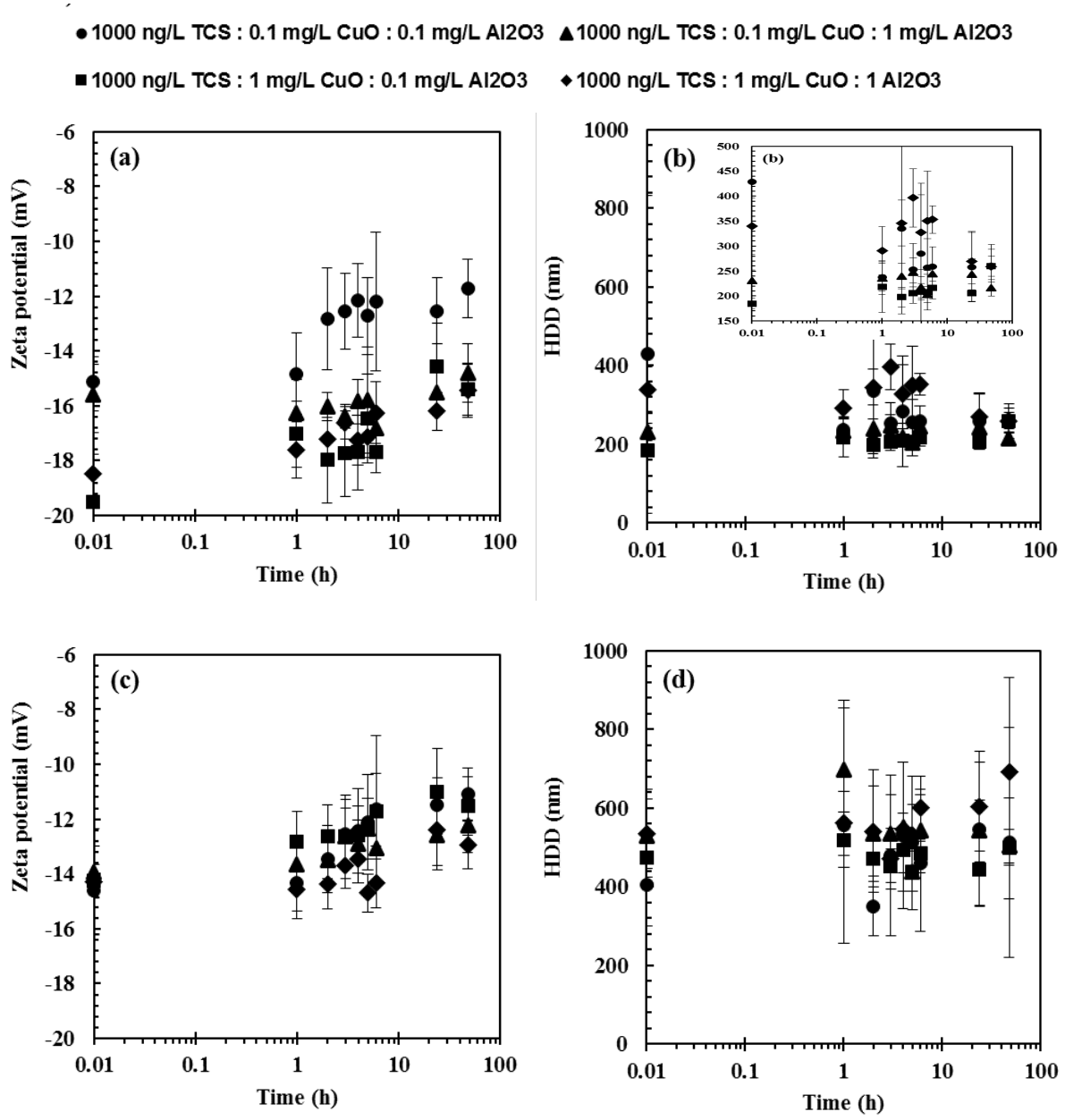

Figure 4.27: ζ-potential and HDD (a and b, respectively) in ER water in presence of TCS, and ζ-potential and HDD (c and d, respectively) in BR water in presence of TCS over 48 h. Error bars represent standard deviations (SD) for three replicates.

© University of Pretoria

Increasing the concentration of TCS to 1000 ng/L in ternary mixtures had no considerable influence on HDD which ranged from 180 to 430 nm in ER (Figure 4.27b) and 350 to700 nm in BR (Figure 4.27d). Similar ranges were observed in presence of 100 ng/L TCS. The comparisons on the influence of 100 and 1000 ng/L TCS on ternary mixtures of ENPs and TCS are summarised in Appendix 4.3. These results show that the studied concentrations of ENPs (0.1 and 1 mg/L) are low enough to be stabilised even by lower concentrations of TCS in the freshwater systems (Table 2.3). In addition, measured environmental concentrations of ENPs are orders of magnitudes lower than 0.1 mg/L used in this study (Donovan et al., 2016; Johnson et al., 2011). Ternary mixtures irrespective of mixture concentrations were more destabilised in BR water samples with higher concentrations of both NOM and electrolytes than in ER. Based on these results, the aggregation of mixtures of ENPs and TCS is characteristically influenced by water chemistry. Hence, in presence of TCS and probably other aromatic organic pollutants, heteroaggregation of ENPs will still occur and aquatic organisms will be exposed to aggregates of mixtures of ENPs and not the pristine ENPs. These findings indicate that in natural water systems, ternary mixtures of ENPs and TCS will be stable and interact with pelagic organisms where they may exert toxicological effects. Results of all aggregation and ζ-potential experiments under the various exposure media are summarized in Appendices. 4.4 to 4.10.

Overall, the enhanced stability of ENPs in presence of TCS has two major implications. Firstly, their high residence time in the water column implies increased transport and bioavailabilty to pelagic organisms where they may induce adverse effects. Secondly, ENPs may increase the toxicity of TCS via trojan horse effect as they are likely to transport adsorbed fractions of TCS into aquatic organisms. These outcomes suggest that pelagic organism are more at risk to mixtures of ENPs and TCS than benthic organisms. The findings herein contribute to the knowledge on transformation of mixtures of ENPs and organic polutants which is critical on their risk assessment in natural water systems.

© University of Pretoria

4.8. Dissolution of ENPs in river water

4.8.1. Dissolution of individual ENPs

Dissolution studies in river water matrixes from ER and BR over 48 h were done to gain insights on the timescale effect on the potential exposure of nAl_2O_3 and nCuO in terms of ionic and particulate forms. Results suggest that dissolution increased with time at a given exposure concentration (0.1 and 1 mg/L). An exposure concentration of 10 mg/L was considered too high and unlikely to be found in the environment, and therefore of limited value in the dissolution studies.

Dissolution of nCuO was observed to be time dependent. For instance, at 2 h it was 0.8% and increased to 1.44% at 48 h in ER water at nominal exposure concentration of 1 mg/L (Table 4.2). Dissolution was higher in ER compared to BR. Hence it was also influenced by river water chemistry. The higher dissolution in ER may be attributed to the low IS leading to enhanced stability of ENPs with resultant high number of active sites for dissolution (Odzak et al., 2015; Son et al., 2015). In addition, low concentration of NOM in ER may also account for the high dissolution since at high concentration, NOM has been reported to impede dissolution of ENPs (Conway et al., 2015). In BR water, at the same nominal exposure concentration of 1 mg/L, dissolution was 1.12% at 48 h. The presence of high NOM (Table 3.1) may have adsorbed the Cu^{2+} ionic species resulting in slightly lower observed concentrations. Moreover, the high IS in BR promoted aggregation which resulted in small surface area of ENPs leading to reduced number of active sites for dissolution (Gondikas et al., 2012; Li et al., 2013; Odzak et al., 2015; Son et al., 2015). Visual MINTEQ predictions on Cu^{2+} distribution in both ER and BR water samples indicate that 100% of the released ions form labile complexes with NOM (Table 4.3). High NOM has been reported to impede dissolution of nCuO in aqueous media (Conway et al., 2015; Miao et al., 2016). For example, Conway et al. (2015) investigated the dissolution of 1 mg/L nCuO in wastewater (pH 7.6, NOM 2.38 mg/L and IS 34.1 mM) and storm runoff water (pH 6.6, NOM 6.49 mg/L and IS 4.4 mM) where dissolution was found to be $< 10\%$ and 0 %, respectively. Copper tends to undergo disproportionation reactions leading to the generation of Cu^0, Cu^+ and Cu^{2+} ionic forms. In the natural aquatic environment, complex forming ions such as Cl^-, SO_4^{2-} and PO_4^{3-} are ubiquitous (Conway et al., 2015; Fang et al., 2017; Heinlaan et al., 2016; Tong et al., 2014). Therefore, this may lead to formation of various precipitation complexes (e.g. CuS and $Cu_3(PO_4)_2$). For example, the presence of sulphates in

© University of Pretoria

ER and BR water samples (Table 3.1) may have led to sulfidation processes forming highly insoluble CuS (Conway et al., 2015; Ma et al., 2014). All these processes may lead to the reduction in the concentration of detectable copper ions.

In addition, copper precipitates as a hydroxide in the pH range of 6.6 to 7.8 with ligands present in freshwater (Dimkpa et al., 2015). This pH range is very close to the pH of the river water used in this study. Hence, copper may have precipitated as a hydroxide. Dissolution of nCuO at 1 mg/L decreased with increasing pH where at pH > 7.7 very low dissolution was observed (< 3%) (Odzak et al., 2014). Hence, the low dissolution observed in this study with river water samples of pH 7.9 and 8.1 (Table 3.1), agrees with previous works (Conway et al., 2015; Heinlaan et al., 2016). The low dissolution of nCuO in freshwater systems implies that the reported toxicity of nCuO in aquatic systems may be largely attributed to the particulates and not the ionic species.

Table 4.2: Dissolution of ENPs in natural river waters river water done in triplicates using ICP-MS and recorded as mean values ± standard deviation

	Cu^{2+} (µg/L)		Al^{3+} (µg/L)	
River/ NC*	0.1 mg/L nCuO	1 mg/L nCuO	0.1 mg/L nAl_2O_3	1 mg/L nAl_2O_3
BR (2h)	4.07 ± 1.05	6.39 ± 0.60	4.36 ± 1.76	17.90 ± 1.21
BR (48 h)	4.75 ± 1.32	8.97 ± 1.41	8.27 ± 1.02	38.23 ± 1.92
ER (2 h)	2.84 ± 0.71	6.40 ± 1.54	14.87 ± 1.25	153.43 ± 8.56
ER (48 h)	3.13 ± 0.38	11.53 ± 2.41	22.29 ± 1.60	162.13 ± 7.87

*NC: nominal concentration. Data recorded as mean ± standard deviations, where $n = 3$.

Dissolution of nAl_2O_3 at nominal exposure concentration of 1 mg/L was higher in ER compared to BR water samples. The effect of time was apparent in BR water were dissolution increased by more than doubled from 2 to 48 h (Table 4.2). In ER water, dissolution increased from 29% at 2 h to 30.6% after 48 h whereas in BR, dissolution was ≤ 8% even after 48 h

© University of Pretoria

(Table 4.2). The dissolution of nAl_2O_3 observed at 1 mg/L over 48 h in this study was much lower compared to the one reported previously (Pakrashi et al., 2012). Pakrashi et al. (2012) studied the dissolution of nAl_2O_3 at the concentration 1 mg/L in lake water and observed dissolution of 94%. However, at lower concentration of 0.1 mg/L, after 48 h, dissolution increased to 15.6% and 42.1% in BR and ER, respectively. Based on Visual MINTEQ prediction on the distribution of Al^{3+} at nominal concentration of 1 mg/L in ER and BR water systems, 93 and 81% of Al^{3+} formed the soluble ionic compound $Al(OH)_4^-$ in ER and BR, respectively (Table 4.4). This may account for the higher dissolution of Al_2O_3 detected in ER water (Table 4.2). At least 5 and 17% of Al^{3+} formed labile complexes with NOM whereas at least 1 and 2% formed hydroxides of aluminium in ER and BR, respectively, as shown in Table 4.4.

Low dissolution, especially in BR water, may be attributed to water chemistry driven-factors such as NOM resulting in formation of complexes with released ions as predicted by Visual MINTEQ (Table 4.4). In addition, adsorption of NOM onto surfaces of ENPs leads to the formation of a coating that impedes dissolution (Ghosh et al., 2008; Pakrashi et al., 2012). Herein, the high dissolution in ER water corresponds to low HDD observed ($\leq$ 250 nm) at 0.1 mg/L compared to results in BR water where aggregates of > 300 nm were formed as shown in Figures 4.15b and d, respectively. In addition, the released ions may undergo chelation with components of freshwater such as NOM (Conway et al., 2015; Yang et al., 2009), making them less available for detection. NOM does not only influence dissolution of ENPs, it also acts as a scavenger for released ions by forming complexes with the released ions (Benjamin, 2002). Due to slightly higher dissolution of nAl_2O_3 in freshwater systems, the reported toxicity of nAl_2O_3 in aquatic systems may be attributed to both ionic species and particulates. These results suggest that at environmentally relevant concentration (< 0.1 mg/L), ENPs may undergo greater dissolution than was observed in the present study.

© University of Pretoria

Table 4.3: Distribution of Cu^{2+} calculated by Visual MINTEQ from dissolved nCuO in ER and BR water samples over 48 h

	ER (% distribution Cu^{2+})		BR (% distribution Cu^{2+})	
Species/ NC*	0.1 mg/L nCuO	1 mg/L nCuO	0.1 mg/L nCuO	1 mg/L nCuO
/$FA_2Cu_{(aq)}$	38.96	38.99	44.87	44.88
/FA_2CuOH(aq)	61.04	61.01	55.13	55.12

*NC: nominal concentration.

The speciation results of dissolved aluminium in ER and BR water samples based on modelling using Visual MINTEQ showed that 100% of dissolved aluminium at nominal concentrations of 0.1 and 1 mg/L nAl_2O_3 formed labile complexes with NOM and OH^- in both river systems (Table 4.4). In ER water, at least 87% of dissolved aluminium formed the anion $Al(OH)_4^-$ and about 12% formed complexes with NOM. In BR water, 69% and 81% of the dissolved aluminium, at nominal concentrations of 0.1 and 1 mg/L nAl_2O_3 respectively, formed the anion $Al(OH)_4^-$. Of the rest, 30% and 17% formed labile complexes with NOM, at nominal concentrations of 0.1 and 1 mg/L nAl_2O_3, respectively. This is summarised in Table 4.4. Visual MINTEQ predicted the absence of any free Al^{3+} for both river water samples. Typically, NOM forms soluble metal complexes at neutral and alkaline pH conditions and most of the complexes formed in the natural water matrixes are labile (Adeleye et al., 2014). Hence, the released metal ions were still detected by ICP-MS.

© University of Pretoria

Table 4.4: Distribution of Al^{3+} calculated by Visual MINTEQ from dissolved nAl_2O_3 in ER and BR water samples over 48 h

	ER (% distribution Al^{3+})		BR (% distribution Al^{3+})	
Species/ NC*	0.1 mg/L nAl_2O_3	1 mg/L nAl_2O_3	0.1 mg/L nAl_2O_3	1 mg/L nAl_2O_3
$Al(OH)^{2+}$	0.03	0.03	0.06	0.07
$Al(OH)_{3(aq)}$	1.33	1.43	1.63	1.92
$Al(OH)_4^-$	86.69	93.18	68.59	80.82
$/FA_2AlOH_{(aq)}$	11.90	5.34	29.58	17.11
$/FA_2Al^+_{(aq)}$	0.05	0.02	0.16	0.09

*NC: nominal concentration.

4.8.2. Dissolution of Binary mixtures of ENPs in river water

Dissolution of binary mixtures of nAl_2O_3 and nCuO in natural water matrixes was investigated over 48 h. The dissolution of nAl_2O_3 from all mixtures was below the detection limit as no Al^{3+} was detected. However, Cu^{2+} was detected from the studied mixtures due to dissolution of nCuO. The dissolution was time dependent at a given exposure concentration (0.1 or 1 mg/L) as shown in Table 4.5.

© University of Pretoria

Table 4.5: Dissolution of nCuO in river water samples done using ICP-MS and recorded as mean values ± standard deviation

	Cu^{2+} (µg/L)				
River*	nCuO 0.1 mg/L*	nCuO 1 mg/L*	(nCuO, nAl_2O_3) (0.1, 1) mg/L*	(nCuO, nAl_2O_3) (1,0.1) mg/L*	(nCuO, nAl_2O_3) (1,1) mg/L*
BR (2h)	4.07 ± 1.05	6.39 ± 0.60	6.33 ± 1.53	15.33 ± 3.06	11.33 ± 1.15
BR (48 h)	4.75 ± 1.32	8.97 ± 1.41	8.00 ± 1.00	15.67 ± 2.89	13.00 ± 0.00
ER (2 h)	2.84 ± 0.71	6.40 ± 1.54	3.33 ± 1.53	6.67 ± 2.08	4.00 ± 0.00
ER (48 h)	3.13 ± 0.38	11.53 ± 2.41	3.00 ± 1.00	5.00 ± 1.00	5.33 ± 1.15

*Nominal concentration of ENPs. Data recorded as mean ± standard deviation, where $n = 3$.

The dissolution of nCuO was 0.80% at 2 h and increased slightly to 1.12% after 48 h in BR water samples at a nominal exposure concentration of 1 mg/L (Table 4.5). However, in the presence of 0.1 mg/L nAl_2O_3, the dissolution increased to 1.92 and 1.96% at 2 and 48 h, respectively. Despite the dissolution of 1 mg/L nCuO being low in BR water, it increased by more than 100% in the presence of 0.1 mg/L nAl_2O_3 at 2 h. These observations are consistent with the reduction in aggregation for the mixture of (1, 0.1) mg/L nCuO and nAl_2O_3, respectively, where HDD decreased from 783 nm at 0 h to 620 nm at 48 h. This decrease in HDD may have led to an increase in the number of available sites for dissolution (Gondikas et al., 2012; Son et al., 2015). Increasing the concentration of nAl_2O_3 in the mixture to 1 mg/L, a slight decrease in dissolution of nCuO was observed at both 2 (1.42%) and 48 h (1.63%). This was in agreement with the observed increase in HDD at 2 h (927 nm) and at 48 (1008 nm) compared to > 805 nm at both 2 and 48 h in presence of 0.1 mg/L nAl_2O_3. The increase in aggregation leads to reduction in the surface area and consequently, fewer available active sites for ion release (Bian et al., 2011; Miao et al., 2010; Xiao et al., 2018). Hence, the observed reduction in dissolution. In addition, the observed decrease in dissolution at higher concentration of nAl_2O_3 may be attributed to adsorption of released Cu^{2+} onto the surfaces of nAl_2O_3 which had a large surface area (50.5 m^2/g) as observed from other studies on various systems (Mansouri et al., 2016; Tong et al., 2014; Wilke et al., 2016).

© University of Pretoria

The dissolution of nCuO in ER water samples at nominal exposure concentration of 0.1 mg/ was 3.55% at 2 h and increased slightly to 3.91% after 48 h (Table 4.5). No significant influence of nAl_2O_3 was observed on the dissolution of nCuO in ER water irrespective of exposure concentration and time (Table 4.5). These results are consistent with the observations under the influence of nAl_2O_3 on the aggregation on nCuO where no significant influence was observed (Figures 4.19b and 4.20b). NOM has been reported to enhance dissolution of ENPs (Jiang et al., 2015; Philippe and Schaumann, 2014; Xiao et al., 2018). Chelation effects on the surfaces of ENPs and binding to the released ions leading to deviation from dissolution equilibrium have been proposed as the mechanisms by which NOM enhances dissolution of ENPs (Jiang et al., 2015; Philippe and Schaumann, 2014). This may account for higher dissolution in BR with higher concentration of NOM (8.16 mg/L) than ER with lower concentration (5.07 mg/L). In addition, IS can promote dissolution for charged species since their activity decreases with increasing IS to the limit of 1.0 M (Grenthe, 1997; Mwaanga, 2012). BR had higher IS (5.35 mM) compared to ER (2.48 mM) as shown in Table 3.1. This may account for the higher dissolution observed in BR. The functional groups present in NOM e.g. carboxylic and phenolic groups, can form complexes with released ions which may lead to a reduction in the amount of detectable ions (Collin et al., 2016). In addition, other ions present in natural water matrixes can form complexes as discussed in section 2.3.2.2. Hence, these results indicate that both water chemistry and presence of other ENPs in the system have significant influence on dissolution of nCuO. The low dissolution of nCuO implies that the observed effects of nCuO to pelagic dwelling organisms may be predominantly associated to the particulate forms as reported in toxicity studies (Abdel-Khalek et al., 2015; Heinlaan et al., 2011; Thit et al., 2017).

4.8.3. Dissolution of Ternary mixtures of ENPs and TCS in river water

The dissolution of nAl_2O_3 and nCuO in ternary mixtures of nAl_2O_3, nCuO and TCS in river water matrixes was studied over 48 h. However, the dissolution of both ENPs in the ternary mixtures were below detection limit for ICP-MS. In both river systems, the presence of TCS stabilised the ENPs as shown in Figures 4.26 and 4.27. The resultant adsorption of TCS onto surfaces of ENPs may have provided a coating which possibly blocked the dissolution sites leading to the absence of detectable ions (Yu et al., 2017). In addition, adsorption of NOM has the potential to impede dissolution of ENPs by blocking active site on surface of ENPs (Deonarine et al., 2011; Yu et al., 2017). The interaction of NOM with other organic pollutants

© University of Pretoria

is influenced by factors including such microdomains within NOM that segregates interactions based on function groups such as aromatic or carbohydrate domains, presence of function groups that promote hydrogen bonding and preference based on configuration and conformation of the molecules and strands at microstructure level (Pignatello, 2012). Since TCS is an aromatic phenol, it may have undergone interactions with NOM leading to changes in the properties of NOM including molecular structure, MW, hydrophobicity, conformation and charge which in turn affect the interaction of NOM with ENPs (Mwaanga, 2012; Stumm and Morgan, 2012). For example, increase in MW of NOM results in increased adsorption of NOM onto the surfaces of ENPs (Mwaanga, 2012). In the current study, adsorption of TCS was evidenced by increased stability of ENPs in presence of TCS such that ternary mixtures of ENPs and TCS had lower HDD (Figure 4.26) compared to binary mixtures of ENPs (Figures 4.17 and 4.19). Increased adsorption of NOM-TCS complexes on surfaces of ENPs may have impeded the dissolution of ENPs by blocking active sites for dissolution on surface of ENPs resulting in the reduction of released metal ions (Behera et al., 2010; Deonarine et al., 2011; Yu et al., 2017). These findings suggest that despite the aggregate size of ternaries being comparable to that of individual ENPs in the same exposure media, ternaries may pose reduced toxic effects to aquatic organisms because of low dissolution as toxicological effects are usually linked to ionic rather than particulate species (Leareng et al., 2020; Song et al., 2020; Tong et al., 2015; Yu et al., 2016).

The low dissolution observed herein for singles, binary and ternary mixtures of ENPs implies that the ecological effects of the studied ENPs are due to particulates species rather than ionic species. The presence of aromatic organic pollutants in natural aquatic systems may reduce the toxicity of ENPs resulting from ionic species but increase the effects due to particulate species as a result of enhanced stability. These findings contribute to the increasing knowledge on the interactions of mixtures of ENPs and organic pollutants. However, more work is necessary to elucidate the underpinning mechanisms of interactions in mixtures responsible for the observed effects.

© University of Pretoria

Chapter 5: Conclusions and recommendations

5.1. Conclusions

This study investigated the influence of water chemistry parameters such as pH, IS and NOM on the transformation of ENPs. The aggregation and dissolution of individual ENPs, binary mixtures of ENPs (ENP-ENP), binary mixtures of ENPs with TCS (ENP-TCS) and ternary mixtures of ENPs and TCS (ENP-ENP-TCS) was studied in aquatic systems at the low concentrations close to what is expected in the natural aquatic environment. This study revealed that the aggregation and dissolution of nAl_2O_3 and nCuO are influenced by water chemistry parameters (pH, IS and NOM), TCS and presence of other ENPs aquatic systems. The critical findings in this study includes the revelation that the aggregation and dissolution of ENPs is influenced not only by water chemistry parameters but also by the presence of other ENPs and organic pollutants in aquatic systems. Three objectives were pursued to achieve the aims of this study:

Objective 1: Transformation of nCuO and nAl_2O_3 in synthetic and river water systems.

The transformation of ENPs in aquatic systems was influenced by pH, IS and NOM. The pH, determined the ζ–potential of ENPs which in turn influenced their state of aggregation. Aggregation of ENPs was observed to reach a maximum at pH_{IEP}. The IS generated by the concentrations of electrolytes, typically encountered in natural aquatic systems, is insufficient to compress the EDL for significant reduction of ζ–potential. Therefore, the IS had an insignificant influence on the aggregation of ENPs. NOM may have adsorbed onto surfaces of ENPs, leading to increased ζ-potentials and impeded aggregation. In river water, with extremely complex composition, the resultant transformation of ENPs is determined by complicated interactions among water chemistry factors. These may counteract each other as is evidenced by higher dissolution rates observed in ER compared to BR water. Also, larger aggregates were observed in BR compared to ER water. In river water systems, ENPs are primarily present as aggregates. The dissolution of ENPs is influenced by NOM coating the surfaces of ENPs. This implies that organisms are seldom exposed to single particle ENPs, but rather to their aggregates or the ions which they released. Because of chelation and precipitation effects, the released ions might not pose the toxicity expected from studies conducted in

© University of Pretoria

synthetic water. In river water, ENPs are generally stable, this implies they are more likely to interact with pelagic than benthic organisms. The observed variations in aggregation and dissolution of ENPs in river water suggest that it is impossible to generalize the fate and transformation of ENPs in aquatic systems.

Objective 2: Interaction of binary mixtures of nCuO and nAl_2O_3 in synthetic and river water

The interaction of binary mixtures of ENPs was influenced by the same water chemistry parameters mentioned before. At circumneutral pH, the ζ-potential was affected by the ratio of the ENPs present in the binary mixtures. It decreased with increasing relative concentration of nCuO. It also increased with increase in IS. However, in both cases, this did not significantly influence the aggregation of ENPs in synthetic water. Adding NOM increased the ζ-potential, possibly due to adsorption of NOM onto the surfaces of ENPs with resultant imparting of negative charge. However, this also had only a marginal influence on aggregation. The reasons might be due to the fact that the changes in the ζ-potential was insufficient to have an effect.

In river water, binary mixtures of ENPs formed larger aggregates, probably due to hetero-aggregation. Larger aggregates were observed in BR compared to ER water. Dissolution of nCuO was enhanced in BR water in the presence of low concentrations of nAl_2O_3. However, this decreased at higher concentration of nAl_2O_3 possibly due to adsorption of Cu^{2+} on the surfaces of nAl_2O_3. Strangely, no significant influence was observed in ER water. Therefore, ecological effects, originating from copper ionic species, appear to be more profound in the presence of low concentrations of nAl_2O_3. Both water chemistry and concentration ratios of ENPs influence the transformation of mixtures of ENPs in aquatic systems. The high stability of mixtures of ENPs in natural water systems implies persistence, i.e. long residence times. This has implications for the aquatic organisms present.

Objective 3: Influence of TCS on the transformation of ENPs as binary and ternary mixtures in river water systems

TCS stabilised ENPs in ER water but destabilised them in BR water. This was due to the influence of differences in the physicochemical parameters (NOM and IS). The influence of TCS on the aggregation of ENPs is similar but more pronounced at low concentrations of

© University of Pretoria

NOM. No significant effect of TCS on ζ-potential of ENPs was observed. The aggregation of ternary mixtures of TCS and ENPs was lower compared to that of binary mixtures of ENPs irrespective of differences in water chemistry. The resultant interaction of TCS and NOM impeded dissolution of ENPs. The ions concentrations were below the detection limit. Hence, in ternary mixtures, the expectation is that ecological effects will be limited. This applies to effects arising from the presence of solvated ionic species, not for particulate ENPs. This confirms that transformation of mixtures is unique and that it may not be possible to predict the behaviour of mixtures based on the behaviour of the individual components alone.

These findings motivate the need to investigate specific interactions that exist between TCS and ENPs and between TCS and NOM to elucidate the mechanisms underpinning the observed transformations.

5.2. Recommendations

The fate and transformation of ENPs are not only influenced by water chemistry but also the presence of organic pollutants and other ENPs in aquatic systems. Therefore, ENPs-specific studies must be conducted to determine their fate and transformation. They simply cannot be predicted based on studies done on other ENPs. The enhanced aggregation of nCuO at low concentration is in contrast with the aggregation trends observed for other ENPs. It warrants further investigation. Hence, the fate and transformation of ENPs in aquatic systems are unique and are not predictable from experimental results based on DIW. Therefore, studies on the fate and transformation of ENP mixtures in natural water systems, at environmentally relevant concentrations, are recommended to support risk assessment of ENPs in the natural environmental compartment. Furthermore, studies linking the exposure media composition with dissolution and/or aggregation of ENPs are highly recommended.

© University of Pretoria

References

ABDEL-KHALEK, A. A., KADRY, M. A., BADRAN, S. R. & MARIE, M.-A. S. 2015. Comparative toxicity of copper oxide bulk and nano particles in Nile tilapia; Oreochromis niloticus: biochemical and oxidative stress. *The Journal of Basic & Applied Zoology.* 72**,** 43-57.

ADAM, V., LOYAUX-LAWNICZAK, S., LABILLE, J., GALINDO, C., DEL NERO, M., GANGLOFF, S., WEBER, T. & QUARANTA, G. 2016. Aggregation behaviour of TiO_2 nanoparticles in natural river water. *Journal of Nanoparticle Research.* 18**,** 13.

ADAMCZYK, Z. & WERONŚKI, P. 1999. Application of the DLVO theory for particle deposition problems. *Advances in Colloid and Interface Science.* 83**,** 137-226.

ADELEYE, A. S., CONWAY, J. R., PEREZ, T., RUTTEN, P. & KELLER, A. A. 2014. Influence of extracellular polymeric substances on the long-term fate, dissolution, and speciation of copper-based nanoparticles. *Environmental science & technology.* 48**,** 12561-12568.

AHAMED, M., AKHTAR, M. J., ALHADLAQ, H. A. & ALROKAYAN, S. A. 2015. Assessment of the lung toxicity of copper oxide nanoparticles: current status. *Nanomedicine.* 10**,** 2365-2377.

AIKEN, G. R., HSU-KIM, H. & RYAN, J. N. 2011a. Influence of dissolved organic matter on the environmental fate of metals, nanoparticles, and colloids. ACS Publications.

AIKEN, G. R., HSU-KIM, H. & RYAN, J. N. 2011b. Influence of dissolved organic matter on the environmental fate of metals, nanoparticles, and colloids. ACS Publications.

ALABRESM, A., MIRSHAHGHASSEMI, S., CHANDLER, G. T., DECHO, A. W. & LEAD, J. 2017. Use of PVP-coated magnetite nanoparticles to ameliorate oil toxicity to an estuarine meiobenthic copepod and stimulate the growth of oil-degrading bacteria. *Environmental Science: Nano.* 4**,** 1859-1865.

AMAL, R., RAPER, J. A. & WAITE, T. 1992. Effect of fulvic acid adsorption on the aggregation kinetics and structure of hematite particles. *Journal of Colloid and Interface Science.* 151**,** 244-257.

AMDE, M., LIU, J.-F., TAN, Z.-Q. & BEKANA, D. 2017. Transformation and bioavailability of metal oxide nanoparticles in aquatic and terrestrial environments. A review. *Environmental Pollution.* 230**,** 250-267.

© University of Pretoria

AMOATEY, P. & BAAWAIN, M. S. 2019. Effects of pollution on freshwater aquatic organisms. *Water Environment Research.*

ANGEL, B. M., BATLEY, G. E., JAROLIMEK, C. V. & ROGERS, N. J. 2013. The impact of size on the fate and toxicity of nanoparticulate silver in aquatic systems. *Chemosphere.* 93**,** 359-365.

ANITA, S., RAMACHANDRAN, T., RAJENDRAN, R., KOUSHIK, C. & MAHALAKSHMI, M. 2011. A study of the antimicrobial property of encapsulated copper oxide nanoparticles on cotton fabric. *Textile Research Journal.* 81**,** 1081-1088.

APPLEROT, G., LELLOUCHE, J., LIPOVSKY, A., NITZAN, Y., LUBART, R., GEDANKEN, A. & BANIN, E. 2012. Understanding the antibacterial mechanism of CuO nanoparticles: revealing the route of induced oxidative stress. *Small.* 8**,** 3326-3337.

ARENAS-LAGO, D., MONIKH, F. A., VIJVER, M. G. & PEIJNENBURG, W. J. 2019. Dissolution and aggregation kinetics of zero valent copper nanoparticles in (simulated) natural surface waters: Simultaneous effects of pH, NOM and ionic strength. *Chemosphere.*

AUFFAN, M., BOTTERO, J.-Y., CHANEAC, C. & ROSE, J. 2010. Inorganic manufactured nanoparticles: how their physicochemical properties influence their biological effects in aqueous environments. *Nanomedicine.* 5**,** 999-1007.

AUFFAN, M., ROSE, J., BOTTERO, J.-Y., LOWRY, G. V., JOLIVET, J.-P. & WIESNER, M. R. 2009. Towards a definition of inorganic nanoparticles from an environmental, health and safety perspective. *Nature nanotechnology.* 4**,** 634.

AZEVEDO, S., HOLZ, T., RODRIGUES, J., MONTEIRO, T., COSTA, F., SOARES, A. & LOUREIRO, S. 2017. A mixture toxicity approach to predict the toxicity of Ag decorated ZnO nanomaterials. *Science of the Total Environment.* 579**,** 337-344.

BAALOUSHA, M. 2009. Aggregation and disaggregation of iron oxide nanoparticles: influence of particle concentration, pH and natural organic matter. *Science of the total Environment.* 407**,** 2093-2101.

BAALOUSHA, M., MANCIULEA, A., CUMBERLAND, S., KENDALL, K. & LEAD, J. R. 2008. Aggregation and surface properties of iron oxide nanoparticles: influence of pH and natural organic matter. *Environmental toxicology and chemistry.* 27**,** 1875-1882.

BADAWY, A. M. E., LUXTON, T. P., SILVA, R. G., SCHECKEL, K. G., SUIDAN, M. T. & TOLAYMAT, T. M. 2010. Impact of environmental conditions (pH, ionic strength,

© University of Pretoria

and electrolyte type) on the surface charge and aggregation of silver nanoparticles suspensions. *Environmental science & technology.* 44**,** 1260-1266.

BARGHAVA, H. & LEONARD, P. 1996. 'Triclosan Application and Safety. *Am. J. Infect. Control.* 24**,** 209.

BATLEY, G. E., KIRBY, J. K. & MCLAUGHLIN, M. J. 2012. Fate and risks of nanomaterials in aquatic and terrestrial environments. *Accounts of chemical research.* 46**,** 854-862.

BAUN, A., SØRENSEN, S. N., RASMUSSEN, R., HARTMANN, N. B. & KOCH, C. B. 2008. Toxicity and bioaccumulation of xenobiotic organic compounds in the presence of aqueous suspensions of aggregates of nano-C60. *Aquatic Toxicology.* 86**,** 379-387.

BEHERA, S. K., OH, S.-Y. & PARK, H.-S. 2010. Sorption of triclosan onto activated carbon, kaolinite and montmorillonite: effects of pH, ionic strength, and humic acid. *Journal of hazardous materials.* 179**,** 684-691.

BENAVIDES, M., FERNÁNDEZ-LODEIRO, J., COELHO, P., LODEIRO, C. & DINIZ, M. S. 2016. Single and combined effects of aluminum (Al_2O_3) and zinc (ZnO) oxide nanoparticles in a freshwater fish, Carassius auratus. *Environmental Science and Pollution Research.* 23**,** 24578-24591.

BENJAMIN, M. M. 2002. Adsorption reactions. *Water Chemistry.* McGraw-Hill New York.

BESHA, A. T., GEBREYOHANNES, A. Y., TUFA, R. A., BEKELE, D. N., CURCIO, E. & GIORNO, L. 2017. Removal of emerging micropollutants by activated sludge process and membrane bioreactors and the effects of micropollutants on membrane fouling: a review. *Journal of environmental chemical engineering.* 5**,** 2395-2414.

BESHA, A. T., LIU, Y., FANG, C., BEKELE, D. N. & NAIDU, R. 2019. Assessing the interactions between micropollutants and nanoparticles in engineered and natural aquatic environments. *Critical Reviews in Environmental Science and Technology.* 1-81.

BESTER, K. 2005. Fate of triclosan and triclosan-methyl in sewage treatmentplants and surface waters. *Archives of Environmental Contamination and Toxicology.* 49**,** 9-17.

BHARTI, B., MEISSNER, J. & FINDENEGG, G. H. 2011. Aggregation of silica nanoparticles directed by adsorption of lysozyme. *Langmuir.* 27**,** 9823-9833.

BHATTACHARJEE, S. 2016. DLS and zeta potential–what they are and what they are not? *Journal of Controlled Release.* 235**,** 337-351.

© University of Pretoria

BHUVANESHWARI, M., BAIROLIYA, S., PARASHAR, A., CHANDRASEKARAN, N. & MUKHERJEE, A. 2016. Differential toxicity of Al_2O_3 particles on Gram-positive and Gram-negative sediment bacterial isolates from freshwater. *Environmental Science and Pollution Research.* 23**,** 12095-12106.

BIAN, S.-W., MUDUNKOTUWA, I. A., RUPASINGHE, T. & GRASSIAN, V. H. 2011. Aggregation and dissolution of 4 nm ZnO nanoparticles in aqueous environments: influence of pH, ionic strength, size, and adsorption of humic acid. *Langmuir.* 27**,** 6059-6068.

BONE, A. J., COLMAN, B. P., GONDIKAS, A. P., NEWTON, K. M., HARROLD, K. H., CORY, R. M., UNRINE, J. M., KLAINE, S. J., MATSON, C. W. & DI GIULIO, R. T. 2012. Biotic and abiotic interactions in aquatic microcosms determine fate and toxicity of Ag nanoparticles: part 2–toxicity and Ag speciation. *Environmental science & technology.* 46**,** 6925-6933.

BOPP, S. K., BAROUKI, R., BRACK, W., DALLA COSTA, S., DORNE, J.-L. C., DRAKVIK, P. E., FAUST, M., KARJALAINEN, T. K., KEPHALOPOULOS, S. & VAN KLAVEREN, J. 2018. Current EU research activities on combined exposure to multiple chemicals. *Environment international.* 120**,** 544-562.

BORM, P., KLAESSIG, F. C., LANDRY, T. D., MOUDGIL, B., PAULUHN, J. R., THOMAS, K., TROTTIER, R. & WOOD, S. 2006. Research strategies for safety evaluation of nanomaterials, part V: role of dissolution in biological fate and effects of nanoscale particles. *Toxicological Sciences.* 90**,** 23-32.

BOSGRA, S., VAN EIJKEREN, J. C. & SLOB, W. 2009. Dose addition and the isobole method as approaches for predicting the cumulative effect of non-interacting chemicals: A critical evaluation. *Critical reviews in toxicology.* 39**,** 418-426.

BOUHAIK, I. S., LEROY, P., OLLIVIER, P., AZAROUAL, M. & MERCURY, L. 2013. Influence of surface conductivity on the apparent zeta potential of TiO2 nanoparticles: Application to the modeling of their aggregation kinetics. *Journal of colloid and interface science.* 406**,** 75-85.

BOXALL, A., TIEDE, K., CHAUDHRY, Q., AITKEN, R., JONES, A., JEFFERSON, B., LEWIS, J. & TEAM, E. 2007a. Current and future predicted exposure to engineered nanoparticles. *Science of the Total Environment.* 390**,** 396-409.

BOXALL, A. B., CHAUDHRY, Q., SINCLAIR, C., JONES, A., AITKEN, R., JEFFERSON, B. & WATTS, C. 2007b. Current and future predicted environmental

© University of Pretoria

exposure to engineered nanoparticles. *Central Science Laboratory, Department of the Environment and Rural Affairs, London, UK.* 89.

BRAUSCH, J. M. & RAND, G. M. 2011. A review of personal care products in the aquatic environment: environmental concentrations and toxicity. *Chemosphere.* 82**,** 1518-1532.

BROWN, M. A., ABBAS, Z., KLEIBERT, A., GREEN, R. G., GOEL, A., MAY, S. & SQUIRES, T. M. 2016. Determination of surface potential and electrical double-layer structure at the aqueous electrolyte-nanoparticle interface. *Physical Review X.* 6**,** 011007.

BRUNETTI, G., DONNER, E., LAERA, G., SEKINE, R., SCHECKEL, K. G., KHAKSAR, M., VASILEV, K., DE MASTRO, G. & LOMBI, E. 2015. Fate of zinc and silver engineered nanoparticles in sewerage networks. *Water research.* 77**,** 72-84.

CAO, G. 2004. Imperial College Press. *Nanostructures & nanomaterials: synthesis, properties & applications.*

CAREY, D. E. & MCNAMARA, P. J. 2015. The impact of triclosan on the spread of antibiotic resistance in the environment. *Frontiers in microbiology.* 5**,** 780.

CARLSON, C. A. 2002. Production and removal processes. *Biogeochemistry of marine dissolved organic matter.* 91-151.

CHALEW, T. E. & HALDEN, R. U. 2009. Environmental exposure of aquatic and terrestrial biota to triclosan and triclocarban 1. *JAWRA Journal of the American Water Resources Association.* 45**,** 4-13.

CHAÚQUE, E., ZVIMBA, J., NGILA, J. & MUSEE, N. 2014. Stability studies of commercial ZnO engineered nanoparticles in domestic wastewater. *Physics and Chemistry of the Earth, Parts A/B/C.* 67**,** 140-144.

CHEKLI, L., PHUNTSHO, S., ROY, M. & SHON, H. K. 2013. Characterisation of Fe-oxide nanoparticles coated with humic acid and Suwannee River natural organic matter. *Science of the Total Environment.* 461**,** 19-27.

CHEKLI, L., ZHAO, Y., TIJING, L., PHUNTSHO, S., DONNER, E., LOMBI, E., GAO, B. & SHON, H. 2015. Aggregation behaviour of engineered nanoparticles in natural waters: characterising aggregate structure using on-line laser light scattering. *Journal of hazardous materials.* 284**,** 190-200.

CHEN, D., CHEN, C., SHEN, W., QUAN, H., CHEN, S., XIE, S., LUO, X. & GUO, L. 2017. MOF-derived magnetic porous carbon-based sorbent: synthesis,

© University of Pretoria

characterization, and adsorption behavior of organic micropollutants. *Advanced Powder Technology.* 28**,** 1769-1779.

CHEN, G., LIU, X. & SU, C. 2012. Distinct effects of humic acid on transport and retention of TiO_2 rutile nanoparticles in saturated sand columns. *Environmental science & technology.* 46**,** 7142-7150.

CHEN, H., CHENG, Y., MENG, D., XUE, G., JIANG, M. & LI, X. 2018. Joint effect of triclosan and copper nanoparticles on wastewater biological nutrient removal. *Environmental technology.* 39**,** 2447-2456.

CHEN, J., GU, B., ROYER, R. A. & BURGOS, W. D. 2003a. The roles of natural organic matter in chemical and microbial reduction of ferric iron. *Science of the Total Environment.* 307**,** 167-178.

CHEN, M., YAMAMURO, S., FARRELL, D. & MAJETICH, S. A. 2003b. Gold-coated iron nanoparticles for biomedical applications. *Journal of applied physics.* 93**,** 7551-7553.

CHOWDHURY, I., WALKER, S. L. & MYLON, S. E. 2013. Aggregate morphology of nano-TiO 2: role of primary particle size, solution chemistry, and organic matter. *Environmental Science: Processes & Impacts.* 15**,** 275-282.

CHU, K. W. & CHOW, K. L. 2002. Synergistic toxicity of multiple heavy metals is revealed by a biological assay using a nematode and its transgenic derivative. *Aquatic Toxicology.* 61**,** 53-64.

COLLIN, B., AUFFAN, M., JOHNSON, A. C., KAUR, I., KELLER, A. A., LAZAREVA, A., LEAD, J. R., MA, X., MERRIFIELD, R. C. & SVENDSEN, C. 2014. Environmental release, fate and ecotoxicological effects of manufactured ceria nanomaterials. *Environmental Science: Nano.* 1**,** 533-548.

COLLIN, B., TSYUSKO, O. V., STARNES, D. L. & UNRINE, J. M. 2016. Effect of natural organic matter on dissolution and toxicity of sulfidized silver nanoparticles to Caenorhabditis elegans. *Environmental Science: Nano.* 3**,** 728-736.

COMMISSION, E. 2011. Commission recommendation of 18 October 2011 on the definition of nanomaterial (2011/696/EU). *Official Journal of the European Communities: Legis.* 275**,** 38.

CONWAY, J. R., ADELEYE, A. S., GARDEA-TORRESDEY, J. & KELLER, A. A. 2015. Aggregation, dissolution, and transformation of copper nanoparticles in natural waters. *Environmental science & technology.* 49**,** 2749-2756.

© University of Pretoria

COOGAN, M. A. & POINT, T. W. L. 2008. Snail bioaccumulation of triclocarban, triclosan, and methyltriclosan in a North Texas, USA, stream affected by wastewater treatment plant runoff. *Environmental Toxicology and Chemistry: An International Journal.* 27**,** 1788-1793.

CROTEAU, M.-N. L., MISRA, S. K., LUOMA, S. N. & VALSAMI-JONES, E. 2014. Bioaccumulation and toxicity of CuO nanoparticles by a freshwater invertebrate after waterborne and dietborne exposures. *Environmental science & technology.* 48**,** 10929-10937.

CUPAIOLI, F. A., ZUCCA, F. A., BORASCHI, D. & ZECCA, L. 2014. Engineered nanoparticles. How brain friendly is this new guest? *Progress in neurobiology.* 119**,** 20-38.

DĄBROWSKI, A. 2001. Adsorption—from theory to practice. *Advances in colloid and interface science.* 93**,** 135-224.

DAS, D., NATH, B. C., PHUKON, P. & DOLUI, S. K. 2013. Synthesis and evaluation of antioxidant and antibacterial behavior of CuO nanoparticles. *Colloids and Surfaces B: Biointerfaces.* 101**,** 430-433.

DEFRIEND, K. A., WIESNER, M. R. & BARRON, A. R. 2003. Alumina and aluminate ultrafiltration membranes derived from alumina nanoparticles. *Journal of membrane science.* 224**,** 11-28.

DEGEN, A. & KOSEC, M. 2000. Effect of pH and impurities on the surface charge of zinc oxide in aqueous solution. *Journal of the European Ceramic Society.* 20**,** 667-673.

DELAY, M., DOLT, T., WOELLHAF, A., SEMBRITZKI, R. & FRIMMEL, F. H. 2011. Interactions and stability of silver nanoparticles in the aqueous phase: Influence of natural organic matter (NOM) and ionic strength. *Journal of Chromatography A.* 1218**,** 4206-4212.

DENG, R., LIN, D., ZHU, L., MAJUMDAR, S., WHITE, J. C., GARDEA-TORRESDEY, J. L. & XING, B. 2017. Nanoparticle interactions with co-existing contaminants: joint toxicity, bioaccumulation and risk. *Nanotoxicology.* 11**,** 591-612.

DEONARINE, A., LAU, B. L., AIKEN, G. R., RYAN, J. N. & HSU-KIM, H. 2011. Effects of humic substances on precipitation and aggregation of zinc sulfide nanoparticles. *Environmental science & technology.* 45**,** 3217-3223.

DERKSEN, J., RIJS, G. & JONGBLOED, R. 2004. Diffuse pollution of surface water by pharmaceutical products. *Water Science and Technology.* 49**,** 213-221.

© University of Pretoria

DHILLON, G. S., KAUR, S., PULICHARLA, R., BRAR, S. K., CLEDÓN, M., VERMA, M. & SURAMPALLI, R. Y. 2015. Triclosan: current status, occurrence, environmental risks and bioaccumulation potential. *International journal of environmental research and public health.* 12**,** 5657-5684.

DIEGOLI, S., MANCIULEA, A. L., BEGUM, S., JONES, I. P., LEAD, J. R. & PREECE, J. A. 2008. Interaction between manufactured gold nanoparticles and naturally occurring organic macromolecules. *Science of the Total Environment.* 402**,** 51-61.

DIMKPA, C. O., MCLEAN, J. E., BRITT, D. W. & ANDERSON, A. J. 2015. Nano-CuO and interaction with nano-ZnO or soil bacterium provide evidence for the interference of nanoparticles in metal nutrition of plants. *Ecotoxicology.* 24**,** 119-129.

DOMINGOS, R. F., BAALOUSHA, M. A., JU-NAM, Y., REID, M. M., TUFENKJI, N., LEAD, J. R., LEPPARD, G. G. & WILKINSON, K. J. 2009. Characterizing manufactured nanoparticles in the environment: multimethod determination of particle sizes. *Environmental science & technology.* 43**,** 7277-7284.

DONINI, C., ROBINSON, D., COLOMBO, P., GIORDANO, F. & PEPPAS, N. 2002. Preparation of poly (methacrylic acid-g-poly (ethylene glycol)) nanospheres from methacrylic monomers for pharmaceutical applications. *International Journal of Pharmaceutics.* 245**,** 83-91.

DONOVAN, A. R., ADAMS, C. D., MA, Y., STEPHAN, C., EICHHOLZ, T. & SHI, H. 2016. Detection of zinc oxide and cerium dioxide nanoparticles during drinking water treatment by rapid single particle ICP-MS methods. *Analytical and bioanalytical chemistry.* 408**,** 5137-5145.

DU PREEZ, J. & YANG, W. 2003. Improving the aqueous solubility of triclosan by solubilization, complexation, and in situ salt formation. *J. Cosmet. Sci.* 54**,** 537-550.

EGERTON, T. A. 2013. The influence of surface alumina and silica on the photocatalytic degradation of organic pollutants. *Catalysts.* 3**,** 338-362.

EL-TRASS, A., ELSHAMY, H., EL-MEHASSEB, I. & EL-KEMARY, M. 2012. CuO nanoparticles: synthesis, characterization, optical properties and interaction with amino acids. *Applied Surface Science.* 258**,** 2997-3001.

FABREGA, J., FAWCETT, S. R., RENSHAW, J. C. & LEAD, J. R. 2009. Silver nanoparticle impact on bacterial growth: effect of pH, concentration, and organic matter. *Environmental science & technology.* 43**,** 7285-7290.

© University of Pretoria

FABREGA, J., LUOMA, S. N., TYLER, C. R., GALLOWAY, T. S. & LEAD, J. R. 2011. Silver nanoparticles: behaviour and effects in the aquatic environment. *Environment international.* 37**,** 517-531.

FAIR, P. A., LEE, H.-B., ADAMS, J., DARLING, C., PACEPAVICIUS, G., ALAEE, M., BOSSART, G. D., HENRY, N. & MUIR, D. 2009. Occurrence of triclosan in plasma of wild Atlantic bottlenose dolphins (Tursiops truncatus) and in their environment. *Environmental Pollution.* 157**,** 2248-2254.

FAJARDO, C., SACCÀ, M., COSTA, G., NANDE, M. & MARTIN, M. 2014. Impact of Ag and Al_2O_3 nanoparticles on soil organisms: In vitro and soil experiments. *Science of the Total Environment.* 473**,** 254-261.

FANG, J., SHIJIRBAATAR, A., LIN, D.-H., WANG, D.-J., SHEN, B. & ZHOU, Z.-Q. 2017. Stability of co-existing ZnO and TiO_2 nanomaterials in natural water: Aggregation and sedimentation mechanisms. *Chemosphere.* 184**,** 1125-1133.

FANG, T., ZHANG, Y., YAN, Y., DAI, C. & ZHANG, J. 2020. Molecular insight into the aggregation and dispersion behavior of modified nanoparticles. *Journal of Petroleum Science and Engineering.* 191**,** 107193.

FATEHAH, M. O., AZIZ, H. A. & STOLL, S. 2014. Nanoparticle Properties, Behavior, Fate in Aquatic Systems and Characterization Methods. *Journal of Colloid Science and Biotechnology.* 3**,** 111-140.

FERREIRA, J. A., MARTIN-NETO, L., VAZ, C. M. & REGITANO, J. B. 2002. Sorption interactions between imazaquin and a humic acid extracted from a typical Brazilian Oxisol. *Journal of environmental quality.* 31**,** 1665-1670.

FERRETTI, R., STOLL, S., ZHANG, J. & BUFFLE, J. 2003. Flocculation of hematite particles by a comparatively large rigid polysaccharide: schizophyllan. *Journal of colloid and interface science.* 266**,** 328-338.

FISS, E. M., RULE, K. L. & VIKESLAND, P. J. 2007. Formation of chloroform and other chlorinated byproducts by chlorination of triclosan-containing antibacterial products. *Environmental science & technology.* 41**,** 2387-2394.

FRENCH, R. A., JACOBSON, A. R., KIM, B., ISLEY, S. L., PENN, R. L. & BAVEYE, P. C. 2009. Influence of ionic strength, pH, and cation valence on aggregation kinetics of titanium dioxide nanoparticles. *Environmental science & technology.* 43**,** 1354-1359.

© University of Pretoria

FROGGETT, S. J., CLANCY, S. F., BOVERHOF, D. R. & CANADY, R. A. 2014. A review and perspective of existing research on the release of nanomaterials from solid nanocomposites. *Particle and fibre toxicology.* 11**,** 17.

GALHARDI, C. M., DINIZ, Y. S., FAINE, L. A., RODRIGUES, H. G., BURNEIKO, R. C., RIBAS, B. O. & NOVELLI, E. L. 2004. Toxicity of copper intake: lipid profile, oxidative stress and susceptibility to renal dysfunction. *Food and chemical toxicology.* 42**,** 2053-2060.

GAO, Y., LUO, Z., HE, N. & WANG, M. K. 2013. Metallic nanoparticle production and consumption in China between 2000 and 2010 and associative aquatic environmental risk assessment. *Journal of nanoparticle research.* 15**,** 1681.

GARDNER, M., COMBER, S., SCRIMSHAW, M. D., CARTMELL, E., LESTER, J. & ELLOR, B. 2012. The significance of hazardous chemicals in wastewater treatment works effluents. *Science of the Total Environment.* 437**,** 363-372.

GARNER, K. L. & KELLER, A. A. 2014. Emerging patterns for engineered nanomaterials in the environment: a review of fate and toxicity studies. *Journal of Nanoparticle Research.* 16**,** 2503.

GAUTHIER, P. T., NORWOOD, W. P., PREPAS, E. E. & PYLE, G. G. 2014. Metal–PAH mixtures in the aquatic environment: a review of co-toxic mechanisms leading to more-than-additive outcomes. *Aquatic toxicology.* 154**,** 253-269.

GE, S., AGBAKPE, M., ZHANG, W. & KUANG, L. 2015. Heteroaggregation between PEI-coated magnetic nanoparticles and algae: effect of particle size on algal harvesting efficiency. *ACS applied materials & interfaces.* 7**,** 6102-6108.

GHOSH, S., MASHAYEKHI, H., PAN, B., BHOWMIK, P. & XING, B. 2008. Colloidal behavior of aluminum oxide nanoparticles as affected by pH and natural organic matter. *Langmuir.* 24**,** 12385-12391.

GODYMCHUK, A., KAREPINA, E., YUNDA, E., BOZHKO, I., LYAMINA, G., KUZNETSOV, D., GUSEV, A. & KOSOVA, N. 2015. Aggregation of manufactured nanoparticles in aqueous solutions of mono-and bivalent electrolytes. *Journal of Nanoparticle Research.* 17**,** 211.

GOMES, T., PEREIRA, C. G., CARDOSO, C., PINHEIRO, J. P., CANCIO, I. & BEBIANNO, M. J. 2012. Accumulation and toxicity of copper oxide nanoparticles in the digestive gland of Mytilus galloprovincialis. *Aquatic Toxicology.* 118**,** 72-79.

© University of Pretoria

GONDIKAS, A. P., MORRIS, A., REINSCH, B. C., MARINAKOS, S. M., LOWRY, G. V. & HSU-KIM, H. 2012. Cysteine-induced modifications of zero-valent silver nanomaterials: implications for particle surface chemistry, aggregation, dissolution, and silver speciation. *Environmental science & technology.* 46**,** 7037-7045.

GOTTSCHALK, F., SUN, T. & NOWACK, B. 2013. Environmental concentrations of engineered nanomaterials: review of modeling and analytical studies. *Environmental Pollution.* 181**,** 287-300.

GRENTHE, I. 1997. Estimations of medium effects on thermodynamic data. *Modelling in aquatic chemistry.*

GRIFFITT, R. J., LUO, J., GAO, J., BONZONGO, J. C. & BARBER, D. S. 2008. Effects of particle composition and species on toxicity of metallic nanomaterials in aquatic organisms. *Environmental Toxicology and Chemistry.* 27**,** 1972-1978.

GU, C., KARTHIKEYAN, K., SIBLEY, S. D. & PEDERSEN, J. A. 2007. Complexation of the antibiotic tetracycline with humic acid. *Chemosphere.* 66**,** 1494-1501.

GUO, L., HUNT, B. J. & SANTSCHI, P. H. 2001. Ultrafiltration behavior of major ions (Na, Ca, Mg, F, Cl, and SO_4) in natural waters. *Water Research.* 35**,** 1500-1508.

GUO, P. 2005. A special issue on bionanotechnology-Preface. *Other Nanotechnology Publications.* 18.

HAISS, W., THANH, N. T., AVEYARD, J. & FERNIG, D. G. 2007. Determination of size and concentration of gold nanoparticles from UV− Vis spectra. *Analytical chemistry.* 79**,** 4215-4221.

HALDEN, R. U. 2014. On the need and speed of regulating triclosan and triclocarban in the United States. ACS Publications.

HALDEN, R. U., LINDEMAN, A. E., AIELLO, A. E., ANDREWS, D., ARNOLD, W. A., FAIR, P., FUOCO, R. E., GEER, L. A., JOHNSON, P. I. & LOHMANN, R. 2017. The Florence statement on triclosan and triclocarban. *Environmental health perspectives.* 125**,** 064501.

HANDY, R. D., OWEN, R. & VALSAMI-JONES, E. 2008. The ecotoxicology of nanoparticles and nanomaterials: current status, knowledge gaps, challenges, and future needs. *Ecotoxicology.* 17**,** 315-325.

HANSEN, S. F., HEGGELUND, L. R., BESORA, P. R., MACKEVICA, A., BOLDRIN, A. & BAUN, A. 2016. Nanoproducts–what is actually available to European consumers? *Environmental Science: Nano.* 3**,** 169-180.

© University of Pretoria

HAZEEM, L. J., BOUOUDINA, M., RASHDAN, S., BRUNET, L., SLOMIANNY, C. & BOUKHERROUB, R. 2016. Cumulative effect of zinc oxide and titanium oxide nanoparticles on growth and chlorophyll a content of Picochlorum sp. *Environmental Science and Pollution Research.* 23**,** 2821-2830.

HE, Y. T., WAN, J. & TOKUNAGA, T. 2008. Kinetic stability of hematite nanoparticles: the effect of particle sizes. *Journal of nanoparticle research.* 10**,** 321-332.

HEINLAAN, M., KAHRU, A., KASEMETS, K., ARBEILLE, B., PRENSIER, G. & DUBOURGUIER, H.-C. 2011. Changes in the Daphnia magna midgut upon ingestion of copper oxide nanoparticles: a transmission electron microscopy study. *Water research.* 45**,** 179-190.

HEINLAAN, M., MUNA, M., KNÖBEL, M., KISTLER, D., ODZAK, N., KÜHNEL, D., MÜLLER, J., GUPTA, G. S., KUMAR, A. & SHANKER, R. 2016. Natural water as the test medium for Ag and CuO nanoparticle hazard evaluation: an interlaboratory case study. *Environmental pollution.* 216**,** 689-699.

HENDREN, C. O., MESNARD, X., DRÖGE, J. & WIESNER, M. R. 2011. Estimating production data for five engineered nanomaterials as a basis for exposure assessment. ACS Publications.

HOLDEN, P. A., KLAESSIG, F., TURCO, R. F., PRIESTER, J. H., RICO, C. M., AVILA-ARIAS, H., MORTIMER, M., PACPACO, K. & GARDEA-TORRESDEY, J. L. 2014. Evaluation of exposure concentrations used in assessing manufactured nanomaterial environmental hazards: are they relevant? *Environmental science & technology.* 48**,** 10541-10551.

HORNYAK, G. L., TIBBALS, H. F., DUTTA, J. & MOORE, J. J. 2008. *Introduction to nanoscience and nanotechnology*, CRC press.

HOTZE, E. M., PHENRAT, T. & LOWRY, G. V. 2010. Nanoparticle aggregation: challenges to understanding transport and reactivity in the environment. *Journal of environmental quality.* 39**,** 1909-1924.

HOU, J., WANG, X., HAYAT, T. & WANG, X. 2017. Ecotoxicological effects and mechanism of CuO nanoparticles to individual organisms. *Environmental Pollution.* 221**,** 209-217.

HULLA, J., SAHU, S. & HAYES, A. 2015. Nanotechnology: History and future. *Human & experimental toxicology.* 34**,** 1318-1321.

© University of Pretoria

HUNTER, R. J. 2013. *Zeta potential in colloid science: principles and applications*, Academic press.

HUYNH, K. A., MCCAFFERY, J. M. & CHEN, K. L. 2014. Heteroaggregation reduces antimicrobial activity of silver nanoparticles: evidence for nanoparticle–cell proximity effects. *Environmental Science & Technology Letters.* 1**,** 361-366.

ILLÉS, E. & TOMBÁCZ, E. 2006. The effect of humic acid adsorption on pH-dependent surface charging and aggregation of magnetite nanoparticles. *Journal of colloid and interface science.* 295**,** 115-123.

ISWARYA, V., BHUVANESHWARI, M., ALEX, S. A., IYER, S., CHAUDHURI, G., CHANDRASEKARAN, P. T., BHALERAO, G. M., CHAKRAVARTY, S., RAICHUR, A. M. & CHANDRASEKARAN, N. 2015. Combined toxicity of two crystalline phases (anatase and rutile) of Titania nanoparticles towards freshwater microalgae: Chlorella sp. *Aquatic toxicology.* 161**,** 154-169.

IVASK, A., JUGANSON, K., BONDARENKO, O., MORTIMER, M., ARUOJA, V., KASEMETS, K., BLINOVA, I., HEINLAAN, M., SLAVEYKOVA, V. & KAHRU, A. 2014. Mechanisms of toxic action of Ag, ZnO and CuO nanoparticles to selected ecotoxicological test organisms and mammalian cells in vitro: a comparative review. *Nanotoxicology.* 8**,** 57-71.

JALALI, M. & JALALI, M. 2016. Geochemistry and background concentration of major ions in spring waters in a high-mountain area of the Hamedan (Iran). *Journal of Geochemical Exploration.* 165**,** 49-61.

JI, J., LONG, Z. & LIN, D. 2011. Toxicity of oxide nanoparticles to the green algae Chlorella sp. *Chemical Engineering Journal.* 170**,** 525-530.

JIANG, C., AIKEN, G. R. & HSU-KIM, H. 2015. Effects of natural organic matter properties on the dissolution kinetics of zinc oxide nanoparticles. *Environmental science & technology.* 49**,** 11476-11484.

JIANG, L., LIU, Y., LIU, S., ZENG, G., HU, X., HU, X., GUO, Z., TAN, X., WANG, L. & WU, Z. 2017. Adsorption of estrogen contaminants by graphene nanomaterials under natural organic matter preloading: comparison to carbon nanotube, biochar, and activated carbon. *Environmental science & technology.* 51**,** 6352-6359.

JOHNSON, A. C., BOWES, M. J., CROSSLEY, A., JARVIE, H. P., JURKSCHAT, K., JÜRGENS, M. D., LAWLOR, A. J., PARK, B., ROWLAND, P. & SPURGEON, D. 2011. An assessment of the fate, behaviour and environmental risk associated with

© University of Pretoria

sunscreen TiO_2 nanoparticles in UK field scenarios. *Science of the Total Environment.* 409**,** 2503-2510.

JOLIVET, J.-P., FROIDEFOND, C., POTTIER, A., CHANÉAC, C., CASSAIGNON, S., TRONC, E. & EUZEN, P. 2004. Size tailoring of oxide nanoparticles by precipitation in aqueous medium. A semi-quantitative modelling. *Journal of Materials Chemistry.* 14**,** 3281-3288.

JOVANOVIĆ, B. 2015. Critical review of public health regulations of titanium dioxide, a human food additive. *Integrated environmental assessment and management.* 11**,** 10-20.

JUN, X., ZHAO, H. Z. & LU, G. H. 2013. Effects of selected metal oxide nanoparticles on multiple biomarkers in Carassius auratus. *Biomedical and Environmental Sciences.* 26**,** 742-749.

JUNGHANS, M., BACKHAUS, T., FAUST, M., SCHOLZE, M. & GRIMME, L. 2006. Application and validation of approaches for the predictive hazard assessment of realistic pesticide mixtures. *Aquatic Toxicology.* 76**,** 93-110.

KALLAY, N. & ŽALAC, S. 2002. Stability of nanodispersions: a model for kinetics of aggregation of nanoparticles. *Journal of colloid and interface science.* 253**,** 70-76.

KANETOSHI, A., OGAWA, H., KATSURA, E. & KANESHIMA, H. 1987. Chlorination of Irgasan DP300 and formation of dioxins from its chlorinated derivatives. *Journal of Chromatography A.* 389**,** 139-153.

KASPRZYK-HORDERN, B., DINSDALE, R. M. & GUWY, A. J. 2008. The occurrence of pharmaceuticals, personal care products, endocrine disruptors and illicit drugs in surface water in South Wales, UK. *Water research.* 42**,** 3498-3518.

KATZ, D. R., CANTWELL, M. G., SULLIVAN, J. C., PERRON, M. M., BURGESS, R. M., HO, K. T. & CHARPENTIER, M. A. 2013. Factors regulating the accumulation and spatial distribution of the emerging contaminant triclosan in the sediments of an urbanized estuary: Greenwich Bay, Rhode Island, USA. *Science of the total environment.* 443**,** 123-133.

KELLER, A. A. & LAZAREVA, A. 2013. Predicted releases of engineered nanomaterials: from global to regional to local. *Environmental Science & Technology Letters.* 1**,** 65-70.

© University of Pretoria

KHAN, R., INAM, M., PARK, D., ZAM ZAM, S., SHIN, S., KHAN, S., AKRAM, M. & YEOM, I. 2018. Influence of Organic Ligands on the Colloidal Stability and Removal of ZnO Nanoparticles from Synthetic Waters by Coagulation. *Processes.* 6**,** 170.

KHANNA, A. 2008. Nanotechnology in high performance paint coatings. *Asian J. Exp. Sci.* 21**,** 25-32.

KIENZLER, A., BOPP, S. K., VAN DER LINDEN, S., BERGGREN, E. & WORTH, A. 2016. Regulatory assessment of chemical mixtures: Requirements, current approaches and future perspectives. *Regulatory Toxicology and Pharmacology.* 80**,** 321-334.

KOH, B. & CHENG, W. 2014. Mechanisms of carbon nanotube aggregation and the reversion of carbon nanotube aggregates in aqueous medium. *Langmuir.* 30**,** 10899-10909.

KOLPIN, D. W., FURLONG, E. T., MEYER, M. T., THURMAN, E. M., ZAUGG, S. D., BARBER, L. B. & BUXTON, H. T. 2002. Pharmaceuticals, hormones, and other organic wastewater contaminants in US streams, 1999− 2000: A national reconnaissance. *Environmental science & technology.* 36**,** 1202-1211.

KUNHIKRISHNAN, A., SHON, H. K., BOLAN, N. S., EL SALIBY, I. & VIGNESWARAN, S. 2015. Sources, distribution, environmental fate, and ecological effects of nanomaterials in wastewater streams. *Critical Reviews in Environmental Science and Technology.* 45**,** 277-318.

LABORDA, F., BOLEA, E., CEPRIÁ, G., GÓMEZ, M. T., JIMÉNEZ, M. S., PÉREZ-ARANTEGUI, J. & CASTILLO, J. R. 2016. Detection, characterization and quantification of inorganic engineered nanomaterials: a review of techniques and methodological approaches for the analysis of complex samples. *Analytica chimica acta.* 904**,** 10-32.

LAETZ, C. A., BALDWIN, D. H., COLLIER, T. K., HEBERT, V., STARK, J. D. & SCHOLZ, N. L. 2008. The synergistic toxicity of pesticide mixtures: implications for risk assessment and the conservation of endangered Pacific salmon. *Environmental health perspectives.* 117**,** 348-353.

LAN, Y. K., CHEN, T. C., TSAI, H. J., WU, H. C., LIN, J. H., LIN, I., LEE, J. F. & CHEN, C. S. 2016. Adsorption behavior and mechanism of antibiotic sulfamethoxazole on carboxylic-functionalized carbon nanofibers-encapsulated Ni magnetic nanoparticles. *Langmuir.* 32**,** 9530-9539.

© University of Pretoria

LANDRY, V., RIEDL, B. & BLANCHET, P. 2008. Alumina and zirconia acrylate nanocomposites coatings for wood flooring: Photocalorimetric characterization. *Progress in Organic Coatings.* 61**,** 76-82.

LE VAN, N., MA, C., SHANG, J., RUI, Y., LIU, S. & XING, B. 2016. Effects of CuO nanoparticles on insecticidal activity and phytotoxicity in conventional and transgenic cotton. *Chemosphere.* 144**,** 661-670.

LEAD, J. R., BATLEY, G. E., ALVAREZ, P. J., CROTEAU, M. N., HANDY, R. D., MCLAUGHLIN, M. J., JUDY, J. D. & SCHIRMER, K. 2018. Nanomaterials in the environment: Behavior, fate, bioavailability, and effects—An updated review. *Environmental toxicology and chemistry.* 37**,** 2029-2063.

LEAD, J. R. & WILKINSON, K. J. 2007. Environmental colloids and particles: current knowledge and future developments. *IUPAC series on Analytical and Physical Chemistry of Environmental Systems.* 10**,** 1.

LEARENG, S. K., UBOMBA-JASWA, E. & MUSEE, N. 2020. Toxicity of zinc oxide and iron oxide engineered nanoparticles to Bacillus subtilis in river water systems. *Environmental Science: Nano.* 7**,** 172-185.

LEE, J., BARTELT-HUNT, S. L., LI, Y. & MORTON, M. 2015. Effect of 17β-estradiol on stability and mobility of TiO2 rutile nanoparticles. *Science of the Total Environment.* 511**,** 195-202.

LEE, J., MAHENDRA, S. & ALVAREZ, P. J. 2010. Nanomaterials in the construction industry: a review of their applications and environmental health and safety considerations. *ACS nano.* 4**,** 3580-3590.

LEHUTSO, R. F., DASO, A. P. & OKONKWO, J. O. 2017. Occurrence and environmental levels of triclosan and triclocarban in selected wastewater treatment plants in Gauteng Province, South Africa. *Emerging Contaminants.* 3**,** 107-114.

LEI, C., SUN, Y., TSANG, D. C. & LIN, D. 2018. Environmental transformations and ecological effects of iron-based nanoparticles. *Environmental pollution.* 232**,** 10-30.

LEVARD, C., HOTZE, E. M., LOWRY, G. V. & BROWN JR, G. E. 2012. Environmental transformations of silver nanoparticles: impact on stability and toxicity. *Environmental science & technology.* 46**,** 6900-6914.

LEWIS, W. K., HARRUFF, B. A., GORD, J. R., ROSENBERGER, A. T., SEXTON, T. M., GULIANTS, E. A. & BUNKER, C. E. 2010. Chemical dynamics of aluminum nanoparticles in ammonium nitrate and ammonium perchlorate matrices: enhanced

© University of Pretoria

reactivity of organically capped aluminum. *The Journal of Physical Chemistry C.* 115**,** 70-77.

LI, H., ZHENG, N., LIANG, N., ZHANG, D., WU, M. & PAN, B. 2016. Adsorption mechanism of different organic chemicals on fluorinated carbon nanotubes. *Chemosphere.* 154**,** 258-265.

LI, L.-Z., ZHOU, D.-M., PEIJNENBURG, W. J., VAN GESTEL, C. A., JIN, S.-Y., WANG, Y.-J. & WANG, P. 2011. Toxicity of zinc oxide nanoparticles in the earthworm, Eisenia fetida and subcellular fractionation of Zn. *Environment International.* 37**,** 1098-1104.

LI, M., LIN, D. & ZHU, L. 2013. Effects of water chemistry on the dissolution of ZnO nanoparticles and their toxicity to Escherichia coli. *Environmental pollution.* 173**,** 97-102.

LI, Y., ZHANG, W., NIU, J. & CHEN, Y. 2012. Mechanism of photogenerated reactive oxygen species and correlation with the antibacterial properties of engineered metal-oxide nanoparticles. *ACS nano.* 6**,** 5164-5173.

LIN, D., TIAN, X., WU, F. & XING, B. 2010. Fate and transport of engineered nanomaterials in the environment. *Journal of Environmental Quality.* 39**,** 1896-1908.

LIST, B. 2008. Reregistration Eligibility Decision for Triclosan. Citeseer.

LIU, J., LEGROS, S., VON DER KAMMER, F. & HOFMANN, T. 2013. Natural organic matter concentration and hydrochemistry influence aggregation kinetics of functionalized engineered nanoparticles. *Environmental science & technology.* 47**,** 4113-4120.

LOOSLI, F., LE COUSTUMER, P. & STOLL, S. 2013. TiO_2 nanoparticles aggregation and disaggregation in presence of alginate and Suwannee River humic acids. pH and concentration effects on nanoparticle stability. *Water research.* 47**,** 6052-6063.

LOOSLI, F., LE COUSTUMER, P. & STOLL, S. 2014a. Effect of natural organic matter on the disagglomeration of manufactured TiO_2 nanoparticles. *Environmental Science: Nano.* 1**,** 154-160.

LOOSLI, F., LE COUSTUMER, P. & STOLL, S. 2014b. Effect of natural organic matter on the disagglomeration of manufactured TiO 2 nanoparticles. *Environmental Science: Nano.* 1**,** 154-160.

LOOSLI, F., VITORAZI, L., BERRET, J.-F. & STOLL, S. 2015a. Isothermal titration calorimetry as a powerful tool to quantify and better understand agglomeration

© University of Pretoria

mechanisms during interaction processes between TiO_2 nanoparticles and humic acids. *Environmental Science: Nano.* 2**,** 541-550.

LOOSLI, F., VITORAZI, L., BERRET, J.-F. & STOLL, S. 2015b. Towards a better understanding on agglomeration mechanisms and thermodynamic properties of TiO_2 nanoparticles interacting with natural organic matter. *Water research.* 80**,** 139-148.

LOPEZ-DOVAL, J. C., FREIXA, A., SANTOS, L., SANCHÍS, J., RODRÍGUEZ-MOZAZ, S., FARRÉ, M., BARCELÓ, D. & SABATER, S. 2019. Exposure to single and binary mixtures of fullerenes and triclosan: Reproductive and behavioral effects in the freshwater snail Radix balthica. *Environmental research.* 108565.

LOUIE, S. M., SPIELMAN-SUN, E. R., SMALL, M. J., TILTON, R. D. & LOWRY, G. V. 2015. Correlation of the physicochemical properties of natural organic matter samples from different sources to their effects on gold nanoparticle aggregation in monovalent electrolyte. *Environmental science & technology.* 49**,** 2188-2198.

LOWRY, G. V., GREGORY, K. B., APTE, S. C. & LEAD, J. R. 2012. Transformations of nanomaterials in the environment. ACS Publications.

LOWRY, G. V., HILL, R. J., HARPER, S., RAWLE, A. F., HENDREN, C. O., KLAESSIG, F., NOBBMANN, U., SAYRE, P. & RUMBLE, J. 2016. Guidance to improve the scientific value of zeta-potential measurements in nanoEHS. *Environmental Science: Nano.* 3**,** 953-965.

LUYTS, K., NAPIERSKA, D., NEMERY, B. & HOET, P. H. 2013. How physico-chemical characteristics of nanoparticles cause their toxicity: complex and unresolved interrelations. *Environmental science: processes & impacts.* 15**,** 23-38.

LV, X., GAO, B., SUN, Y., SHI, X., XU, H. & WU, J. 2014. Effects of humic acid and solution chemistry on the retention and transport of cerium dioxide nanoparticles in saturated porous media. *Water, Air, & Soil Pollution.* 225**,** 2167.

MA, R., STEGEMEIER, J., LEVARD, C., DALE, J. G., NOACK, C. W., YANG, T., BROWN, G. E. & LOWRY, G. V. 2014. Sulfidation of copper oxide nanoparticles and properties of resulting copper sulfide. *Environmental Science: Nano.* 1**,** 347-357.

MACKAY, D. & BOETHLING, R. S. 2000. *Handbook of property estimation methods for chemicals: environmental health sciences*, CRC press.

MAHDAVI, M., SHARIFPUR, M., AHMADI, M. H. & MEYER, J. P. 2019. Aggregation study of Brownian nanoparticles in convective phenomena. *Journal of Thermal Analysis and Calorimetry.* 135**,** 111-121.

© University of Pretoria

MAHDAVI, S., JALALI, M. & AFKHAMI, A. 2015. Heavy metals removal from aqueous solutions by Al 2 O 3 nanoparticles modified with natural and chemical modifiers. *Clean technologies and environmental policy.* 17**,** 85-102.

MAJEDI, S. M., KELLY, B. C. & LEE, H. K. 2014. Role of combinatorial environmental factors in the behavior and fate of ZnO nanoparticles in aqueous systems: a multiparametric analysis. *Journal of hazardous materials.* 264**,** 370-379.

MAJUMDER, D. D., BANERJEE, R., ULRICHS, C., MEWIS, I. & GOSWAMI, A. 2007. Nano-materials: Science of bottom-up and top-down. *IETE technical review.* 24**,** 9-25.

MAJZIK, A. & TOMBÁCZ, E. 2007a. Interaction between humic acid and montmorillonite in the presence of calcium ions I. Interfacial and aqueous phase equilibria: Adsorption and complexation. *Organic Geochemistry.* 38**,** 1319-1329.

MAJZIK, A. & TOMBÁCZ, E. 2007b. Interaction between humic acid and montmorillonite in the presence of calcium ions II. Colloidal interactions: Charge state, dispersing and/or aggregation of particles in suspension. *Organic Geochemistry.* 38**,** 1330-1340.

MANSANO, A. S., SOUZA, J. P., CANCINO-BERNARDI, J., VENTURINI, F. P., MARANGONI, V. S. & ZUCOLOTTO, V. 2018. Toxicity of copper oxide nanoparticles to Neotropical species Ceriodaphnia silvestrii and Hyphessobrycon eques. *Environmental Pollution.* 243**,** 723-733.

MANSOORI, G. A. 2002. Advances in atomic & molecular nanotechnology. *United Nations Tech Monitor; UN-APCTT Tech Monitor, 2002; Special Issue: 53.* 59.

MANSOURI, B., MALEKI, A., JOHARI, S. A., SHAHMORADI, B., MOHAMMADI, E., SHAHSAVARI, S. & DAVARI, B. 2016. Copper bioaccumulation and depuration in common carp (Cyprinus carpio) following co-exposure to TiO_2 and CuO nanoparticles. *Archives of environmental contamination and toxicology.* 71**,** 541-552.

MANUSADŽIANAS, L., CAILLET, C., FACHETTI, L., GYLYTĖ, B., GRIGUTYTĖ, R., JURKONIENĖ, S., KARITONAS, R., SADAUSKAS, K., THOMAS, F. & VITKUS, R. 2012. Toxicity of copper oxide nanoparticle suspensions to aquatic biota. *Environmental toxicology and chemistry.* 31**,** 108-114.

MARIE, T., MÉLANIE, A., LENKA, B., JULIEN, I., ISABELLE, K., CHRISTINE, P., ELISE, M., CATHERINE, S., BERNARD, A. & ESTER, A. 2014. Transfer, transformation, and impacts of ceria nanomaterials in aquatic mesocosms simulating a pond ecosystem. *Environmental science & technology.* 48**,** 9004-9013.

© University of Pretoria

MASHOCK, M. J., ZANON, T., KAPPELL, A. D., PETRELLA, L. N., ANDERSEN, E. C. & HRISTOVA, K. R. 2016. Copper oxide nanoparticles impact several toxicological endpoints and cause neurodegeneration in Caenorhabditis elegans. *PloS one.* 11.

MATILAINEN, A., VEPSÄLÄINEN, M. & SILLANPÄÄ, M. 2010. Natural organic matter removal by coagulation during drinking water treatment: a review. *Advances in colloid and interface science.* 159**,** 189-197.

MATSOUKAS, T., DESAI, T. & LEE, K. 2015. Engineered nanoparticles and their applications. *Journal of Nanomaterials.* 2015.

MAVROCORDATOS, D., PRONK, W. & BOLLER, M. 2004. Analysis of environmental particles by atomic force microscopy, scanning and transmission electron microscopy. *Water Science and Technology.* 50**,** 9-18.

MAYNARD, A. D. 2011. Don't define nanomaterials. *Nature.* 475**,** 31.

MCCLESKEY, R. B., NORDSTROM, D. K. & RYAN, J. N. 2012. Comparison of electrical conductivity calculation methods for natural waters. *Limnology and Oceanography: Methods.* 10**,** 952-967.

MEYER, D. E., CURRAN, M. A. & GONZALEZ, M. A. 2009. An examination of existing data for the industrial manufacture and use of nanocomponents and their role in the life cycle impact of nanoproducts. ACS Publications.

MIAO, A. J., ZHANG, X. Y., LUO, Z., CHEN, C. S., CHIN, W. C., SANTSCHI, P. H. & QUIGG, A. 2010. Zinc oxide–engineered nanoparticles: dissolution and toxicity to marine phytoplankton. *Environmental Toxicology and Chemistry.* 29**,** 2814-2822.

MIAO, L., WANG, C., HOU, J., WANG, P., AO, Y., LI, Y., GENG, N., YAO, Y., LV, B. & YANG, Y. 2016. Aggregation and removal of copper oxide (CuO) nanoparticles in wastewater environment and their effects on the microbial activities of wastewater biofilms. *Bioresource technology.* 216**,** 537-544.

MIRANDA, R., DA SILVEIRA, A. D., DE JESUS, I., GRÖTZNER, S., VOIGT, C., CAMPOS, S., GARCIA, J., RANDI, M., RIBEIRO, C. O. & NETO, F. F. 2016. Effects of realistic concentrations of TiO 2 and ZnO nanoparticles in Prochilodus lineatus juvenile fish. *Environmental Science and Pollution Research.* 23**,** 5179-5188.

MISRA, S. K., DYBOWSKA, A., BERHANU, D., LUOMA, S. N. & VALSAMI-JONES, E. 2012. The complexity of nanoparticle dissolution and its importance in nanotoxicological studies. *Science of the total environment.* 438**,** 225-232.

© University of Pretoria

MONIKH, F. A., PRAETORIUS, A., SCHMID, A., KOZIN, P., MEISTERJAHN, B., MAKAROVA, E., HOFMANN, T. & VON DER KAMMER, F. 2018. Scientific rationale for the development of an OECD test guideline on engineered nanomaterial stability. *NanoImpact.* 11**,** 42-50.

MONTASERI, H. & FORBES, P. B. 2016. A review of monitoring methods for triclosan and its occurrence in aquatic environments. *TrAC Trends in Analytical Chemistry.* 85**,** 221-231.

MONTASERI, H. & FORBES, P. B. 2018. A triclosan turn-ON fluorescence sensor based on thiol-capped core/shell quantum dots. *Spectrochimica Acta Part A: Molecular and Biomolecular Spectroscopy.* 204**,** 370-379.

MUDUNKOTUWA, I. A., RUPASINGHE, T., WU, C.-M. & GRASSIAN, V. H. 2011. Dissolution of ZnO nanoparticles at circumneutral pH: a study of size effects in the presence and absence of citric acid. *Langmuir.* 28**,** 396-403.

MUELLER, N. C. & NOWACK, B. 2008. Exposure modeling of engineered nanoparticles in the environment. *Environmental science & technology.* 42**,** 4447-4453.

MUI, J., NGO, J. & KIM, B. 2016. Aggregation and colloidal stability of commercially available Al_2O_3 nanoparticles in aqueous environments. *Nanomaterials.* 6**,** 90.

MURPHY, E. M., ZACHARA, J. M., SMITH, S. C., PHILLIPS, J. L. & WIETSMA, T. W. 1994. Interaction of hydrophobic organic compounds with mineral-bound humic substances. *Environmental science & technology.* 28**,** 1291-1299.

MUSEE, N. 2011a. Nanotechnology risk assessment from a waste management perspective: Are the current tools adequate? *Human & experimental toxicology.* 30**,** 820-835.

MUSEE, N. 2011b. Nanowastes and the environment: Potential new waste management paradigm. *Environment international.* 37**,** 112-128.

MUSEE, N. 2011c. Simulated environmental risk estimation of engineered nanomaterials: a case of cosmetics in Johannesburg City. *Human & experimental toxicology.* 30**,** 1181-1195.

MUSEE, N. 2018. Environmental risk assessment of triclosan and triclocarban from personal care products in South Africa. *Environmental pollution.* 242**,** 827-838.

MUSEE, N., ZVIMBA, J. N., SCHAEFER, L. M., NOTA, N., SIKHWIVHILU, L. M. & THWALA, M. 2014. Fate and behavior of ZnO-and Ag-engineered nanoparticles and a bacterial viability assessment in a simulated wastewater treatment plant. *Journal of Environmental Science and Health, Part A.* 49**,** 59-66.

© University of Pretoria

MWAANGA, P. 2012. The behavior and toxicity of metal oxide nanoparticles in aqueous solution.

MWAANGA, P., CARRAWAY, E. R. & SCHLAUTMAN, M. A. 2014. Preferential sorption of some natural organic matter fractions to titanium dioxide nanoparticles: influence of pH and ionic strength. *Environmental monitoring and assessment.* 186**,** 8833-8844.

NAASZ, S., ALTENBURGER, R. & KÜHNEL, D. 2018. Environmental mixtures of nanomaterials and chemicals: The Trojan-horse phenomenon and its relevance for ecotoxicity. *Science of the Total Environment.* 635**,** 1170-1181.

NAG, S. K., DAS SARKAR, S. & MANNA, S. K. 2018. Triclosan–an antibacterial compound in water, sediment and fish of River Gomti, India. *International Journal of Environmental Health Research.* 28**,** 461-470.

NAIDU, R., ESPANA, V. A. A., LIU, Y. & JIT, J. 2016. Emerging contaminants in the environment: risk-based analysis for better management. *Chemosphere.* 154**,** 350-357.

NAIKA, H. R., LINGARAJU, K., MANJUNATH, K., KUMAR, D., NAGARAJU, G., SURESH, D. & NAGABHUSHANA, H. 2015. Green synthesis of CuO nanoparticles using Gloriosa superba L. extract and their antibacterial activity. *Journal of Taibah University for Science.* 9**,** 7-12.

NANDA, K., MAISELS, A., KRUIS, F., FISSAN, H. & STAPPERT, S. 2003. Higher surface energy of free nanoparticles. *Physical review letters.* 91**,** 106102.

NATIONS, S., WAGES, M., CAÑAS, J. E., MAUL, J., THEODORAKIS, C. & COBB, G. P. 2011. Acute effects of Fe_2O_3, TiO_2, ZnO and CuO nanomaterials on Xenopus laevis. *Chemosphere.* 83**,** 1053-1061.

NAVRATILOVA, J., PRAETORIUS, A., GONDIKAS, A., FABIENKE, W., VON DER KAMMER, F. & HOFMANN, T. 2015. Detection of engineered copper nanoparticles in soil using single particle ICP-MS. *International journal of environmental research and public health.* 12**,** 15756-15768.

NEBBIOSO, A. & PICCOLO, A. 2013. Molecular characterization of dissolved organic matter (DOM): a critical review. *Analytical and bioanalytical chemistry.* 405**,** 109-124.

NGHIEM, L. D. & COLEMAN, P. J. 2008. NF/RO filtration of the hydrophobic ionogenic compound triclosan: transport mechanisms and the influence of membrane fouling. *Separation and Purification Technology.* 62**,** 709-716.

© University of Pretoria

NIDHIN, M., INDUMATHY, R., SREERAM, K. & NAIR, B. U. 2008. Synthesis of iron oxide nanoparticles of narrow size distribution on polysaccharide templates. *Bulletin of Materials Science.* 31**,** 93-96.

NOWACK, B. & BUCHELI, T. D. 2007. Occurrence, behavior and effects of nanoparticles in the environment. *Environmental pollution.* 150**,** 5-22.

OCHEKPE, N. A., OLORUNFEMI, P. O. & NGWULUKA, N. C. 2009. Nanotechnology and drug delivery part 1: background and applications. *Tropical journal of pharmaceutical research.* 8.

ODZAK, N., KISTLER, D., BEHRA, R. & SIGG, L. 2014. Dissolution of metal and metal oxide nanoparticles in aqueous media. *Environmental pollution.* 191**,** 132-138.

ODZAK, N., KISTLER, D., BEHRA, R. & SIGG, L. 2015. Dissolution of metal and metal oxide nanoparticles under natural freshwater conditions. *Environmental Chemistry.* 12**,** 138-148.

ODZAK, N., KISTLER, D. & SIGG, L. 2017. Influence of daylight on the fate of silver and zinc oxide nanoparticles in natural aquatic environments. *Environmental Pollution.* 226**,** 1-11.

OKUMURA, T. & NISHIKAWA, Y. 1996. Gas chromatography—mass spectrometry determination of triclosans in water, sediment and fish samples via methylation with diazomethane. *Analytica Chimica Acta.* 325**,** 175-184.

OMAR, F. M., AZIZ, H. A. & STOLL, S. 2014. Aggregation and disaggregation of ZnO nanoparticles: influence of pH and adsorption of Suwannee River humic acid. *Science of the total environment.* 468**,** 195-201.

OTTOFUELLING, S., VON DER KAMMER, F. & HOFMANN, T. 2011. Commercial titanium dioxide nanoparticles in both natural and synthetic water: comprehensive multidimensional testing and prediction of aggregation behavior. *Environmental science & technology.* 45**,** 10045-10052.

PAKRASHI, S., DALAI, S., PRATHNA, T., TRIVEDI, S., MYNENI, R., RAICHUR, A. M., CHANDRASEKARAN, N. & MUKHERJEE, A. 2013. Cytotoxicity of aluminium oxide nanoparticles towards fresh water algal isolate at low exposure concentrations. *Aquatic Toxicology.* 132**,** 34-45.

PAKRASHI, S., DALAI, S., SNEHA, B., CHANDRASEKARAN, N. & MUKHERJEE, A. 2012. A temporal study on fate of Al_2O_3 nanoparticles in a fresh water microcosm at

© University of Pretoria

environmentally relevant low concentrations. *Ecotoxicology and environmental safety.* 84**,** 70-77.

PAN, B. & XING, B. 2008. Adsorption mechanisms of organic chemicals on carbon nanotubes. *Environmental science & technology.* 42**,** 9005-9013.

PAPE-LINDSTROM, P. A. & LYDY, M. J. 1997. Synergistic toxicity of atrazine and organophosphate insecticides contravenes the response addition mixture model. *Environmental Toxicology and Chemistry.* 16**,** 2415-2420.

PEMBERTON, R. M. & HART, J. P. 1999. Electrochemical behaviour of triclosan at a screen-printed carbon electrode and its voltammetric determination in toothpaste and mouthrinse products. *Analytica chimica acta.* 390**,** 107-115.

PENG, C., SHEN, C., ZHENG, S., YANG, W., HU, H., LIU, J. & SHI, J. 2017a. Transformation of CuO nanoparticles in the aquatic environment: influence of pH, electrolytes and natural organic matter. *Nanomaterials.* 7**,** 326.

PENG, C., ZHANG, W., GAO, H., LI, Y., TONG, X., LI, K., ZHU, X., WANG, Y. & CHEN, Y. 2017b. Behavior and potential impacts of metal-based engineered nanoparticles in aquatic environments. *Nanomaterials.* 7**,** 21.

PETERS, R., TEN DAM, G., BOUWMEESTER, H., HELSPER, H., ALLMAIER, G., VD KAMMER, F., RAMSCH, R., SOLANS, C., TOMANIOVÁ, M. & HAJSLOVA, J. 2011. Identification and characterization of organic nanoparticles in food. *TrAC Trends in Analytical Chemistry.* 30**,** 100-112.

PETOSA, A. R., JAISI, D. P., QUEVEDO, I. R., ELIMELECH, M. & TUFENKJI, N. 2010. Aggregation and deposition of engineered nanomaterials in aquatic environments: role of physicochemical interactions. *Environmental science & technology.* 44**,** 6532-6549.

PHAM, H. & NGUYEN, Q. P. 2014. Effect of silica nanoparticles on clay swelling and aqueous stability of nanoparticle dispersions. *Journal of Nanoparticle Research.* 16**,** 1-11.

PHENRAT, T., SONG, J. E., CISNEROS, C. M., SCHOENFELDER, D. P., TILTON, R. D. & LOWRY, G. V. 2010. Estimating attachment of nano-and submicrometer-particles coated with organic macromolecules in porous media: development of an empirical model. *Environmental science & technology.* 44**,** 4531-4538.

© University of Pretoria

PHILIPPE, A. & SCHAUMANN, G. E. 2014. Interactions of dissolved organic matter with natural and engineered inorganic colloids: a review. *Environmental science & technology.* 48**,** 8946-8962.

PICCINNO, F., GOTTSCHALK, F., SEEGER, S. & NOWACK, B. 2012. Industrial production quantities and uses of ten engineered nanomaterials in Europe and the world. *Journal of Nanoparticle Research.* 14**,** 1109.

PICCOLO, A. 2001. The supramolecular structure of humic substances. *Soil science.* 166**,** 810-832.

PIGNATELLO, J. J. 2011. Interactions of anthropogenic organic chemicals with natural organic matter and black carbon in environmental particles. *Biophysico-Chemical Processes of Anthropogenic Organic Compounds in Environmental Systems.* 1-50.

PIGNATELLO, J. J. 2012. Dynamic interactions of natural organic matter and organic compounds. *Journal of soils and sediments.* 12**,** 1241-1256.

PIRELA, S. V., PYRGIOTAKIS, G., BELLO, D., THOMAS, T., CASTRANOVA, V. & DEMOKRITOU, P. 2014. Development and characterization of an exposure platform suitable for physico-chemical, morphological and toxicological characterization of printer-emitted particles (PEPs). *Inhalation toxicology.* 26**,** 400-408.

PIRIYAWONG, V., THONGPOOL, V., ASANITHI, P. & LIMSUWAN, P. 2012. Preparation and characterization of alumina nanoparticles in deionized water using laser ablation technique. *Journal of Nanomaterials.* 2012.

PRASHANTH, P., RAVEENDRA, R., HARI KRISHNA, R., ANANDA, S., BHAGYA, N., NAGABHUSHANA, B., LINGARAJU, K. & RAJA NAIKA, H. 2015. Synthesis, characterizations, antibacterial and photoluminescence studies of solution combustion-derived α-Al_2O_3 nanoparticles. *Journal of Asian Ceramic Societies.* 3**,** 345-351.

PRESTON, S., COAD, N., TOWNEND, J., KILLHAM, K. & PATON, G. I. 2000. Biosensing the acute toxicity of metal interactions: are they additive, synergistic, or antagonistic? *Environmental Toxicology and Chemistry: An International Journal.* 19**,** 775-780.

QUIK, J. T., LYNCH, I., VAN HOECKE, K., MIERMANS, C. J., DE SCHAMPHELAERE, K. A., JANSSEN, C. R., DAWSON, K. A., STUART, M. A. C. & VAN DE MEENT, D. 2010. Effect of natural organic matter on cerium dioxide nanoparticles settling in model fresh water. *Chemosphere.* 81**,** 711-715.

© University of Pretoria

RABE, M., VERDES, D. & SEEGER, S. 2011. Understanding protein adsorption phenomena at solid surfaces. *Advances in colloid and interface science.* 162**,** 87-106.

RAGHUPATHI, K. R., KOODALI, R. T. & MANNA, A. C. 2011. Size-dependent bacterial growth inhibition and mechanism of antibacterial activity of zinc oxide nanoparticles. *Langmuir.* 27**,** 4020-4028.

RAMASWAMY, B. R., SHANMUGAM, G., VELU, G., RENGARAJAN, B. & LARSSON, D. J. 2011. GC–MS analysis and ecotoxicological risk assessment of triclosan, carbamazepine and parabens in Indian rivers. *Journal of hazardous materials.* 186**,** 1586-1593.

RITSON, J., GRAHAM, N., TEMPLETON, M., CLARK, J., GOUGH, R. & FREEMAN, C. 2014. The impact of climate change on the treatability of dissolved organic matter (DOM) in upland water supplies: a UK perspective. *Science of the Total Environment.* 473**,** 714-730.

ROBICHAUD, C. O., UYAR, A. E., DARBY, M. R., ZUCKER, L. G. & WIESNER, M. R. 2009. Estimates of upper bounds and trends in nano-TiO2 production as a basis for exposure assessment. ACS Publications.

ROMANELLO, M. B. & DE CORTALEZZI, M. M. F. 2013. An experimental study on the aggregation of TiO2 nanoparticles under environmentally relevant conditions. *Water research.* 47**,** 3887-3898.

RÖMER, I., GAVIN, A. J., WHITE, T. A., MERRIFIELD, R. C., CHIPMAN, J. K., VIANT, M. R. & LEAD, J. R. 2013. The critical importance of defined media conditions in Daphnia magna nanotoxicity studies. *Toxicology letters.* 223**,** 103-108.

ROSSNER, A., SNYDER, S. A. & KNAPPE, D. R. 2009. Removal of emerging contaminants of concern by alternative adsorbents. *Water research.* 43**,** 3787-3796.

RUSANOV, A. I. 2005. Surface thermodynamics revisited. *Surface Science Reports.* 58**,** 111-239.

SABALIUNAS, D., WEBB, S. F., HAUK, A., JACOB, M. & ECKHOFF, W. S. 2003. Environmental fate of triclosan in the River Aire Basin, UK. *Water research.* 37**,** 3145-3154.

SADIQ, I. M., PAKRASHI, S., CHANDRASEKARAN, N. & MUKHERJEE, A. 2011. Studies on toxicity of aluminum oxide (Al_2O_3) nanoparticles to microalgae species: Scenedesmus sp. and Chlorella sp. *Journal of Nanoparticle Research.* 13**,** 3287-3299.

© University of Pretoria

SALEH, N. B., PFEFFERLE, L. D. & ELIMELECH, M. 2010. Influence of biomacromolecules and humic acid on the aggregation kinetics of single-walled carbon nanotubes. *Environmental science & technology.* 44**,** 2412-2418.

SALTIEL, C., CHEN, Q., MANICKAVASAGAM, S., SCHADLER, L., SIEGEL, R. & MENGUC, M. 2004. Identification of the dispersion behavior of surface treated nanoscale powders. *Journal of Nanoparticle Research.* 6**,** 35-46.

SANTSCHI, P. H., BALNOIS, E., WILKINSON, K. J., ZHANG, J., BUFFLE, J. & GUO, L. 1998. Fibrillar polysaccharides in marine macromolecular organic matter as imaged by atomic force microscopy and transmission electron microscopy. *Limnology and Oceanography.* 43**,** 896-908.

SCHIEßL, K., BABICK, F. & STINTZ, M. 2012. Calculation of double layer interaction between colloidal aggregates. *Advanced Powder Technology.* 23**,** 139-147.

SCHWARZENBACH, R. P., ESCHER, B. I., FENNER, K., HOFSTETTER, T. B., JOHNSON, C. A., VON GUNTEN, U. & WEHRLI, B. 2006. The challenge of micropollutants in aquatic systems. *Science.* 313**,** 1072-1077.

SCHWEIZER, H. P. 2001. Triclosan: a widely used biocide and its link to antibiotics. *FEMS microbiology letters.* 202**,** 1-7.

SHARMA, R., BISEN, D., SHUKLA, U. & SHARMA, B. 2012. X-ray diffraction: a powerful method of characterizing nanomaterials. *Recent research in science and technology.* 4.

SIKDER, M., CROTEAU, M.-N., POULIN, B. A. & BAALOUSHA, M. 2021. Effect of Nanoparticle Size and Natural Organic Matter Composition on the Bioavailability of Polyvinylpyrrolidone-Coated Platinum Nanoparticles to a Model Freshwater Invertebrate. *Environmental Science & Technology.* 55**,** 2452-2461.

SIKDER, M., LEAD, J. R., CHANDLER, G. T. & BAALOUSHA, M. 2018. A rapid approach for measuring silver nanoparticle concentration and dissolution in seawater by UV–Vis. *Science of The Total Environment.* 618**,** 597-607.

SIKDER, M., WANG, J., POULIN, B. A., TFAILY, M. M. & BAALOUSHA, M. 2020. Nanoparticle size and natural organic matter composition determine aggregation behavior of polyvinylpyrrolidone coated platinum nanoparticles. *Environmental Science: Nano.* 7**,** 3318-3332.

SINGER, H., MÜLLER, S., TIXIER, C. & PILLONEL, L. 2002. Triclosan: occurrence and fate of a widely used biocide in the aquatic environment: field measurements in

© University of Pretoria

wastewater treatment plants, surface waters, and lake sediments. *Environmental science & technology.* 36**,** 4998-5004.

SINGH, J., KAUR, G. & RAWAT, M. 2016. A brief review on synthesis and characterization of copper oxide nanoparticles and its applications. *J. Bioelectron. Nanotechnol.* 1.

SINGH, R. P., SHUKLA, V. K., YADAV, R. S., SHARMA, P. K., SINGH, P. K. & PANDEY, A. C. 2011. Biological approach of zinc oxide nanoparticles formation and its characterization. *Adv. Mater. Lett.* 2**,** 313-317.

SMITH, S. 2013. US Disinfectant & Antimicrobial Chemicals Market. PRWeb.

SOLOVITCH, N., LABILLE, J., ROSE, J., CHAURAND, P., BORSCHNECK, D., WIESNER, M. R. & BOTTERO, J.-Y. 2010. Concurrent aggregation and deposition of TiO2 nanoparticles in a sandy porous media. *Environmental science & technology.* 44**,** 4897-4902.

SON, D. I., YOU, C. H. & KIM, T. W. 2009. Structural, optical, and electronic properties of colloidal CuO nanoparticles formed by using a colloid-thermal synthesis process. *Applied surface science.* 255**,** 8794-8797.

SON, J., VAVRA, J. & FORBES, V. E. 2015. Effects of water quality parameters on agglomeration and dissolution of copper oxide nanoparticles (CuO-NPs) using a central composite circumscribed design. *Science of the total Environment.* 521**,** 183-190.

SONG, K., ZHANG, W., SUN, C., HU, X., WANG, J. & YAO, L. 2020. Dynamic cytotoxicity of ZnO nanoparticles and bulk particles to Escherichia coli: a view from unfixed ZnO particle: Zn2+ ratio. *Aquatic Toxicology.* 105407.

SOUSA, V. S. & TEIXEIRA, M. R. 2013. Aggregation kinetics and surface charge of CuO nanoparticles: the influence of pH, ionic strength and humic acids. *Environmental Chemistry.* 10**,** 313-322.

SREERAM, K. J., INDUMATHY, R., RAJARAM, A., NAIR, B. U. & RAMASAMI, T. 2006. Template synthesis of highly crystalline and monodisperse iron oxide pigments of nanosize. *Materials research bulletin.* 41**,** 1875-1881.

STANKUS, D. P., LOHSE, S. E., HUTCHISON, J. E. & NASON, J. A. 2011. Interactions between natural organic matter and gold nanoparticles stabilized with different organic capping agents. *Environmental science & technology.* 45**,** 3238-3244.

© University of Pretoria

STUDER, A. M., LIMBACH, L. K., VAN DUC, L., KRUMEICH, F., ATHANASSIOU, E. K., GERBER, L. C., MOCH, H. & STARK, W. J. 2010. Nanoparticle cytotoxicity depends on intracellular solubility: comparison of stabilized copper metal and degradable copper oxide nanoparticles. *Toxicology letters.* 197**,** 169-174.

STUMM, W. & MORGAN, J. J. 2012. *Aquatic chemistry: chemical equilibria and rates in natural waters*, John Wiley & Sons.

SUN, D. D. & LEE, P. F. 2012. TiO2 microsphere for the removal of humic acid from water: Complex surface adsorption mechanisms. *Separation and purification technology.* 91**,** 30-37.

SUN, T. Y., BORNHÖFT, N. A., HUNGERBÜHLER, K. & NOWACK, B. 2016. Dynamic probabilistic modeling of environmental emissions of engineered nanomaterials. *Environmental science & technology.* 50**,** 4701-4711.

SURIYANON, N., PUNYAPALAKUL, P. & NGAMCHARUSSRIVICHAI, C. 2013. Mechanistic study of diclofenac and carbamazepine adsorption on functionalized silica-based porous materials. *Chemical engineering journal.* 214**,** 208-218.

TALLING, J. 2010. Potassium—a non-limiting nutrient in fresh waters? *Freshwater Reviews.* 3**,** 97-104.

TANTRA, R., SCHULZE, P. & QUINCEY, P. 2010. Effect of nanoparticle concentration on zeta-potential measurement results and reproducibility. *Particuology.* 8**,** 279-285.

TEO, B. K. & SUN, X. 2006. From top-down to bottom-up to hybrid nanotechnologies: road to nanodevices. *Journal of cluster science.* 17**,** 529-540.

THIO, B. J. R., ZHOU, D. & KELLER, A. A. 2011. Influence of natural organic matter on the aggregation and deposition of titanium dioxide nanoparticles. *Journal of hazardous materials.* 189**,** 556-563.

THIT, A., HUGGINS, K., SELCK, H. & BAUN, A. 2017. Acute toxicity of copper oxide nanoparticles to Daphnia magna under different test conditions. *Toxicological & Environmental Chemistry.* 99**,** 665-679.

THWALA, M., KLAINE, S. J. & MUSEE, N. 2016. Interactions of metal-based engineered nanoparticles with aquatic higher plants: A review of the state of current knowledge. *Environmental toxicology and chemistry.* 35**,** 1677-1694.

THWALA, M., MUSEE, N., SIKHWIVHILU, L. & WEPENER, V. 2013. The oxidative toxicity of Ag and ZnO nanoparticles towards the aquatic plant Spirodela punctuta

© University of Pretoria

and the role of testing media parameters. *Environmental Science: Processes & Impacts.* 15**,** 1830-1843.

TIEDE, K., BOXALL, A. B., TEAR, S. P., LEWIS, J., DAVID, H. & HASSELLÖV, M. 2008. Detection and characterization of engineered nanoparticles in food and the environment. *Food additives and contaminants.* 25**,** 795-821.

TIEDE, K., DUDKIEWICZ, A., BOXALL, A. & LEWIS, J. 2015. Case study–characterization of nanomaterials in food products. *Frontiers of Nanoscience.* Elsevier.

TILLER, C. L. & O'MELIA, C. R. 1993. Natural organic matter and colloidal stability: models and measurements. *Colloids and Surfaces A: Physicochemical and Engineering Aspects.* 73**,** 89-102.

TONG, T., FANG, K., THOMAS, S. A., KELLY, J. J., GRAY, K. A. & GAILLARD, J.-F. O. 2014. Chemical interactions between nano-ZnO and nano-TiO_2 in a natural aqueous medium. *Environmental science & technology.* 48**,** 7924-7932.

TONG, T., WILKE, C. M., WU, J., BINH, C. T. T., KELLY, J. J., GAILLARD, J.-F. O. & GRAY, K. A. 2015. Combined toxicity of nano-ZnO and nano-TiO_2: from single-to multinanomaterial systems. *Environmental science & technology.* 49**,** 8113-8123.

TRENHOLM, R. A., VANDERFORD, B. J., HOLADY, J. C., REXING, D. J. & SNYDER, S. A. 2006. Broad range analysis of endocrine disruptors and pharmaceuticals using gas chromatography and liquid chromatography tandem mass spectrometry. *Chemosphere.* 65**,** 1990-1998.

UNRINE, J. M., COLMAN, B. P., BONE, A. J., GONDIKAS, A. P. & MATSON, C. W. 2012. Biotic and abiotic interactions in aquatic microcosms determine fate and toxicity of Ag nanoparticles. Part 1. Aggregation and dissolution. *Environmental science & technology.* 46**,** 6915-6924.

UVAROV, V. & POPOV, I. 2013. Metrological characterization of X-ray diffraction methods at different acquisition geometries for determination of crystallite size in nano-scale materials. *Materials Characterization.* 85**,** 111-123.

VAN HOECKE, K., DE SCHAMPHELAERE, K. A., VAN DER MEEREN, P., SMAGGHE, G. & JANSSEN, C. R. 2011. Aggregation and ecotoxicity of CeO_2 nanoparticles in synthetic and natural waters with variable pH, organic matter concentration and ionic strength. *Environmental pollution.* 159**,** 970-976.

© University of Pretoria

VAN KOETSEM, F., VERSTRAETE, S., VAN DER MEEREN, P. & DU LAING, G. 2015. Stability of engineered nanomaterials in complex aqueous matrices: settling behaviour of CeO_2 nanoparticles in natural surface waters. *Environmental research.* 142**,** 207-214.

VANCE, M. E., KUIKEN, T., VEJERANO, E. P., MCGINNIS, S. P., HOCHELLA JR, M. F., REJESKI, D. & HULL, M. S. 2015. Nanotechnology in the real world: Redeveloping the nanomaterial consumer products inventory. *Beilstein journal of nanotechnology.* 6**,** 1769-1780.

VIDYA, P. & CHITRA, K. 2017. Assessment of acute toxicity (LC50-96 h) of aluminium oxide, silicon dioxide and titanium dioxide nanoparticles on the freshwater fish, Oreochromis mossambicus (Peters, 1852). *Int J Fish Aquat Stud.* 5**,** 327-332.

VINDEDAHL, A. M., STREHLAU, J. H., ARNOLD, W. A. & PENN, R. L. 2016. Organic matter and iron oxide nanoparticles: aggregation, interactions, and reactivity. *Environmental Science: Nano.* 3**,** 494-505.

VISCONTI, F., DE PAZ, J. & RUBIO, J. 2010. An empirical equation to calculate soil solution electrical conductivity at 25° C from major ion concentrations. *European Journal of Soil Science.* 61**,** 980-993.

WANG, D., GAO, Y., LIN, Z., YAO, Z. & ZHANG, W. 2014. The joint effects on Photobacterium phosphoreum of metal oxide nanoparticles and their most likely coexisting chemicals in the environment. *Aquatic toxicology.* 154**,** 200-206.

WANG, H., WICK, R. L. & XING, B. 2009. Toxicity of nanoparticulate and bulk ZnO, Al_2O_3 and TiO_2 to the nematode Caenorhabditis elegans. *Environmental Pollution.* 157**,** 1171-1177.

WANG, H., ZHAO, X., HAN, X., TANG, Z., LIU, S., GUO, W., DENG, C., GUO, Q., WANG, H. & WU, F. 2017. Effects of monovalent and divalent metal cations on the aggregation and suspension of Fe_3O_4 magnetic nanoparticles in aqueous solution. *Science of the Total Environment.* 586**,** 817-826.

WANG, L.-F., HABIBUL, N., HE, D.-Q., LI, W.-W., ZHANG, X., JIANG, H. & YU, H.-Q. 2015. Copper release from copper nanoparticles in the presence of natural organic matter. *Water research.* 68**,** 12-23.

WANG, N., HSU, C., ZHU, L., TSENG, S. & HSU, J.-P. 2013. Influence of metal oxide nanoparticles concentration on their zeta potential. *Journal of colloid and interface science.* 407**,** 22-28.

© University of Pretoria

WANG, Z., LI, J., ZHAO, J. & XING, B. 2011. Toxicity and internalization of CuO nanoparticles to prokaryotic alga Microcystis aeruginosa as affected by dissolved organic matter. *Environmental science & technology.* 45**,** 6032-6040.

WANG, Z., ZHANG, K., ZHAO, J., LIU, X. & XING, B. 2010. Adsorption and inhibition of butyrylcholinesterase by different engineered nanoparticles. *Chemosphere.* 79**,** 86-92.

WANG, Z., ZHANG, L., ZHAO, J. & XING, B. 2016. Environmental processes and toxicity of metallic nanoparticles in aquatic systems as affected by natural organic matter. *Environmental Science: Nano.* 3**,** 240-255.

WARD, J. E. & KACH, D. J. 2009. Marine aggregates facilitate ingestion of nanoparticles by suspension-feeding bivalves. *Marine environmental research.* 68**,** 137-142.

WIESNER, M. R., LOWRY, G. V., ALVAREZ, P., DIONYSIOU, D. & BISWAS, P. 2006. Assessing the risks of manufactured nanomaterials. ACS Publications.

WIGGER, H., HACKMANN, S., ZIMMERMANN, T., KÖSER, J., THÖMING, J. & VON GLEICH, A. 2015. Influences of use activities and waste management on environmental releases of engineered nanomaterials. *Science of the Total Environment.* 535**,** 160-171.

WILKE, C. M., PETERSEN, C., ALSINA, M. A., GAILLARD, J.-F. & GRAY, K. A. 2019. Photochemical interactions between n-Ag_2S and n-TiO_2 amplify their bacterial stress response. *Environmental Science: Nano.* 6**,** 115-126.

WILKE, C. M., TONG, T., GAILLARD, J.-F. O. & GRAY, K. A. 2016. Attenuation of microbial stress due to Nano-Ag and nano-TiO_2 interactions under dark conditions. *Environmental science & technology.* 50**,** 11302-11310.

WONG, K.-F. V. & KURMA, T. 2008. Transport properties of alumina nanofluids. *Nanotechnology.* 19**,** 345702.

XIAO, Y., VIJVER, M. G. & PEIJNENBURG, W. J. 2018. Impact of water chemistry on the behavior and fate of copper nanoparticles. *Environmental pollution.* 234**,** 684-691.

XIE, Z., EBINGHAUS, R., FLÖSER, G., CABA, A. & RUCK, W. 2008. Occurrence and distribution of triclosan in the German Bight (North Sea). *Environmental Pollution.* 156**,** 1190-1195.

YAN, S., SUBRAMANIAN, S. B., TYAGI, R., SURAMPALLI, R. Y. & ZHANG, T. C. 2009. Emerging contaminants of environmental concern: source, transport, fate, and treatment. *Practice Periodical of Hazardous, Toxic, and Radioactive Waste Management.* 14**,** 2-20.

© University of Pretoria

YANG, K., LIN, D. & XING, B. 2009. Interactions of humic acid with nanosized inorganic oxides. *Langmuir.* 25**,** 3571-3576.

YANG, Y., LONG, C.-L., LI, H.-P., WANG, Q. & YANG, Z.-G. 2016. Analysis of silver and gold nanoparticles in environmental water using single particle-inductively coupled plasma-mass spectrometry. *Science of the Total Environment.* 563**,** 996-1007.

YANG, Y., OK, Y. S., KIM, K.-H., KWON, E. E. & TSANG, Y. F. 2017. Occurrences and removal of pharmaceuticals and personal care products (PPCPs) in drinking water and water/sewage treatment plants: A review. *Science of the Total Environment.* 596**,** 303-320.

YE, N., WANG, Z., FANG, H., WANG, S. & ZHANG, F. 2017. Combined ecotoxicity of binary zinc oxide and copper oxide nanoparticles to Scenedesmus obliquus. *Journal of Environmental Science and Health, Part A.* 52**,** 555-560.

YE, N., WANG, Z., WANG, S., FANG, H. & WANG, D. 2018a. Aqueous aggregation and stability of graphene nanoplatelets, graphene oxide, and reduced graphene oxide in simulated natural environmental conditions: complex roles of surface and solution chemistry. *Environmental Science and Pollution Research.* 25**,** 10956-10965.

YE, N., WANG, Z., WANG, S., FANG, H. & WANG, D. 2018b. Dissolved organic matter and aluminum oxide nanoparticles synergistically cause cellular responses in freshwater microalgae. *Journal of Environmental Science and Health, Part A.* 53**,** 651-658.

YIN, Y., SHEN, M., TAN, Z., YU, S., LIU, J. & JIANG, G. 2015. Particle coating-dependent interaction of molecular weight fractionated natural organic matter: impacts on the aggregation of silver nanoparticles. *Environmental science & technology.* 49**,** 6581-6589.

YING, G.-G. & KOOKANA, R. S. 2007. Triclosan in wastewaters and biosolids from Australian wastewater treatment plants. *Environment international.* 33**,** 199-205.

YOKOYAMA, A., SRINIVASAN, K. & FOGLER, H. 1989. Stabilization mechanism by acidic polysaccharides. Effects of electrostatic interactions on stability and peptization. *Langmuir.* 5**,** 534-538.

YU, R., WU, J., LIU, M., ZHU, G., CHEN, L., CHANG, Y. & LU, H. 2016. Toxicity of binary mixtures of metal oxide nanoparticles to Nitrosomonas europaea. *Chemosphere.* 153**,** 187-197.

© University of Pretoria

YU, S., LIU, J., YIN, Y. & SHEN, M. 2017. Interactions between engineered nanoparticles and dissolved organic matter: A review on mechanisms and environmental effects. *Journal of Environmental Sciences.* 63**,** 198-217.

YUNG, M. M., WONG, S. W., KWOK, K. W., LIU, F., LEUNG, Y., CHAN, W., LI, X., DJURIŠIĆ, A. & LEUNG, K. M. 2015. Salinity-dependent toxicities of zinc oxide nanoparticles to the marine diatom Thalassiosira pseudonana. *Aquatic Toxicology.* 165**,** 31-40.

ZHANG, Y., CHEN, Y., WESTERHOFF, P. & CRITTENDEN, J. 2009. Impact of natural organic matter and divalent cations on the stability of aqueous nanoparticles. *Water research.* 43**,** 4249-4257.

ZHANG, Y., LEU, Y.-R., AITKEN, R. & RIEDIKER, M. 2015. Inventory of engineered nanoparticle-containing consumer products available in the Singapore retail market and likelihood of release into the aquatic environment. *International journal of environmental research and public health.* 12**,** 8717-8743.

ZHANG, Z., KONG, F., VARDHANABHUTI, B., MUSTAPHA, A. & LIN, M. 2012. Detection of engineered silver nanoparticle contamination in pears. *Journal of agricultural and food chemistry.* 60**,** 10762-10767.

ZHAO, J.-L., YING, G.-G., LIU, Y.-S., CHEN, F., YANG, J.-F. & WANG, L. 2010. Occurrence and risks of triclosan and triclocarban in the Pearl River system, South China: from source to the receiving environment. *Journal of Hazardous Materials.* 179**,** 215-222.

ZHAO, J., WANG, Z., DAI, Y. & XING, B. 2013. Mitigation of CuO nanoparticle-induced bacterial membrane damage by dissolved organic matter. *Water research.* 47**,** 4169-4178.

ZHENG, X., WU, R. & CHEN, Y. 2011. Effects of ZnO nanoparticles on wastewater biological nitrogen and phosphorus removal. *Environmental science & technology.* 45**,** 2826-2832.

ZHOU, D. & KELLER, A. A. 2010. Role of morphology in the aggregation kinetics of ZnO nanoparticles. *Water research.* 44**,** 2948-2956.

ZHU, X., ZHU, L., CHEN, Y. & TIAN, S. 2009. Acute toxicities of six manufactured nanomaterial suspensions to Daphnia magna. *Journal of nanoparticle research.* 11**,** 67-75.

© University of Pretoria

ZIETZ, B. P., DIETER, H. H., LAKOMEK, M., SCHNEIDER, H., KEßLER-GAEDTKE, B. & DUNKELBERG, H. 2003. Epidemiological investigation on chronic copper toxicity to children exposed via the public drinking water supply. *Science of the Total Environment.* 302**,** 127-144.

ZOOK, J. M., RASTOGI, V., MACCUSPIE, R. I., KEENE, A. M. & FAGAN, J. 2011. Measuring agglomerate size distribution and dependence of localized surface plasmon resonance absorbance on gold nanoparticle agglomerate size using analytical ultracentrifugation. *ACS nano.* 5**,** 8070-8079.

© University of Pretoria

Appendix 3.1: Analysis certificate of the humic acid (HA)

SIGMA-ALDRICH

3050 Spruce Street, Saint Louis, MO 63103 USA
Email USA: techserv@sial.com Outside USA: eurtechserv@sial.com

Certificate of Analysis

Product Name:	HUMIC ACID technical
Product Number:	53680
Batch Number:	BCBS1775V
Brand:	Aldrich
CAS Number:	1415-93-6
Formula:	
Formula Weight:	
Quality Release Date:	29 JUN 2016

TEST	SPECIFICATION	RESULT
APPEARANCE (COLOR)	BLACK	BLACK
APPEARANCE (FORM)	POWDER OR CRYSTALS	POWDER
THIN LAYER CHROMATOGR.	CORRESPONDS TO STANDARD	CORRESPONDS TO STANDARD
SOLUBILITY (COLOR)	BROWN TO VERY DARK BROWN	VERY DARK BROWN
SOLUBILITY (TURBIDITY)	TURBID TO VERY TURBID (>200 NTIJ)	VERY TURBID (>200 NTU)
SOLUBILITY (METHOD)	0.1G IN IOML WATER	0.1G IN 10 ML WATER
		5.9
RESIDUE ON IGNITION		27.7 0/0

Dr. Claudia Geitner
Manager Quality Control
Buchs, Switzerland

Dr. Claudia Geitner

© University of Pretoria

Appendix 4.1: Illustrates the influence of pH on aggregation of 1 mg/L nAl2O3 or nCuO in DIW over 48 h.

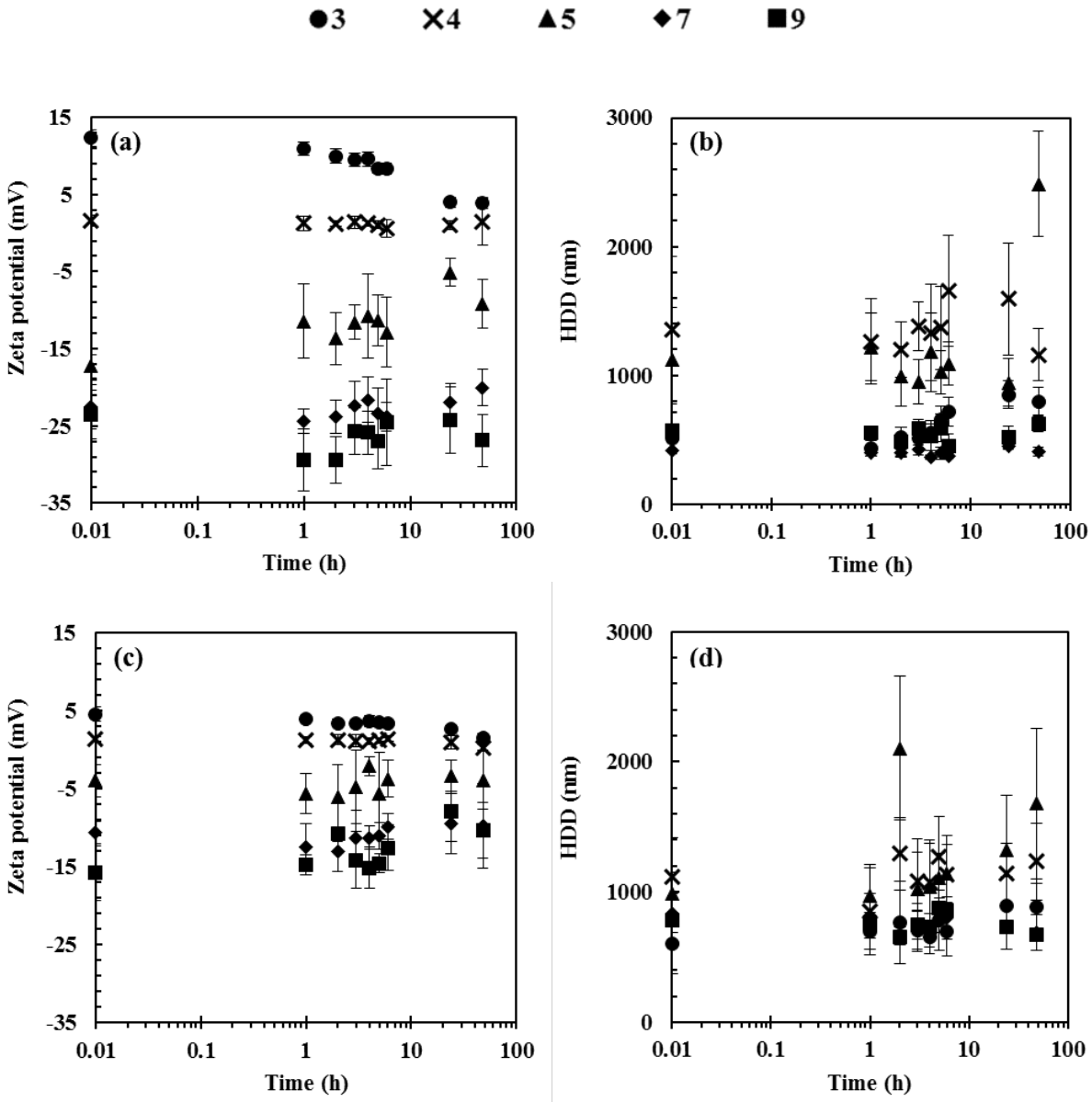

The ζ-potential and HDD for nAl_2O_3 (a and b, respectively), and nCuO (c and d, respectively) in DIW within pH range of 3–9 over 48 h at 1 mg/L. Error bars represent standard deviations (SD) for three replicates.

© University of Pretoria

Appendix 4.2: Illustrates the influence of pH on aggregation of 10 mg/L nAl_2O_3 or nCuO in DIW over 48 h

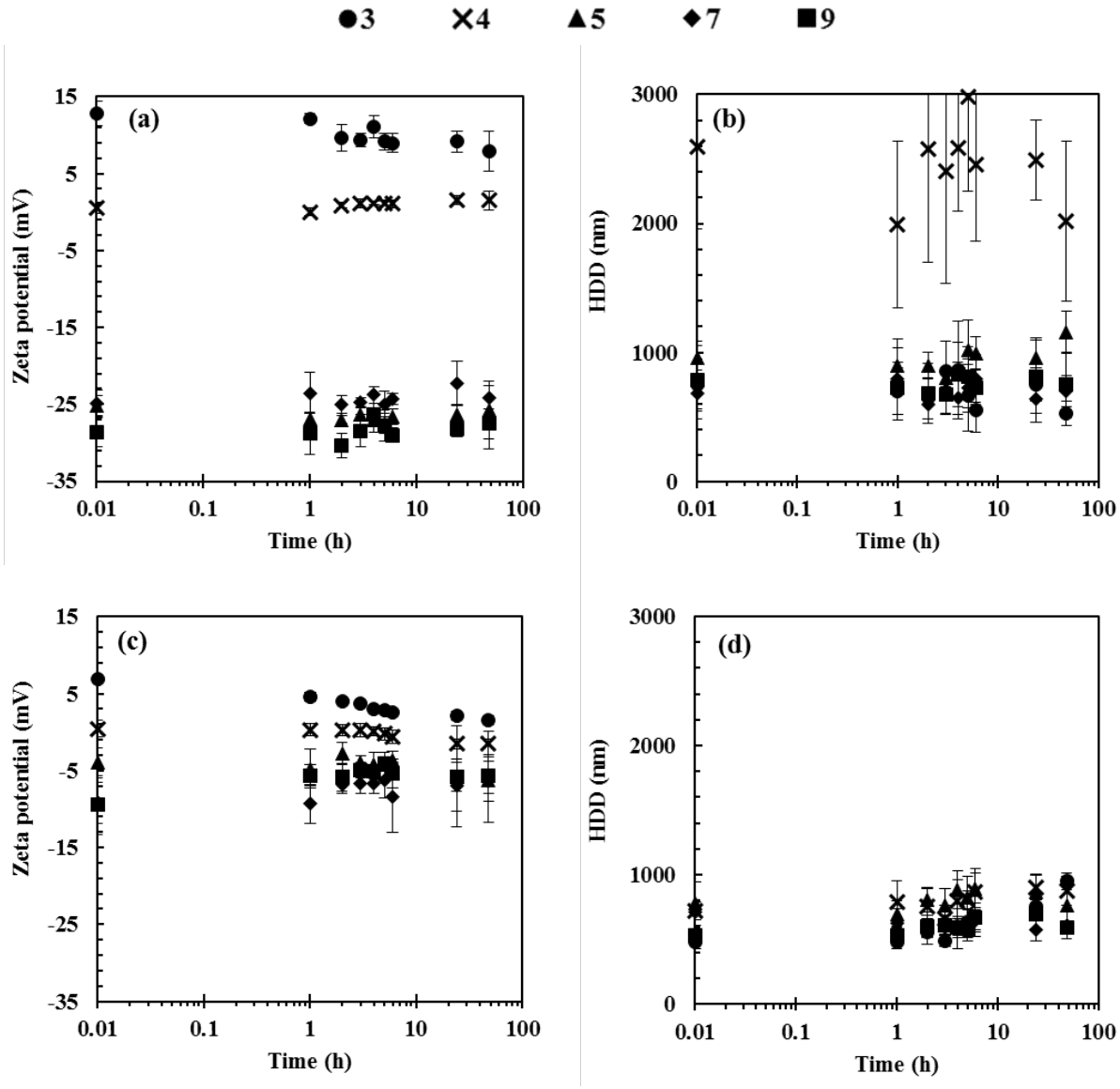

The ζ-potential and HDD for nAl_2O_3 (a and b, respectively), and nCuO (c and d, respectively) in DIW within pH range of 3–9 over 48 h at 10 mg/L. Error bars represent standard deviations (SD) for three replicates.

© University of Pretoria

Appendix 4.3: Illustrates the influence of TCS on aggregation of ternary mixtures of nAl_2O_3, nCuO and TCS in rivers water over 48 h

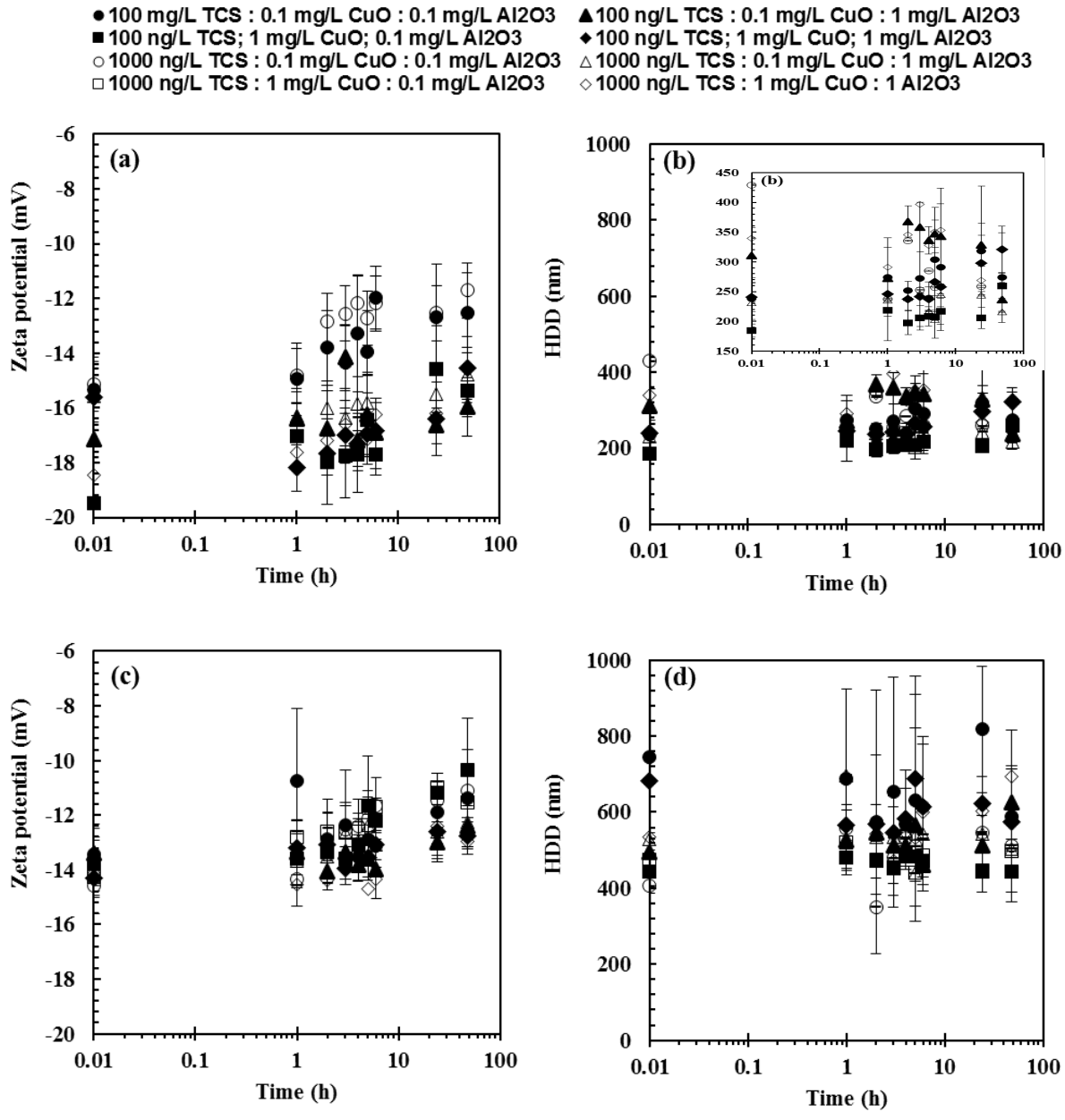

The ζ-potential and HDD (a and b, respectively) in ER water, and (c and d, respectively) in BR water over 48 h. Error bars represent standard deviations (SD) for three replicates.

© University of Pretoria

Appendix 4.4: Summary of aggregation and ζ-potential (ZP) results of nCuO in various exposure media over 48 h.

Exposure media	0.1 mg/L		1 mg/L		10 mg/L	
	ZP (mV)	HDD (nm)	ZP (mV)	HDD (nm)	ZP (mV)	HDD (nm)
pH 7	-8 ─ -11	925 ─ 1433	-9 ─ -13	664 ─ 889	-6 ─ -9	576 ─ 716
IS (1 mM NaCl)	-5 ─ -10	727 ─ 1317	-5 ─ -7	684 ─ 1150	-5 ─ -7	598 ─ 790
IS (10 mM NaCl)	-3 ─ -5	852 ─ 1189	-3 ─ -5	778 ─ 1150	-3 ─ -4	742 ─ 1192
HA (1 mg/L)	-23 ─ -28	489 ─ 648	-19 ─ -27	572 ─ 767	-20 ─ -24	444 ─ 619
HA (10 mg/L)	-30 ─ -35	340 ─ 563	-28 ─ -35	373 ─ 507	-28 ─ -34	405 ─ 470
ER water	-8 ─ -13	229 ─ 249	-9 ─ -16	312 ─ 366	-14 ─ -19	376 ─ 494
BR water	-10 ─ -11	273 ─ 302	-11 ─ -12	340 ─ 395	-11 ─ -13	382 ─ 515

© University of Pretoria

Appendix 4.5: Summary of aggregation and ζ-potential (ZP) results of nAl_2O_3 in various exposure media over 48 h.

Exposure media	0.1 mg/L		1 mg/L		10 mg/L	
	ZP (mV)	HDD (nm)	ZP (mV)	HDD (nm)	ZP (mV)	HDD (nm)
pH 7	-13 ─ -19	663 ─ 794	-20 ─ -24	365 ─ 453	-22 ─ -25	596 ─ 798
IS (1 mM NaCl)	-8 ─ -14	661 ─ 998	-14 ─ -23	722 ─ 995	-20 ─ -29	599 ─ 798
IS (10 mM NaCl)	-5 ─ -9	801 ─ 1234	-9 ─ -19	694 ─ 1007	-17 ─ -23	874 ─ 2097
HA (1 mg/L)	-20 ─ -27	389 ─ 545	-24 ─ -26	349 ─ 393	-24 ─ -26	518 ─ 638
HA (10 mg/L)	-32 ─ -36	379 ─ 475	-32 ─ -36	432 ─ 519	-33 ─ -35	413 ─ 468
ER water	-9 ─ -14	204 ─ 264	-14 ─ -15	248 ─ 444	-14 ─ -16	601 ─ 752
BR water	-9 ─ -11	321 ─ 341	-11 ─ -13	351 ─ 440	-13 ─ -14	581 ─ 895

© University of Pretoria

Appendix 4.6: Summary of results on influence of nAl_2O_3 on aggregation and ζ-potential (ZP) of nCuO in various exposure media over 48 h.

Exposure media	(1 mg/L nCuO, 0.1 mg/L nAl_2O_3)		(1 mg/L nCuO, 1 mg/L nAl_2O_3)		(1 mg/L nCuO, 10 mg/L nAl_2O_3)	
	ZP (mV)	HDD (nm)	ZP (mV)	HDD (nm)	ZP (mV)	HDD (nm)
pH 7	-6 ─ -10	601 ─ 834	-13 ─ -18	397 ─ 608	-17 ─ -19	542 ─ 744
IS (1 mM NaCl)	-9 ─ -13	695 ─ 916	-14 ─ -17	828 ─ 1327	-16 ─ -18	541 ─ 1719
IS (10 mM NaCl)	-6 ─ -11	838 ─ 1160	-15 ─ -22	813 ─ 2403	-22 ─ -26	1037 ─ 3138
HA (1 mg/L)	-24 ─ -29	497 ─ 630	-25 ─ -28	645 ─ 773	-27 ─ -29	692 ─ 778
HA (10 mg/L)	-31 ─ -35	426 ─ 573	-30 ─ -33	468 ─ 559	-34 ─ -36	501 ─ 606
ER water	-12 ─ -16	256 ─ 386	-15 ─ -17	331 ─ 422	-14 ─ -16	462 ─ 602
BR water	-7 ─ -13	619 ─ 827	-11 ─ -12	705 ─ 1050	-12 ─ -13	712 ─ 1682

© University of Pretoria

Appendix 4.7: Summary of results on influence of nCuO on aggregation and ζ-potential (ZP) of nAl_2O_3 in various exposure media over 48 h.

Exposure media	(1 mg/L nAl_2O_3, 0.1 mg/L nCuO)		(1 mg/L nAl_2O_3, 1 mg/L nCuO)		(1 mg/L nAl_2O_3, 10 mg/L nCuO)	
	ZP (mV)	HDD (nm)	ZP (mV)	HDD (nm)	ZP (mV)	HDD (nm)
pH 7	-16 ─ -21	342 ─ 445	-13 ─ -18	396 ─ 608	-4 ─ -13	607 ─ 955
IS (1 mM NaCl)	-16 ─ -18	756 ─ 1191	-14 ─ -17	828 ─ 1327	-10 ─ -14	713 ─ 1668
IS (10 mM NaCl)	-15 ─ -24	1109 ─ 1995	-15 ─ -22	813 ─ 2403	-13 ─ -16	695 ─ 2606
HA (1 mg/L)	-25 ─ -30	799 ─ 945	-25 ─ -28	645 ─ 773	-23 ─ -27	554 ─ 659
HA (10 mg/L)	-31 ─ -34	524 ─ 624	-30 ─ -33	468 ─ 559	-30 ─ -37	345 ─ 530
ER water	-15 ─ -16	287 ─ 363	-15 ─ -17	331 ─ 422	-15 ─ -18	346 ─ 464
BR water	-11 ─ -13	908 ─ 1191	-11 ─ -12	705 ─ 1050	-11 ─ -13	606 ─ 863

© University of Pretoria

Appendix 4.8: Summary of results on influence of TCS on aggregation and ζ-potential (ZP) of nCuO in river water over 48 h.

Exposure media	(0.1 mg/L nCuO, 100 ng/L TCS)		(0.1 mg/L nCuO, 1000 ng/L TCS)		(1 mg/L nCuO, 100 ng/L TCS)		(1 mg/L nCuO, 1000 ng/L TCS)	
	ZP (mV)	HDD (nm)	ZP (mV)	HDD (nm)	ZP (mV)	HDD (nm)	ZP (mV)	HDD (nm)
ER water	-13 — -15	165 — 174	-14 — -17	153 — 169	-12 — -19	162 — 201	-13 — -19	172 — 226
BR water	-4 — -11	291 — 677	-9 — -12	320 — 665	-11 — -16	465 — 631	-11 — -14	432 — 764

Appendix 4.9: Summary of results on influence of TCS on aggregation and ζ-potential (ZP) of nAl_2O_3 in river water over 48 h.

Exposure media	(0.1 mg/L nAl_2O_3, 100 ng/L TCS)		(0.1 mg/L nAl_2O_3, 1000 ng/L TCS)		(1 mg/L nAl_2O_3, 100 ng/L TCS)		(1 mg/L nAl_2O_3, 1000 ng/L TCS)	
	ZP (mV)	HDD (nm)	ZP (mV)	HDD (nm)	ZP (mV)	HDD (nm)	ZP (mV)	HDD (nm)
ER water	-14 — -16	173 — 190	-15 — -16	174 — 184	-16 — -18	187 — 205	-17 — -18	194 — 208
BR water	-12 — -14	341 — 617	-12 — -14	413 — 568	-14 — -17	326 — 416	-14 — -17	365 — 477

© University of Pretoria

Appendix 4.10: Summary of results on aggregation and ζ-potential (ZP) of ternary mixtures in river water over 48 h.

Mixture Composition	ER water		BR water	
(TCS (ng/L); nCuO (mg/L); nAl_2O_3 (mg/L))	ZP (mV)	HDD (nm)	ZP (mV)	HDD (nm)
(100; 0.1; 0.1)	-12 ─ -15	238 ─ 318	-11 ─ -13	568 ─ 817
(100; 0.1; 1)	-14 ─ -17	237 ─ 367	-12 ─ -14	461 ─ 626
(100; 1; 0.1)	-16 ─ -19	196 ─ 295	-10 ─ -14	443 ─ 484
(100; 1; 1)	-15 ─ -18	237 ─ 321	-13 ─ -14	545 ─ 683
(1000; 0.1; 0.1)	-12 ─ -15	238 ─ 429	-11 ─ -15	351 ─ 556
(1000; 0.1; 1)	-15 ─ -17	203 ─ 247	-12 ─ -14	504 ─ 781
(1000; 1; 0.1)	-15 ─ -19	185 ─ 260	-11 ─ -14	440 ─ 519
(100; 1; 1)	-15 ─ -18	259 ─ 397	-13 ─ -15	471 ─ 694

© University of Pretoria